Assessing Historical Trends in Snowpack Variability Across the Northern Rocky Mountains using Remote Sensing and Dendrochronology Approaches

A DISSERTATION
SUBMITTED TO THE FACULTY OF
UNIVERSITY OF MINNESOTA
BY

Christopher John Crawford

IN PARTIAL FULFILLMENT OF THE REQUIREMENTS
FOR THE DEGREE OF
DOCTOR OF PHILOSOPHY

Kurt F. Kipfmueller and Steve M. Manson

June 2013

Acknowledgements

This research was possible because of the contributions of many individuals and grant funding streams. My deepest gratitude is extended to my parents, Bobby and Sandra Crawford, who stood behind me every step of the way while I completed my graduate education. A very special thanks is extended to my advisers, Kurt Kipfmueller and Steve Manson, and Ph.D. committee members Marvin Bauer and Kathy Klink, for their mentoring efforts, intellectual contributions, and invaluable guidance, advice, and feedback during my graduate education. I would like to thank Christian Ferguson for his unconditional enthusiasm, effort, and assistance during two field seasons of tree-ring core sample collection across the northern Rocky Mountain region. I would like to especially thank Marvin Bauer for his support, direction, and encouragement to utilize the historical Landsat image archive for satellite climate data record development. Finally, I would like to thank my dendrochronology lab group (*Minnesota Dendroecology Lab* and *Center for Dendrochronology*) and GIS/spatial analysis (*Human-Environment Geographic Information Science* (HEGIS)) lab group for their helpful feedback during my graduate research at the University of Minnesota.

I would like to also take this opportunity to extend additional appreciation to a number of individuals who have made specific and important contributions to this research. I would like to thank Dorothy Hall, George Riggs, and James Foster for their valuable perspectives on my snow remote sensing work during and after my fellowship visit to the Cryospheric Sciences Laboratory at NASA Goddard Space Flight Center. I would like to thank Scott St. George for his intellectual and statistical contributions to my climate-based research. I would like to especially thank Dan Griffin for his intellectual input and assistance with tree-ring analysis during graduate school as we walked parallel paths to Ph.D. completion. I would like to thank my roommate and tree-ring confidant Max Torbenson for his insight, feedback, and quantitative perspective during the development of my tree-ring research. Finally, I would like to thank Grant Elliot and Matt Salzer who provided important sounding boards for my research ideas including a willingness to review and improve preliminary work.

I am very grateful for my personal relationships during my time as a graduate student. I would like to thank Elizabeth Waring for her support and willingness to extend her professional travel benefits to me so that I could broaden my professional networks and enable my research to gain visibility at professional conferences early in my graduate career. I would like to thank my close friends, Aaron and Julie Schilz, for providing a relaxing social environment to refresh and recharge my internal self during graduate school. I would like to thank my Yoga teachers for guiding me through difficult times when balance seemed beyond my reach. Finally, I want to especially thank Beth Vanderscheuren for her enthusiasm, support, and love during the latter stages of Ph.D. completion. Thanks Beth for understanding my intense passion for the research I undertake.

This research was funded by a NASA Earth and Space Science Fellowship (NNX10AO73H), the Association of American Geographers (AAG), AAG Mountain Geography Specialty Group, AAG Paleoenvironmental Specialty Group, American

Alpine Club, University of Minnesota Graduate School, University of Minnesota College of Liberals Arts (CLA), CLA Graduate Research Partnership Program, and University of Minnesota Department of Geography.

Abstract

Mountain snowpack across the western United States is declining because of warming spring temperatures during the modern period. Earlier snowmelt has been documented for numerous localities throughout the American West using ground-based snow-water-equivalent measurements and gauged streamflow. This research uses historical satellite imagery, tree-ring records, and instrumental climate observations from the northern Rocky Mountain (NRM) region to evaluate the climatic controls on mountain snowpack spatiotemporal variability, assess historical spring snowmelt trends, and contextualize modern climatic change with pre-instrumental climate variability. A suite of methodological approaches is employed to develop and calibrate satellite, tree-ring, and instrumental climate records using time-series analysis techniques. Together, these NRM region climate records suggest that precipitation in the form of mountain snowpack extent varies on interannual to decadal timescales. Of more importance, spring mountain snowpack appears to be decreasing in areal extent during the 20th and early 21st centuries driven largely by modern spring warming.

Table of Contents

Chapter 3: MODIS Terra Collection 6 Fractional Snow Cover Validation in Mountainous Terrain using Landsat TM and ETM+

Chapter 4: Evidence for Spring Mountain Snowpack Retreat from a Landsat-Derived Snow Cover Climate Data Record

Chapter 5: Annual and Sub-annual Precipitation Reconstructions for the Craters of the Moon Lava Complex, Eastern Snake River Plain, USA

List of Tables

List of Figures

Chapter 2: Multitemporal Snow Cover Mapping in Mountainous Terrain for Landsat Climate Data Record Development

Chapter 3: MODIS Terra Collection 6 Fractional Snow Cover Validation in Mountainous Terrain using Landsat TM and ETM+

Chapter 4: Evidence for Spring Mountain Snowpack Retreat from a Landsat-Derived Snow Cover Climate Data Record

Chapter 5: Annual and Sub-annual Precipitation Reconstructions for the Craters of the Moon Lava Complex, Eastern Snake River Plain, USA

Chapter 1: Introduction

1.1 Dissertation Synopsis

This dissertation research project tackles one central question. Is northern Rocky Mountain (NRM) snowpack undergoing significant decline in response to warming surface temperatures during the modern period? The southern extent of the NRMs is geographically located in the interior northwestern United States, encompassing portions of Idaho, western Montana, and western Wyoming. Much of the focus and work on NRM climate and snowpack in this dissertation is centered on the eastern Snake River Plain (SRP), central Idaho, and southwestern Montana sub-regions. Three main physiographic features define this mountainous region including the SRP in southern Idaho, the Idaho Batholith in western Idaho, and fault-block mountain ranges in east central Idaho and southwestern Montana. Tributary and river systems forming within the NRMs feed continental Missouri and Columbia River hydrological basins. Disjoint open forests are common within upper and lower forest margins, whereas, closed-canopy forests dominate the entire forest zone. Alpine regions include tundra spp., bare rock and scree, and lakes of variable size. A mixed assemblage of shrubs, grasslands, and sedges occupy regions below the lower forest border. Agricultural practices and human settlements can be found along riparian corridors at the lowest elevations.

NRM climate can be broadly classified as semi-arid with distinct cool and warm seasons from November-April and July-August, respectively. Precipitation over the annual cycle is evenly distributed, although certain localities show tendencies towards bi-modal seasonality (Mock 1996; Shinker 2010). The SRP is dominated by a winter

precipitation regime composed mainly of snowfall, whereas the central Idaho and southwestern Montana mountains receive peak maxima during spring. The north-south orientation of the Idaho Batholith combined with westward maritime moisture transport from the Pacific Ocean exerts strong controls on windward (leeward) rain shadow patterns between west and east central Idaho. NRM snowpack is classified as continental with accumulation beginning in November and reaching maximum depth in early April before melt begins during spring (April-June) (Cayan 1996). Elevational change between alpine basins and valley floors results in different levels of exposure to the 'free atmosphere' (Daly, Conklin, and Unsworth 2010; Barry 1981); therefore, mountain meteorological processes and patterns can be quite different because of complex airflow patterns and valley temperature inversions (Barry 1981). This complex interaction between physiography, temperature, precipitation, and snowfall makes it difficult to scale-up these dissertation results and discussions on climate and snowpack across mountainous terrain; hence, the emphasis on sub-regional case studies.

This dissertation advances remote sensing and dendrochronology methods, contributes primary climate data records, and establishes a foundation to evaluate NRM climate and snowpack variability on seasonal to decadal timescales. Specific dissertation contributions include (1) a multitemporal method to map snow cover area (SCA) in mountainous terrain from Landsat for climate data record (CDR) development; (2) a cross-sensor snow map validation between MODIS Terra and Landsat TM and ETM+ during spring snowmelt; (3) a spring SCA reconstruction for the central Idaho and southwestern Montana mountains over 20th and 21st centuries using a Landsat snow cover

CDR and surface temperature records; and (4) annual and sub-annual precipitation reconstructions for the eastern SRP using tree-records from the Craters of the Moon National Monument.

1.2 Problem Statement

Warming surface temperatures during the post-industrial era threatens future freshwater resources across the arid western US (Barnett, Adam, and Lettenmaier 2005; Pederson et al. 2011; Service 2004). Current trends in mountain snowpack show widespread decline across many regions of the American West since the 1950s. This response has been linked to warming temperatures accompanied by an earlier onset of spring (Dyer and Mote 2007; Moore, Harper, and Greenwood 2007; Mote et al. 2005; Pierce et al. 2008; Hamlet et al. 2005; Cayan et al. 2001; McCabe and Clark 2005; Stewart, Cayan, and Dettinger 2005). However, the time period available for in-depth evaluation of this trend is confined to roughly the last fifty years, and based almost solely on snow course and snow telemetry (SNOTEL) snow-water-equivalent (SWE) measurements. Consequently, there is an urgent need to expand our understanding of the temperature-snowpack relationship over multiple scales (Barry 1992; Groisman et al. 1994; Barry, Fallot, and Armstrong 1995; Barry 2002). This can be achieved by extending the timescale of analysis over a broader spatial domain, and in return, sharpens our ability to separate anthropogenically-induced climate change trends from natural climate variability.

This dissertation research is intended to advance knowledge on the dynamics between NRM climate variability and snowpack change on paleo- and modern timescales. Western US energy production, agriculture, recreation, and natural

ecosystems rely on the snow-fed streamflow brought about by cool season mountain snowpack accumulation and subsequent melt. Modern climate change compromises the continued availability of snow-dominated freshwater resources for an expanding built-environment infrastructure across the western US (Milly et al. 2008; Otterstrom and Shumway 2003; Service 2004). This freshwater dependency makes economic and social systems vulnerable to abrupt changes in supply. More importantly, with accelerated warming, NRM snowpack stands to undergo significant solid-to-liquid phase transition because of lower elevational stature and freezing line changes (i.e., 0 degrees Celsius isotherm) relative to higher terrain elsewhere in the Rockies.

Recent evidence indicates that snow is melting earlier and faster (Mote et al. 2005), and rain instead of snow is occurring earlier in the winter season (Knowles, Dettinger, and Cayan 2006). This has important implications for the timing and amount seasonal streamflow and runoff. Historically, peak streamflow from snowmelt across the NRMs occurred in early June, but with spring warming, the possibility emerges for a shorter seasonal accumulation window and earlier, and perhaps smaller peak streamflows (McCabe and Clark 2005; Moore, Harper, and Greenwood 2007; Stewart, Cayan, and Dettinger 2005). Also, if snowpack melts earlier and more rapidly, this has the potential to overwhelm hydrological infrastructure and could lead to or exacerbate flooding and summer water shortages. Additional temperature-induced threats include seasonal shifts in timing and magnitude of snowfall and streamflow, threats to hydropower energy production, and greater wildfire risk (Bales et al. 2006; Heyerdahl, Morgan, and Riser 2008; Westerling et al. 2006). This dissertation uses remote sensing and

dendrochronology approaches to contextualize recently observed NRM mountain snowpack trends relative to long-term variability over multiple scales.

1.3 Challenges for Mountain Climate Research

The paucity of instrumental climate stations in mountainous regions has plagued mountain climate research for decades (Barry 1992; Beniston 2003). For the western US, a high proportion of instrumental climate stations are located in valleys (Menne, Williams, and Vose 2009). Spatial placement of instrumental station networks have been designed to support weather prediction, hydrological forecasting, and climate monitoring (Bales et al. 2006). The current instrumental network coverage possesses important scientific value for broad domain two-dimensional climate study, but for mountain studies that include elevation as a third dimension, data coverage does not always satisfy the statistical confidence required for longer timescales of analysis, adequate replication in space, and high spatiotemporal resolution. As a result, climate data record availability currently limits process-based understanding on climate variability and change in mountainous regions, especially in alpine zones where climate inputs like snowpack support lowland freshwater demands.

Instrumental climate networks require financial capital with declared operational commitments to maintain data collection and distribution. Shrinking US federal budgets, including future budget outlooks, paint a grim picture for instrumental climate station additions. Therefore, it is essential to develop new strategies for mountain climate research that exploit other data sources. In an attempt to overcome these limitations, this dissertation research uses remote sensing and dendrochronology methods to develop

primary climate data records for the NRMs. Using existing instrumental climate records that include temperature, precipitation, and SNOTEL SWE observations, satellite CDRs and tree-ring climate proxies are calibrated, analyzed, and interpreted using least-squared regression and time-series analysis techniques. This multi-data integration method is intended to advance scientific approaches to mountain climate research.

1.4 Instrumental, Satellite, and Tree-Ring Proxy Data

Modern climate data records originate from ground and balloon-based instruments and satellite platforms. Paleoclimate records are derived from core sample extractions from environmental proxies such as tree rings, ice cores, and lake and ocean sediments. Each type of climate record has a unique observational timescale, spatial resolution, signal-to-noise (*SN*) ratio, and error and uncertainty. Even though climate signal strength varies with the type of record, quality control documentation enable experimental designs to take advantage of data attributes known to formulate a strong climate signal. For example, ground-based instruments measure surface air temperatures well over time, and satellite platforms retrieve snow albedo at high spatiotemporal resolutions. Constructing a statistical model that merges air temperature with snow albedo blends the strongest climate signals present in both records. This dissertation uses secondary instrumental climate records produced by other entities in-conjunction with primary climate data record development to address specific research questions.

Three climate data types are used: (1) ground-based instrumental climate records; (2) multispectral satellite retrievals from five Landsat platforms and Moderate Resolution Imaging spectroradiometer (MODIS) Terra Collection 6 (C6) snow products; and (3)

tree-ring records. Secondary instrumental climate records originate from gridded (Mitchell and Jones 2005), spatially interpolated (Daly et al. 2008), and single station (Serreze et al. 1999) datasets. A primary Landsat snow cover CDR was derived from raw multispectral digital numbers retrieved during the Landsat mission. The Landsat images were collected from the image archive at the USGS EROS Data Center (http://eros.usgs.gov/). Secondary MODIS Terra C6 swath fractional snow cover products were acquired directly from George Riggs at NASA Goddard Space Flight Center. Tree-ring records were collected from trees growing at the lower forest border on the Craters of the Moon lava complex.

1.5 Methodological Approaches and Statistical Techniques

Time is the unifying domain for this dissertation research. Time-series probability theory is concerned with 'stationary' where no systematic change in the mean and variance is contained within an observed time-series (Chatfield 2004). In most cases, discretely observed non-stationary processes (i.e., data acquisitions) must be transformed into a stationary process to exploit time-series theory and analysis (Chatfield 2004). For this dissertation, secondary instrumental climate records have already been constructed to meet this criterion. On the other hand, primary satellite snow cover CDR development from Landsat required an image processing method, a standardization approach, a probability distribution evaluation, quality control assessment, and statistical validation. Primary tree-ring records were developed using a standard dendrochronological approach (Fritts 1976), although evolving techniques were applied to improve sub-annual resolution.

Both remote sensing and dendrochronology approaches rely heavily on environmental observations acquired in the time domain for data design, development, and analysis. Time seemed to be the most intuitive domain to merge instrumental climate records with snow cover CDRs and tree-ring records. Remote sensing algorithms applied to each Landsat image included image registration, planetary reflectance conversion, cloud cover masking, cloud shadow masking, topographic normalization, and snow albedo retrieval. Linear regression techniques were applied to establish cross-sensor interoperability and snow map validation. Spring SCA was reconstructed over 20th and early 21st centuries using a Landsat CDR, surface temperature records, and linear regression with predicted residual error sum-of-squares (PRESS) cross-validation (Michaelsen 1987). Annual and sub-annual tree-ring chronologies were constructed from raw tree-ring width measurements using conservative standardization techniques (Cook et al. 1995; Cook and Peters 1997). Tree-ring climate signals were identified with correlation analysis using Monte-Carlo simulations (Meko, Touchan, and Anchukaitis 2011). Multiple linear regressions with a PRESS cross-validation approach were employed to develop tree-ring based climate reconstructions.

Beyond the statistical methods used to develop and standardize snow cover CDRs and tree-ring records, three main time-series analysis techniques were used to evaluate and interpret SCA and tree-ring based climate reconstructions. First, linear regression modeling with PRESS cross-validation was used to reconstruct SCA where Landsat SCA estimates were the *dependent* variable, and instrumental climate records were the *independent* variables. Second, spectral estimation, binomial filtering, and a modified

Mann-Kendall trend test (Yue and Wang 2004) were used to distinguish modern SCA climate change trends from natural internal SCA variability. Lastly, singular spectrum analysis (Ghil et al. 2002; Vautard and Ghil 1989) was used to extract the dominant frequencies of precipitation variability that exhibited significant power at annual and sub-annual timescales. The behavior in past climate regimes was also documented and allowed for perspective on climate variability and change during the modern period.

1.6 Multiple Lines of Evidence Framework

Merging multiple types of climate data records to address one central question was the underlying conceptual framework and operational motivation for this dissertation research. Implementing this framework required the use of instrumental, satellite, and tree-ring data sources, and included a suite of different methodological approaches and techniques to arrive at interpretable NRM climate and snowpack records. Following Barry et al. (1995) discussion of climate variability and change during the 20th century, it became apparent that no one data source or method was satisfactory to obtain all the information required to assess NRM climate and snowpack variability. Therefore, in addition to the multi-data multi-method approach outlined above, I decided to adopt a reductionist's multiple lines of evidence narrative to tell independent stories about climate variability and change that I hoped would inform the central question.

This particular framework is a possible alternative to current paradigms in climate research that seem to be moving towards proxy-climate model comparisons (Hughes and Ammann 2009) with an increasing reliance on simulation and projection model results (Duffy et al. 2006; Meehl et al. 2008; Meehl and Teng 2012). While this line of reasoning

coupled with sophisticated mathematical manipulation is sure to inform future climates and provide a certain flavor of model validation, it is imperative to remember the 'Rule of Parsimony' or otherwise known as 'Occam's Razor' when attempting to explain past and present climate variability and change. Future climate change remains skillfully unpredictable (Mehta et al. 2011), but pursuing a multiple lines of evidence framework guarantees that ground-based instruments, satellite retrievals, and tree-rings will show climate variability at multiple temporal and spatial scales, but even so, modern climate change should be observable across independent climate data records indicating strong verification for trends such mountain snowpack decline.

1.7 Summary of Objectives

The central question under investigation in this dissertation is as follows: Is northern Rocky Mountain (NRM) snowpack undergoing significant decline in response to warming surface temperatures during the modern period? Chapters two-five represent either original method or specific case study research papers that have been crafted for a peer-review journal audience of sufficient impact. Each chapter proposes one or more objectives that address questions specific to that study. Chapter two proposes a multitemporal snow cover mapping method in mountainous terrain for Landsat climate data record development. Chapter three undertakes a cross-sensor snow map validation during springmelt in mountainous terrain between MODIS Terra and Landsat TM and ETM+. Chapter four compares a Landsat snow cover CDR with ground-based SNOTEL SWE and surface temperature and precipitation observations, and then spring SCA is reconstructed for a NRM sub-region over 20th and early 21st centuries. Chapter five uses

lower forest border tree-ring records from the Craters of the Moon National Monument to reconstruct annual and sub-annual precipitation variability over the past 500 years. Chapter six contains specific chapter conclusions, general conclusions, and future research directions.

References

Bales, R. C., N. P. Molotch, T. H. Painter, M. D. Dettinger, R. Rice, and J. Dozier. 2006. "Mountain hydrology of the western United States." *Water Resources Research* no. 42 (8):13. doi: W0843210.1029/2005wr004387.

Barnett, T. P., J. C. Adam, and D. P. Lettenmaier. 2005. "Potential impacts of a warming climate on water availability in snow-dominated regions." *Nature* no. 438 (7066):303-309. doi: 10.1038/nature04141.

Barry, R. G. 1981. *Mountain Weather and Climate*. New York: Methuen.

———. 1992. "Mountain climatology and past and potential future climatic changes in mountainous regions - A review." *Mountain Research and Development* no. 12 (1):71-86.

Barry, R. G., J. M. Fallot, and R. L. Armstrong. 1995. "Twentieth-century variability in snow-cover conditions and approaches to detecting and monitoring changes: Status and prospects." *Progress in Physical Geography* no. 19 (4):520-532. doi: 10.1177/030913339501900405.

Barry, Roger G. 2002. "The role of snow and ice in the global climate system: A review." *Polar Geography* no. 26 (3):235 - 246.

Beniston, M. 2003. "Climatic change in mountain regions: A review of possible impacts." *Climatic Change* no. 59 (1-2):5-31.

Cayan, D. R. 1996. "Interannual climate variability and snowpack in the western United States." *Journal of Climate* no. 9 (5):928-948.

Cayan, D. R., S. A. Kammerdiener, M. D. Dettinger, J. M. Caprio, and D. H. Peterson. 2001. "Changes in the onset of spring in the western United States." *Bulletin of the American Meteorological Society* no. 82 (3):399-415.

Chatfield, C. 2004. *The Analysis of Time Series, an Introduction*. six ed. New York: Chapman and Hall/CRC.

Cook, E. R., K. R. Briffa, D. M. Meko, D. A. Graybill, and G. Funkhouser. 1995. "The segment length curse in long tree-ring chronology development for paleoclimatic studies." *Holocene* no. 5 (2):229-237.

Cook, E. R., and K. Peters. 1997. "Calculating unbiased tree-ring indices for the study of climate and environmental change." *The Holocene* no. 7:361-370.

Daly, C., D. R. Conklin, and M. H. Unsworth. 2010. "Local atmospheric decoupling in complex topography alters climate change impacts." *International Journal of Climatology* no. 30 (12):1857-1864. doi: 10.1002/joc.2007.

Daly, C., M. Halbleib, J. I. Smith, W. P. Gibson, M. K. Doggett, G. H. Taylor, J. Curtis, and P. P. Pasteris. 2008. "Physiographically sensitive mapping of climatological temperature and precipitation across the conterminous United States." *International Journal of Climatology* no. 28 (15):2031-2064. doi: 10.1002/joc.1688.

Duffy, P. B., R. W. Arritt, J. Coquard, W. Gutowski, J. Han, J. Iorio, J. Kim, L. R. Leung, J. Roads, and E. Zeledon. 2006. "Simulations of present and future climates in the western United States with four nested regional climate models." *Journal of Climate* no. 19 (6):873-895. doi: 10.1175/jcli3669.1.

Dyer, J. L., and T. L. Mote. 2007. "Trends in snow ablation over North America." *International Journal of Climatology* no. 27 (6):739-748. doi: 10.1002/joc.1426.

Fritts, H. C. 1976. *Tree Rings and Climate*. Caldwell, New Jersey: The Blackburn Press.

Ghil, M., M. R. Allen, M. D. Dettinger, K. Ide, D. Kondrashov, M. E. Mann, A. W. Robertson, A. Saunders, Y. Tian, F. Varadi, and P. Yiou. 2002. "Advanced spectral methods for climatic time series." *Reviews of Geophysics* no. 40 (1). doi: 100310.1029/2000rg000092.

Groisman, P. Y., T. R. Karl, R. W. Knight, and G. L. Stenchikov. 1994. "Changes of snow cover, temperature, and radiative heat-balance over the northern-hemisphere." *Journal of Climate* no. 7 (11):1633-1656.

Hamlet, A. F., P. W. Mote, M. P. Clark, and D. P. Lettenmaier. 2005. "Effects of temperature and precipitation variability on snowpack trends in the western United States." *Journal of Climate* no. 18 (21):4545-4561.

Heyerdahl, E. K., P. Morgan, and J. P. Riser. 2008. "Multi-season climate synchronized historical fires in dry forests (1650-1900), northern Rockies, USA." *Ecology* no. 89 (3):705-716.

Hughes, M. K., and C. M. Ammann. 2009. "The future of the past-an earth system framework for high resolution paleoclimatology: editorial essay." *Climatic Change* no. 94 (3-4):247-259. doi: 10.1007/s10584-009-9588-0.

Knowles, N., M. D. Dettinger, and D. R. Cayan. 2006. "Trends in snowfall versus rainfall in the Western United States." *Journal of Climate* no. 19 (18):4545-4559.

McCabe, G. J., and M. P. Clark. 2005. "Trends and variability in snowmelt runoff in the western United States." *Journal of Hydrometeorology* no. 6 (4):476-482.

Meehl, G. A., J. M. Arblaster, G. Branstator, and H. van Loon. 2008. "A coupled air-sea response mechanism to solar forcing in the Pacific region." *Journal of Climate* no. 21 (12):2883-2897. doi: 10.1175/2007jcli1776.1.

Meehl, G. A., and H. Y. Teng. 2012. "Case studies for initialized decadal hindcasts and predictions for the Pacific region." *Geophysical Research Letters* no. 39. doi: L2270510.1029/2012gl053423.

Mehta, V., G. Meehl, L. Goddard, J. Knight, A. Kumar, M. Latif, T. Lee, A. Rosati, and D. Stammer. 2011. "Decadal climate predictability and prediction: Where are we?" *Bulletin of the American Meteorological Society* no. 92 (5):637-640. doi: 10.1175/2010bams3025.1.

Meko, D. M., R. Touchan, and K. J. Anchukaitis. 2011. "Seascorr: A MATLAB program for identifying the seasonal climate signal in an annual tree-ring time series." *Computers & Geosciences*. doi: 10.1016/j.cageo.2011.01.013.

Menne, M. J., C. N. Williams, and R. S. Vose. 2009. "The US historical climatology network monthly temperature data, version 2." *Bulletin of the American Meteorological Society* no. 90 (7):993-1007. doi: 10.1175/2008bams2613.1.

Michaelsen, J. 1987. "Cross-validation in statistical climate forecast models." *Journal of Applied Meteorology* no. 26:1589-1600.

Milly, P. C. D., J. Betancourt, M. Falkenmark, R. M. Hirsch, Z. W. Kundzewicz, D. P. Lettenmaier, and R. J. Stouffer. 2008. "Climate change - Stationarity is dead: Whither water management?" *Science* no. 319 (5863):573-574. doi: 10.1126/science.1151915.

Mitchell, T. D., and P. D. Jones. 2005. "An improved method of constructing a database of monthly climate observations and associated high-resolution grids." *International Journal of Climatology* no. 25 (6):693-712. doi: 10.1002/joc.1181.

Mock, C. J. 1996. "Climatic controls and spatial variations of precipitation in the western United States." *Journal of Climate* no. 9 (5):1111-1125.

Moore, J. N., J. T. Harper, and M. C. Greenwood. 2007. "Significance of trends toward earlier snowmelt runoff, Columbia and Missouri Basin headwaters, western United States." *Geophysical Research Letters* no. 34 (16):5. doi: L1640210.1029/2007gl031022.

Mote, P. W., A. F. Hamlet, M. P. Clark, and D. P. Lettenmaier. 2005. "Declining mountain snowpack in western north America." *Bulletin of the American Meteorological Society* no. 86 (1):39-49. doi: 10.1175/bams-86-1-39.

Otterstrom, Samuel M., and J. Matthew Shumway. 2003. "Deserts and oases: the continuing concentration of population in the American Mountain West." *Journal of Rural Studies* no. 19 (4):445-462.

Pederson, G. T., S. T. Gray, C. A. Woodhouse, J. L. Betancourt, D. B. Fagre, J. S. Littell, E. Watson, B. H. Luckman, and L. J. Graumlich. 2011. "The Unusual Nature of Recent Snowpack Declines in the North American Cordillera." *Science* no. 333 (6040):332-335. doi: 10.1126/science.1201570.

Pierce, D. W., T. P. Barnett, H. G. Hidalgo, T. Das, C. Bonfils, B. D. Santer, G. Bala, M. D. Dettinger, D. R. Cayan, A. Mirin, A. W. Wood, and T. Nozawa. 2008. "Attribution of Declining Western US Snowpack to Human Effects." *Journal of Climate* no. 21 (23):6425-6444. doi: 10.1175/2008jcli2405.1.

Serreze, M. C., M. P. Clark, R. L. Armstrong, D. A. McGinnis, and R. S. Pulwarty. 1999. "Characteristics of the western United States snowpack from snowpack telemetry (SNOTEL) data." *Water Resources Research* no. 35 (7):2145-2160. doi: 10.1029/1999wr900090.

Service, R. F. 2004. "Water resources: As the West goes dry." *Science* no. 303 (5661):1124-1127.

Shinker, J. J. 2010. "Visualizing spatial heterogeneity of western U.S. climate variability." *Earth Interactions* no. 14. doi: 1010.1175/2010ei323.1.

Stewart, I. T., D. R. Cayan, and M. D. Dettinger. 2005. "Changes toward earlier streamflow timing across western North America." *Journal of Climate* no. 18 (8):1136-1155. doi: 10.1175/jcli3321.1.

Vautard, R., and M. Ghil. 1989. "Singular spectrum analysis in nonlinear dynamics, with applications to paleoclimatic time-series." *Physica D* no. 35 (3):395-424. doi: 10.1016/0167-2789(89)90077-8.

Westerling, A. L., H. G. Hidalgo, D. R. Cayan, and T. W. Swetnam. 2006. "Warming and earlier spring increase western US forest wildfire activity." *Science* no. 313 (5789):940-943. doi: 10.1126/science.1128834.

Yue, S., and C. Y. Wang. 2004. "The Mann-Kendall test modified by effective sample size to detect trend in serially correlated hydrological series." *Water Resources Management* no. 18 (3):201-218. doi: 10.1023/b:warm.0000043140.61082.60.

Chapter 2: Multitemporal Snow Cover Mapping in Mountainous Terrain for Landsat Climate Data Record Development

A multitemporal method to map snow cover in mountainous terrain is proposed to guide Landsat climate data record (CDR) development. The Landsat image archive including MSS, TM, and ETM+ imagery was used to construct a prototype Landsat snow cover CDR for the interior northwestern United States. Landsat snow cover CDRs are designed to capture snow cover area (SCA) variability at discrete bi-monthly intervals that correspond to ground-based snow telemetry (SNOTEL) snow-water-equivalent (SWE) measurements. The June 1 bi-monthly interval was selected for initial CDR development, and was based on peak snowmelt timing for this mountainous region. Fifty-four Landsat images from 1975-2011 were pre-processed that included image registration, top-of-atmosphere (TOA) reflectance conversion, cloud and shadow masking, and topographic normalization. Snow covered pixels were retrieved using the normalized difference snow index (NDSI) and unsupervised classification, and pixels having greater (less) than 50% snow cover were classified presence (absence). A normalized SCA equation was derived to independently estimate SCA given missing image coverage and cloud-shadow contamination. Relative frequency maps of missing pixels were assembled to assess whether systematic biases were embedded within this Landsat CDR. Our results suggest that it is possible to confidently estimate historical bi-monthly SCA from partially cloudy Landsat images. This multitemporal method is intended to guide Landsat CDR development for freshwater-scarce regions of the western US to monitor climate-driven changes in mountain snowpack extent.

1. Introduction

Continental ice sheets, sea ice, permafrost, and hemispheric-scale seasonal snow cover play an important role in regulating Earth's radiation balance, and poleward-equatorial latent heat transport during hemispheric cool-seasons (Barry 2002). Equally important, mountain glaciers and seasonal snow cover (extent) in the form of mountain snowpack (depth) feed seasonal streamflow and replenish hydrological catchments (Barnett, Adam, and Lettenmaier 2005; Winther and Hall 1999). Across the arid western US, mountain ranges serve as seasonal water towers that hold and release snowpack freshwater resources through successive snow accumulation and melt. Snow-fed streamflow contributes approximately 50-70% to the total western US annual water budget (Cayan 1996). With an automated temporally discrete snow telemetry (SNOTEL) snow-water-equivalent (SWE) measurement network already in place for hydrological forecasting (Serreze et al. 1999), it is quite clear that spatially-explicit, satellite-derived climate data record (CDR) development can augment western US mountain snow cover area (SCA) monitoring on past, present, and future timescales.

Evidence is mounting for alarming declines in western US mountain snowpack as well as decreasing Northern Hemisphere spring snow cover extent (Hamlet et al. 2005; Mote et al. 2005; Pierce et al. 2008; Derksen and Brown 2012; Brown and Robinson 2011). Declining snowpack trends have been linked to warming springtime temperatures that trigger earlier and faster snowmelt (Cayan et al. 2001; Westerling et al. 2006). (Knowles, Dettinger, and Cayan 2006) find in their assessment of precipitation-snow ratios that snowpack in lower elevation zones are melting faster with temperature-driven

phase changes in water. Therefore, blending spatially derived snow cover CDRs, topographic models, SNOTEL SWE, and instrumental climate observations using time-series analysis techniques could advance efforts to examine historical trends in mountain snowpack extent, but has not been attempted because of lacking satellite CDR availability.

Over the past four decades, optical remote sensing has provided a critically important data source for observing Earth's changing cryosphere. Multispectral imagery acquired by Advanced Very-High Resolution Radiometer (AVHRR), Moderate Resolution Imaging Spectroradiometer (MODIS), Landsat multispectral scanner system (MSS), Landsat Thematic Mapper (TM), and Landsat Enhanced Thematic Mapper Plus (ETM+) platforms at different pixel resolutions enable snow cover retrieval over continental regions. Snow exhibits high-moderately high reflectances at visible wavelengths and low reflectances at near-infrared wavelengths (Warren 1982; Wiscombe and Warren 1980). These spectral characteristics allow for pixel level snow retrieval and classification at acceptable thematic and spatial accuracy (Dozier 1984; Dozier and Painter 2004; Hall and Martinec 1985). Specific advantages to monitoring snow cover using satellite platforms include daily-weekly image acquisitions, broad-scale spatial coverage over remote mountain and high latitude regions (Dozier 1989; Dozier and Painter 2004; Hall and Martinec 1985; Rosenthal and Dozier 1996), and most importantly, the Landsat mission provides a fairly continuous historical image record at recurrent intervals. This paper uses the entire Landsat image archive to map mountain SCA since the 1970s.

A multitemporal method is proposed to guide Landsat snow cover CDR development for freshwater-scarce regions of the western US. Historically, the cost of digital imagery hindered multitemporal mapping and use of partially cloudy images. With a now freely available image archive at the USGS EROS Data Center (http://eros.usgs.gov/) from Landsat's MSS, TM, and ETM+ mission, the opportunity to construct CDRs on climatically relevant timescales is now possible without the high cost. On the other hand, raw data availability first requires that sound methods for Landsat CDR development be outlined through a concept description and data demonstration. This initial step ensures that Landsat snow cover CDR products are spatially and temporally accurate, radiometrically consistent, and interoperable with MODIS snow products from the outset (Hall, Riggs, et al. 2002).

This paper introduces an operational multitemporal method to map SCA in mountainous terrain to support Landsat CDR development. A prototype Landsat snow cover CDR for peak snowmelt is demonstrated for an interior northwestern US sub-region, namely the central Idaho and southwestern Montana mountains. This continental sub-region was selected for its Pacific Ocean influenced climatology, intermountain hydrological basin significance, and high topographic relief within the broader northern Rocky Mountain region. This study region is also motivated by the need for more basic satellite research on continental snow cover patterns and processes in mountainous terrain. The paper is organized as follows. Section two outlines a multitemporal method for snow cover mapping in mountainous terrain using the Landsat image archive. This section describes how Landsat snow cover CDRs are derived using a normalized SCA

equation, and assesses whether the prototype Landsat CDR contains systematic biases that arise from missing imagery and/or cloud-shadow contamination. The Landsat snow cover CDR is then evaluated to determine whether scale parameterization influences the probability distribution and time domain variance of SCA. Sections three presents results obtained from the multitemporal method and prototype SCA time-series. Section four discusses current Landsat snow cover CDR development including efforts to monitor climate-driven changes in mountain snowpack extent.

2. Multitemporal Method for Landsat CDR Development

2.1 *Landsat Archival Imagery and Study Region Description*

Landsat World Reference System (WRS) -1 and WRS-2 path-row image acquisitions over the prototype study region depend on the sensor and year of acquisition (Table 1). For this June 1 snow cover CDR, Landsat MSS, TM, ETM+ SLC-on, and ETM+ SLC-off images were collected during the Julian dates 143 and 158 for 1973-2011. Scan line coverage (SLC) 'on' and 'off' images reflect time periods for 'pre' and 'post' sensor malfunctions on Landsat ETM+. Landsat ETM+ SLC-off images have stripes that contain missing pixels across the image. SLC-off pixels have no data and are considered missing coverage. All images were pre-processed, mosaicked, and classified for snow cover using the multitemporal method outlined below.

The Landsat snow cover CDR demonstrated is a prototype time-series of June 1 SCA for the central Idaho and southwestern Montana mountains (Figure 1). This June 1

Table 1. Archival Landsat imagery used for June 1 snow cover CDR development.

Landsat Sensor	Julian Bi-Monthly Interval	Time Period	Path-Rows	Images Used (n)
MSS 1-3	143-158	1973-1983	42-29, 43-29	5
MSS 4-5	143-158	1982-1995	39-29, 40-29	4
TM 4-5	143-158	1984-2011	39-29, 40-29	33
ETM+ 7 SLC-on	143-158	1999-2003	39-29, 40-29	4
ETM+ 7 SLC-off	143-158	2003-2011	39-29, 40-29	8

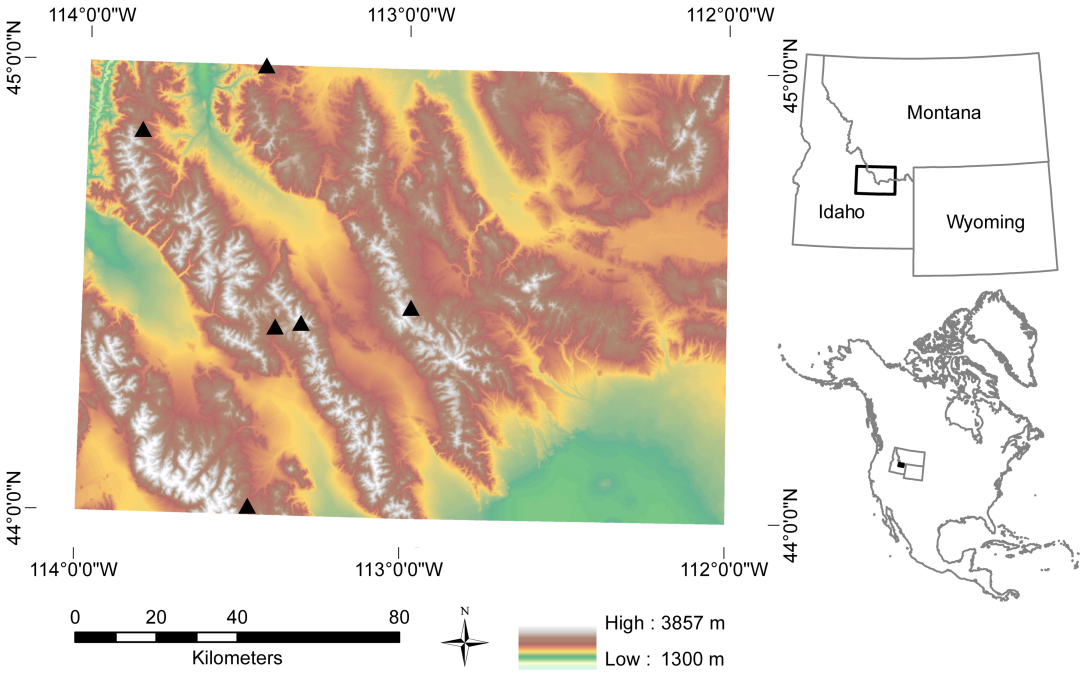

Figure 1. Central Idaho-southwestern Montana snow cover CDR region. The black triangles show SNOTEL SWE measurement sites used for bi-monthly snow cover CDR design.

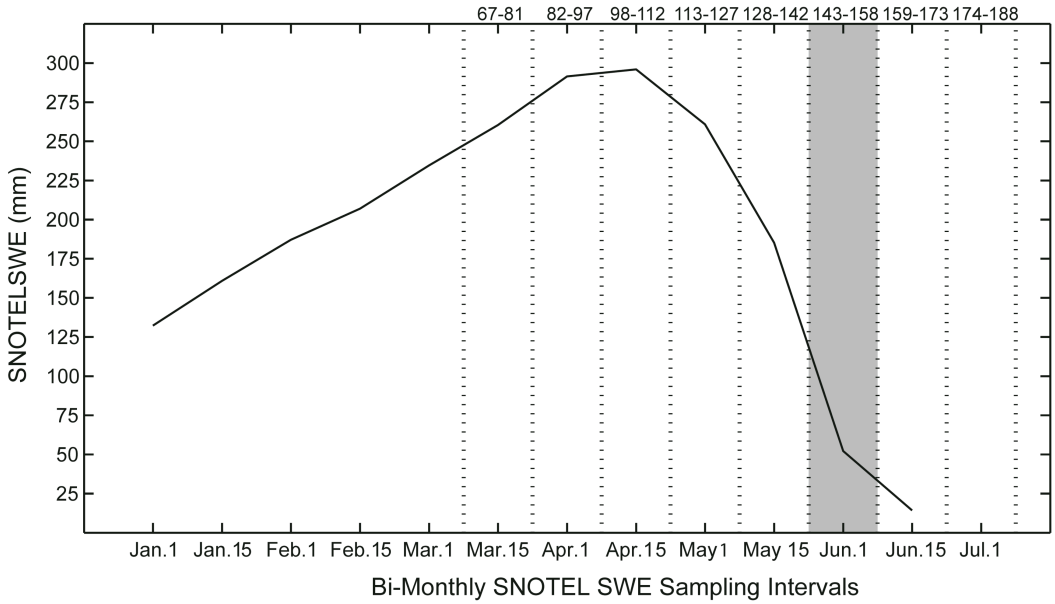

Figure 2. Bi-monthly Landsat snow cover CDR design. All available Landsat images from the entire image archive are assigned into discrete bi-monthly Julian sampling intervals. The thick black line represents a snowpack accumulation-melt curve based on observed mean bi-monthly SWE measurements for 1976-2010. Mean SWE estimates were derived from a regionalization of six SNOTEL sites across the study region (http://www.wcc.nrcs.usda.gov/snow). The gray shading indicates the June 1 Landsat snow cover CDR bi-monthly interval.

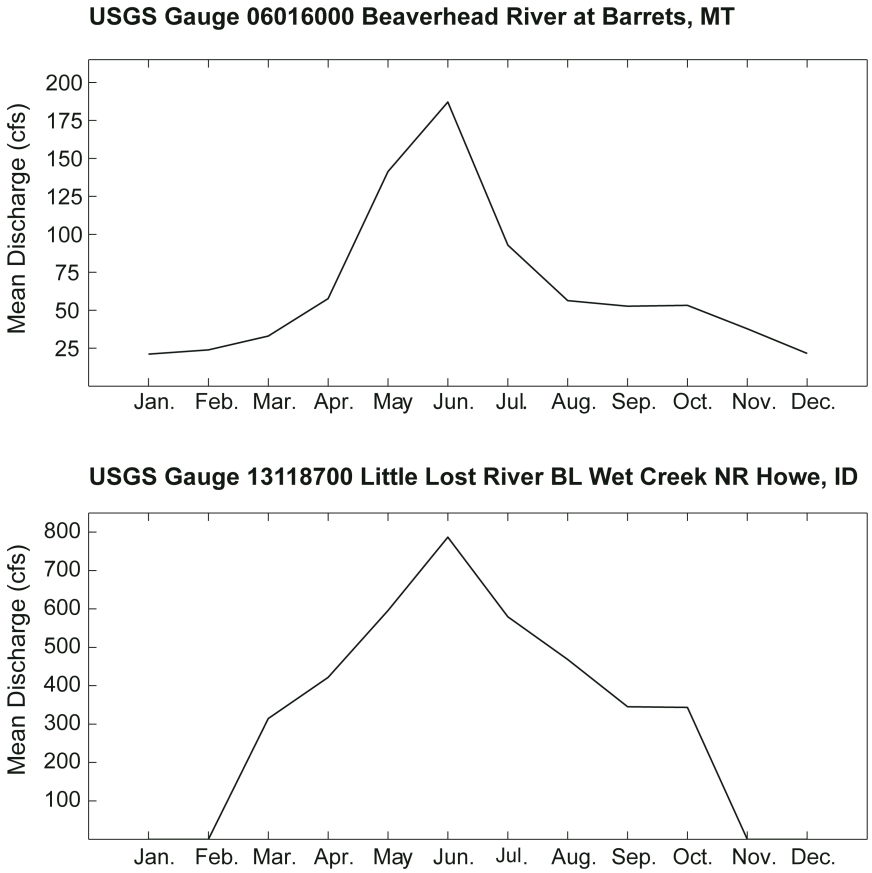

Figure 3. Gauged mean monthly discharge, cubic feet per second (cfs) for Little Lost and Beaverhead Rivers in central Idaho and southwestern Montana. Historical mean monthly discharge estimates for Little Lost (1958-2011) and Beaverhead (1908-2011) gauges were summarized for the period of record. Beaverhead discharge estimates for Nov.-Feb. were not available for the full period of record. Note: discharge estimates are provisional and subject to revision by the USGS.

CDR captures SCA variability during peak snowmelt for 1975-2011 (Figures 2 and 3). Much of the SCA on or near June 1 for this region is confined to mid-high elevations – low elevation zones have already melted out. The central Idaho and southwestern Montana mountains are situated within a continental semi-arid climate zone (Mitchell 1976) with both local and regional hydrological significance. These snow-fed rivers and tributaries form the headwaters of the Columbia and Missouri River basins and support potable water uses, hydropower generation, fisheries migration, agricultural irrigation, and recreation.

2.2 *Landsat Snow Cover CDR Design*

Seasonal mountain snowpack across the Idaho-Montana region begins to accumulate in mid-October and reaches maximum SWE around early-mid April (Cayan 1996). During the winter season (December-March), SCA in mountainous terrain more or less remains near maximum coverage at high elevations with lower elevations exhibiting daily-weekly variability due to short-term meteorological conditions. Once spring arrives, snow cover (snowpack) begins to successively melt with increasing solar irradiance, decreasing albedo, and warming springtime temperatures. Thus, variability in mountain SCA during snow accumulation and snowmelt periods has been, is, and will continue to be retrieved by each Landsat overpass.

Landsat snow cover CDR development is limited by the 16-18 day repeat schedule, which roughly corresponds to a bi-monthly interval. This temporal structure enables the potential to fully use all available Landsat images through compositing, especially in areas where image overlap allows 8-9 day coverage. Landsat snow cover

CDRs are based on SNOTEL SWE bi-monthly sampling intervals centered on days 1 and 15 of each calendar month (Serreze et al. 1999), where Landsat images on days 8 - 22 are assigned to the mid-month interval, and days 23 - 7 mark the end-beginning month interval (Figure 2). These discrete bi-monthly intervals allow for SCA to be mapped at seasonal, interannual, and decadal timescales across a defined spatial domain. This spatial domain involves a latitude-longitude grid that covers an explicit geographic area. This Landsat CDR grid design provides a workable geographic scale to manage data volume and overlapping images, preserve spectral properties, and facilitate statistical integration with gridded ground-based instrumental climate records.

2.3 *Image Registration*

Geo-referencing images to a target coordinate system requires either ground control points or ancillary spatial data such as a digital elevation model (DEM) to accurately assign pixels to an exact latitude-longitude position (Seidel, Ade, and Lichtenegger 1983). Most available Landsat images from the EROS Data Center have already been processed to a standard-level of geometric and terrain accuracy (http://landsat.usgs.gov/Landsat_Processing_Details.php). Geometric errors may exist with older MSS images. This requires careful treatment on an image basis when assembling multitemporal sequences.

For this multitemporal method, unregistered images are geo-referenced to a geometrically accurate image (i.e., preferably the same sensor with minimal cloud coverage) using an automatic tie-point algorithm. Automatic tie-points are selected by correlating the unregistered image with a geo-referenced image using a distributional grid

of stratified points with maximum correlation. An affine transformation is then applied to generate a Root Mean Squared Error (RSME) statistic. A RSME threshold of less than 0.5 (i.e., half the pixel resolution) is the geometric accuracy standard for Landsat snow cover CDRs.

2.4 *Radiometric Calibration*

Radiometric normalization across multiple sensors and different dates of imagery is required to preserve spectral-radiometric properties and temporal consistency between multitemporal image sequences (Chander, Markham, and Helder 2009; Chavez 1996; Song et al. 2001). For example, sensor radiometric differences exist between Landsat MSS, TM, and ETM+ platforms because spectral bandwidths have been placed at different wavelengths along the electromagnetic spectrum. This influences retrieval of pixel-level spectral radiance across a continuous spectrum. Furthermore, each image was acquired on different days where atmospheric conditions and illumination angles in mountainous terrain were variable between images (Meyer et al. 1993). Given these between sensor and multi-date differences, each image must be standardized by calibrating to an absolute radiometric scale.

Landsat imagery downloads from the EROS Data Center are delivered in a geotiff format that contains raw unprocessed digital numbers (DN values). Radiometric calibration first requires that DN values for each spectral band be converted to an at-sensor radiance value using Landsat sensor-specific calibration coefficients (Chander and Markham 2003). Calibration coefficients ensure that at-sensor radiance measurements acquired during the sensor's mission incorporate corrections for measurement changes,

mechanical malfunctions, and instrument deterioration (Chander, Markham, and Barsi 2007; Chander, Markham, and Helder 2009). Landsat images used for snow cover CDR development have been calibrated using the published calibration parameter files (http://landsat.usgs.gov/science_calibration.php).

The next step in radiometric calibration involves converting the at-sensor radiance to a planetary reflectance value. This at-sensor reflectances conversion can either be implemented for the top-of-the-atmosphere (TOA) or the surface (Chander, Markham, and Helder 2009; Vermote and Kotchenova 2008). Several atmospheric correction methods have been developed, and often include either a partial or full correction that relies on ancillary data inputs (Chander, Markham, and Helder 2009; Chavez 1996; Coppin and Bauer 1994; Song et al. 2001; Vermote and Kotchenova 2008; Vermote et al. 1997). These model inputs include spectral-band solar irradiance, earth-sun distance, sun elevation, optical thickness, and atmospheric aerosols, but even so, it remains unclear whether a full atmospheric correction actually produces superior results (Song et al. 2001). For Landsat snow cover CDRs, a TOA conversion following the methods in Chander et al. (2009) was applied using a cosine correction to account for diffuse irradiance. This TOA conversion was decidedly appropriate at a minimum for preserving radiometric consistency across multiple Landsat sensors.

2.5 *Cloud Masking*

Cloud cover contamination remains a significant challenge for optical remote sensing in planetary regions where climatological patterns produce transient, frequent, and persistent cloud cover. Since the Landsat image record contains partially cloudy

images, a robust cloud-masking algorithm to remove cloudy pixels is required. Several cloud-masking approaches have been developed for specific sensor-platforms (Ackerman et al. 1998; Hagolle et al. 2010; Huang et al. 2010; Irish et al. 2006) that use multispectral band criteria to examine reflectance change and the thermal band to further separate cloudy pixels from non-cloudy pixels. Landsat specific algorithms include the automated cloud cover assessment (ACCA) algorithm developed by Irish et al. (2006) to estimate cloud cover content on Landsat ETM+ images. More recently, Huang et al. (2010) developed a Landsat cloud algorithm that uses a DEM, the thermal band, and cloud-free confident forest pixels to identify cloudy pixels. Most studies agree that including the thermal band improves algorithm performance (Hagolle et al. 2010; Huang et al. 2010; Irish et al. 2006).

Although the ACCA is computationally complex and process intensive by design, this algorithm is able to separate pixels containing snow from pixels containing clouds, and distinguish warm clouds from cold clouds using spectral signatures and thermal band cloud population statistics. The ACCA takes advantage of TM and ETM+ bands 2-6 by engaging a four-step process that first develops spectral and thermal band cloud signatures, performs thermal band cloud separation, assigns and aggregates cloudy pixels, and fills cloud holes (Irish et al., 2006). Lacking middle infrared and thermal spectral bands on MSS limits automatic detection of clouds, shadows, and discrimination between snow and clouds. Clouds and shadows were subjectively removed by visually identifying neighborhoods of dark pixels (i.e., shadows) that were adjacent to brightly illuminated pixels (i.e., clouds).

2.6 *Shadow Masking*

Cloud shadows are an inevitable outcome of cloud cover contamination. The spectral characteristics of cloud shadow pixels are largely absorptive with dark low reflectance responses across visible, near and middle infrared wavelengths. The aerial extent of cloud shadow contamination is contingent on time of year, time of acquisition, latitudinal position, topographic relief, cloud area, cloud height, and solar illumination. Because cloud shadows share a similar spectral response with water and heavily shaded mountainous slopes, simple spectral reflectance thresholding is not adequate for shadow detection. Hutchison et al. (2009) and Huang et al. (2010) have developed a cloud shadow detection method that includes cloud pixel location, cloud pixel height, and solar geometry inputs to project shadow pixel location. Once shadow pixel locations have been approximated, a moving window is engaged to guide the search for shadow pixels exhibiting distinct spectral reflectances (Hutchison et al. 2009).

Applying the solar geometry cloud shadow detection method first requires a cloud mask. Next, a cloud height estimate is computed for each cloudy pixel using both daily surface air temperature (i.e., image acquisition date) and Landsat band-6 pixel temperature. Daily mean surface air temperature observations used for cloud height estimation originate from the NCEP 10-meter reanalysis network (Kalnay et al. 1996; Masek et al. 2006). For cloudy pixels, normalized temperature anomalies are calculated by subtracting band-6 temperatures from the surface air temperature. Using the normal lapse rate conversion of 6.4 degrees Celsius decrease for every 1000-meter vertical increase, cloud heights for each pixel can be approximated (Huang et al. 2010). Below

the standard pressure level of 700 hpa, temperature change does not always obey the normal lapse rate (Minder, Mote, and Lundquist 2010). In these instances, approximated cloud heights may be substantially over or underestimated. Also, actual shadow locations are cast from cloud bottoms rather than cloud tops; therefore, thermal band optical depth may contribute additional uncertainty to cloud height estimates. To reduce uncertainty, a range of cloud-shadow projections for each pixel is generated using a scale factor (i.e., cloud height multiplied by 1.5 or 2 for example) in the denominator of the cloud-shadow projection equation (Hutchison et al. 2009; Masek et al. 2006). The final step involves using a moving window with a local neighborhood operation to find pixels that show a shadow spectral response. A 20 by 20 pixel window (Hutchison et al. 2009) is used to search for projected shadow pixels with a spectral reflectance of < 0.10 for the near infrared (band-4) and < 0.10 for the middle infrared (band-5) wavelengths. If a pixel satisfies this threshold criterion, it is flagged as a shadow (Huang et al. 2010).

2.7 *Topographic Normalization*

Land surface radiance represents a combined response to direct and diffuse solar irradiance that reflects the sun's illumination angle and local topographic angle during time of overpass (Dozier and Frew 1990; Lu et al. 2008; Meyer et al. 1993; Smith, Lin, and Ranson 1980; Teillet, Guindon, and Goodenough 1982). This spectral response is wavelength and land cover dependent (Meyer et al. 1993), and in mountainous terrain, these effects are especially pronounced because of steep slopes and directly opposing aspects. As a result, images with mountainous terrain need to be normalized for both the sun's zenith angle and local illumination angle. Telliet et al. (1982) and others suggest

that applying this correction is particularly important for multitemporal image analysis, and for improving classification accuracy.

Several quantitative methods for reducing topographic effects have been proposed that require empirical or semi-empirical correction parameters (Meyer et al., 1993). A key parameter of any correction method is whether Lambertian flat surface scattering is assumed. Smith et al. (1980) found that for Landsat MSS data, a Lambertian assumption was generally correct only for slopes below 25 degrees and sun zenith angles less than 45 degrees. As an alternative, Minneart's correction is generally a preferred method, and requires a derivation of an image specific *k* value that measures the degree to which a surface is Lambertian. Landsat CDRs include an image-based Minneart correction to reduce topographic effects. Using a 10-meter USGS DEM and sun elevation and azimuth parameters contained within the image metadata, illumination layers are generated following the equations found in Meyer et al. (1993). The local illumination DEM layer is then resampled to 30-meter pixels using a nearest neighbor calculation. A stratified random sample from slopes greater than 20 degrees are then collected from the local illumination layer and the Landsat illumination image to derive *k*. Both populations are log transformed, and using linear regression, the slope of the regression line (*k* value) is computed for TM and ETM+ spectral bands 1-5 and 7, and MSS spectral bands 4-7. Finally, Minneart's correction is applied back to each spectral band using wavelength specific *k* values.

2.8 *Image Mosaicking*

When mapping regions where multiple Landsat images cover a target spatial domain, mosaicking is required to obtain a composite image. The main objectives for mosaicking are to maximize cloud-free coverage, piece together images from multiple sensors having different image properties, and ensure that original spectral-radiometric properties have not been compromised. Landsat CDRs hierarchically select images having the lowest cloud cover content to serve as the target image. Image mosaicking is then executed using a simple computational overlap function.

Landsat's 16-18 day image acquisition frequency does limit snow cover mapping. In some instances, Landsat's coverage may not be able to resolve the difference between resident snow cover and transient snowfall (Li et al. 2008). This would result in a tendency to inflate SCA, but even so, individual SCA anomaly years could be identified using statistical tests and ancillary information from SNOTEL SWE, daily MODIS SCA maps, and/or preceding bi-monthly Landsat snow cover CDRs. Mosaicking Landsat images from different acquisition dates, sometimes even five to seven days, does present a caveat for snow cover mapping.

2.9 *Snow Cover Classification*

Snow is highly reflective at visible wavelengths, and is clearly distinguishable from other land surface features (Hall and Martinec 1985; Seidel and Martinec 2004). Clouds are also highly reflective, but diverge with snow at middle infrared wavelengths. While middle infrared cloud reflectances remain high, reflectances for snow are absorptive (Dozier 1989; Hall, Riggs, and Salomonson 1995). Spectral bands at visible and middle infrared wavelengths allow for spectral discrimination between snow and

clouds (Dozier and Painter 2004; Hall, Riggs, and Salomonson 1995). Classifying snow cover in multispectral imagery is accomplished using either a binary (Seidel and Martinec 2004) or fractional method (Rosenthal and Dozier 1996; Salomonson and Appel 2004). These two approaches stem from the normalized difference snow index (NDSI), a spectral band ratio, or subpixel unmixing, a simultaneous linear equation that separates vegetation, soils, and lithology endmembers from snow. Both methods have been shown to yield acceptable snow cover classification accuracy (Hall et al. 2001; Hall et al. 1998; Hall, Kelly, et al. 2002; Hall and Riggs 2007; Hall, Riggs, and Salomonson 1995; Hall et al. 2000; Rittger, Painter, and Dozier 2012; Salomonson and Appel 2004). The NDSI uses TM and ETM+ bands 2 and 5, and MODIS bands 4 and 6 (Hall and Riggs 2011). Pixels with snow cover greater than 50% have been found to have a NDSI value greater than 0.4 (Hall, Riggs, and Salomonson 1995; Hall and Riggs 2011). Snow beneath dense forests can degrade the NDSI response (Klein, Hall, and Riggs 1998). They suggest including a normalized difference vegetation index (NDVI) threshold in conjunction with NDSI to improve snow cover detection because the spectral response of vegetation with snow has low NDVI values.

2.9.1 *TM and ETM+*

Landsat snow cover CDRs from TM and ETM+ use NDSI to retrieve and binary classify pixel level snow presence (absence) greater (less) than 50% snow cover. This threshold-based snow classification scheme for Landsat mimics the MODIS method (Riggs, Hall, and Salomonson 2006). Landsat pixels are classified as snow if NDSI is greater than 0.4, band 2 is greater than 0.11, and band 4 is greater than 0.10. The band 2

threshold aids in the discrimination between snow and water, and the band 4 threshold prevents dark targets as being erroneously identified as snow (Riggs, Hall, and Salomonson 2006). At this time, the NDVI threshold (Klein, Hall, and Riggs 1998) has been excluded because of Landsat's fine spatial resolution, and uncertainty whether this response inflates the snow signal during the spring melt season. Excluding this criterion from the Landsat NDSI classification scheme possibly reduces SCA in dense forest and around the snow-covered to snow-free transition zone.

2.9.2 *MSS*

MSS snow-cloud separation is not possible using an automated approach. As stated earlier, cloud cover was visually identified using shadow detection as a guiding criterion, and then cloud and shadow pixels were manually removed. Because clouds and shadows have been removed during MSS image-processing, highly reflective pixels indicate snow cover presence. Using an ISO data-clustering algorithm on MSS bands, 30 individual classes are initially identified using spectral band means and standard deviations. Each class is then interpreted to be snow or snow-free. Only cluster classes showing a clear homogenous snow cover response are selected for classification. Pixels having a mixed snow cover signal are difficult to identify because of the mixed spectral responses from snow-free surfaces (Rosenthal and Dozier 1996; Dozier and Painter 2004).

2.10 *Landsat SCA Estimation*

Landsat snow cover CDRs are constructed on bi-monthly timescales to estimate SCA from multispectral measurements over a spatially explicit domain. Every useable

Landsat image from the archive is pre-processed, classified for snow cover, and input into a Landsat image chronology. An inevitable component of CDR construction is that visible Landsat image coverage will vary over time. For a given spatial domain, total land surface area (m^2) is calculated using a 10-m USGS DEM. This area calculation is the total amount of land surface area that snow can cover at any time including inland water bodies. This rationale forms the basis for a normalized SCA estimate that is independent from image coverage. Landsat SCA percent coverage for each annual bi-monthly interval is estimated using the following equation:

$$\text{Normalized SCA} = [\text{visible SCA } (m^2) / (\text{land surface area } (m^2) - (\text{missing visible coverage } (m^2) + \text{cloud-shadow contamination } (m^2)))]$$

This ratio assumes no change in land surface area, only a change in visible coverage and SCA. An estimate of visible coverage also accompanies Landsat snow cover CDRs. Normalized SCA estimates can be derived from four possible image combinations: cloud-free, partially cloudy, partially cloudy with SLC-off, and partially cloudy with missing coverage (Figure 4).

2.11 *Landsat CDR Homogeneity*

Ground-based, upper air, and satellite CDR homogeneity has and remains a long-standing data development, production, and distribution objective (Peterson et al. 1998). This quality control process is particularly important for historical records, and ensures that climate data users can access, analyze, and interpret specific datasets without concern that 'non-climatic' factors such as technological change, instrumentation location change, or measurement protocol have influenced the observations in time (Peterson et al. 1998). For historical satellite retrievals, these 'non-climatic' factors can largely be addressed

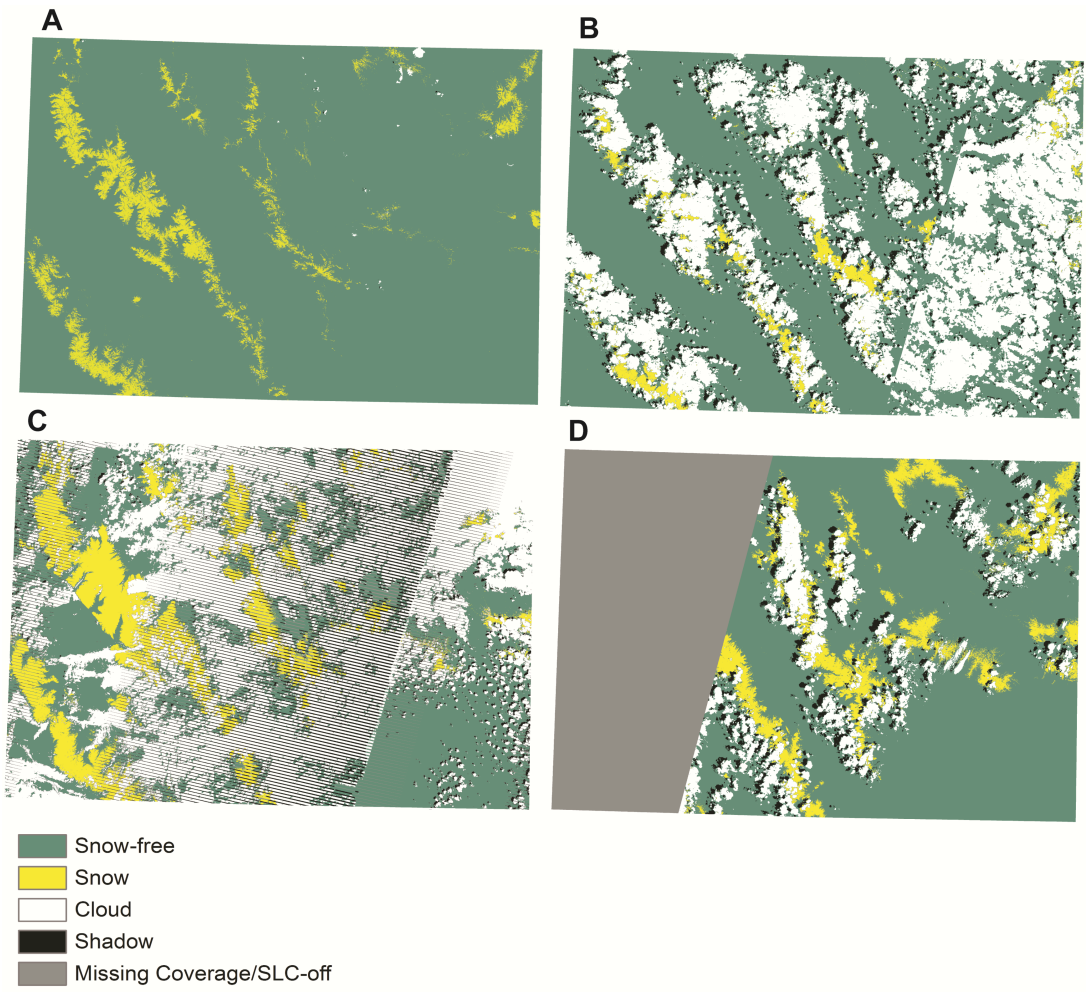

Figure 4. Possible Landsat image combinations for normalized SCA estimation: A) cloud-free SCA map; B) partially cloudy SCA map; C) partially cloudy SCA map with SLC-off; and D) partially cloudy SCA map with missing coverage.

during image pre-processing, but for Landsat snow cover CDRs, additional quality assurance steps are required to account for missing image coverage and cloud-shadow contamination when estimating normalized SCA.

If systematic biases are embedded within Landsat snow cover CDRs, they will originate from either missing image coverage, clouds, shadows, or forest canopy effects (Kane et al. 2008). A primary concern for Landsat snow cover mapping, especially historical imagery, is that the accumulated and combined effects of image acquisition frequency, visible coverage, and cloud-shadow contamination will introduce uncontrollable 'non-climatic factors' into SCA estimation. Even though snow cover distribution and scaling across mountainous terrain has been shown to be possible (Seidel and Martinec 2004), identifying spatially where potential error could emerge is necessary for assessing Landsat CDR quality and homogeneity in time.

Pixel level relative frequency maps of missing image coverage were assembled using no coverage, cloud, and shadow masks derived during image processing. MSS and TM/ETM+ frequency maps were assembled separately because of differing pixel resolution and methods for constructing cloud and shadow masks. Relative frequency maps for MSS and TM/ETM+ visible and non-visible (i.e., combined missing coverage, clouds, and shadows) pixels were tallied across the Landsat CDR.

2.12 *Landsat CDR Statistical Quality*

Time-series data usually originate from equally spaced continuous observations in time (i.e., Landsat images), and are derived based on discretely measured values (i.e., SCA) at specific time periods (Chatfield 2004). Time-series theory requires that a non-

stationary stochastic process with periodic and/or seasonal variations are transformed into a stationary process, in this case Landsat SCA, where there is no systematic change in the mean or variance over time (Chatfield 2004). Landsat snow cover CDRs are designed to capture bi-monthly SCA with the motivation to statistically merge SCA with other related climatic time-series such as SWE, temperature, and precipitation. Before doing so, it is important to evaluate whether the proposed normalized SCA equation produces a scale independent, normal SCA probability distribution that is stationary in time.

To quantify that SCA is scale independent in horizontal and vertical domains, two separate snow cover CDRs have been derived using elevation as a standardized control. The first June 1 SCA CDR has been constructed for the full spatial domain, and the second has been constructed for the alpine domain above 2500 meters. Lilliefor's test for normality is used to determine whether SCA has a normal or non-normal statistical distribution with an unspecified mean and variance (Conover 1980). Student's t-test for correlated samples, and simple correlation is used to test whether SCA mean and variance is statistically different, and shares statistically significant covariance if constrained by scale parameters.

3. Results

June 1 SCA estimates were produced for 30 of the 39 possible years. The June 1 SCA CDR for central Idaho and southwestern Montana spans 1975-2011 with missing years in 1973, 1974, 1978-1982, 1987, and 1988 because of either missing coverage or cloud-shadow contamination (Figure 5). Pixel level relative frequency maps show that if SCA estimation is biased, it is more influenced by missing image coverage than cloud-

shadow contamination (Figure 6). Each TM/ETM+ (Figure 6a) and MSS (Figure 6b) frequency map reveals areas across the full spatial domain having missing coverage that closely resemble adjacent Landsat path-row swath coverage. In the MSS map, scanline striping and manually edited cloud-shadow cover polygons are evident.

Lilliefor's test for normality confirmed that June 1 SCA estimates are non-normal even with a sample size of 30 years (Table 2). It is important to note that June 1 SCA estimates for 1990 and 2002 have been identified as statistical outliers, and may be influenced by transient snowfall at higher elevations during the melt season. Student's t-test for correlated samples between separately derived full and alpine domain (i.e., above 2500 meters) June 1 SCA CDRs indicates a statistical difference between the mean and variance (Table 3). The correlation coefficient between June 1 SCA CDRs is 0.97 ($p<0.001$, two-tailed).

4. Discussion

The Landsat mission and its moderate spatial resolution, unequaled image record length, and acquisition schedule can supplement operational SCA mapping on bi-monthly to decadal timescales. Bi-monthly snow cover CDR design and development is based on using multispectral images from multiple sensors to retrieve SCA during bi-monthly SNOTEL SWE measurement intervals collected across the western US. However, this multitemporal snow cover mapping method does have inherent limitations that need to be fully acknowledged from the outset. Primary limiting factors include data gaps in historical coverage, image acquisition frequency, and the potential for transient snowfall during snow accumulation and snowmelt seasons. Secondary limitations originate from

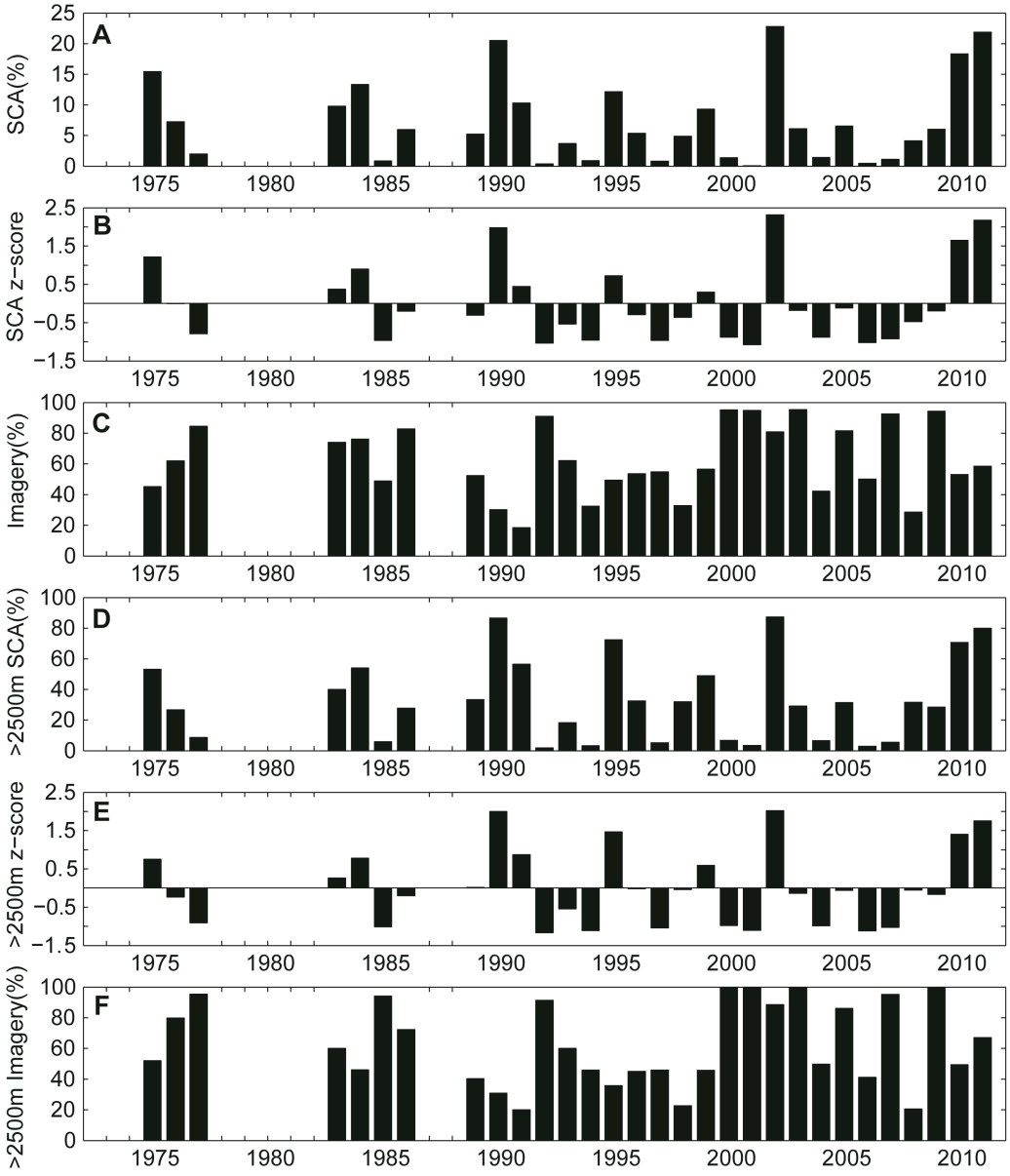

Figure 5. Landsat June 1 snow cover CDR: a) June 1 SCA estimates for the full spatial domain; b) full spatial domain standard normal SCA estimates using the 30-year SCA mean and standard deviation; c) percent visible image coverage for each full domain SCA estimate; d) June 1 SCA estimates for the alpine domain above 2500 meters; e) alpine domain standard normal SCA estimates using the 30-year SCA mean and standard deviation; and f) percentage of visible image coverage for each alpine domain SCA estimate. Years 1973, 1974, 1978-1982, 1987, and 1988 are missing SCA estimates and are marked with line ticks.

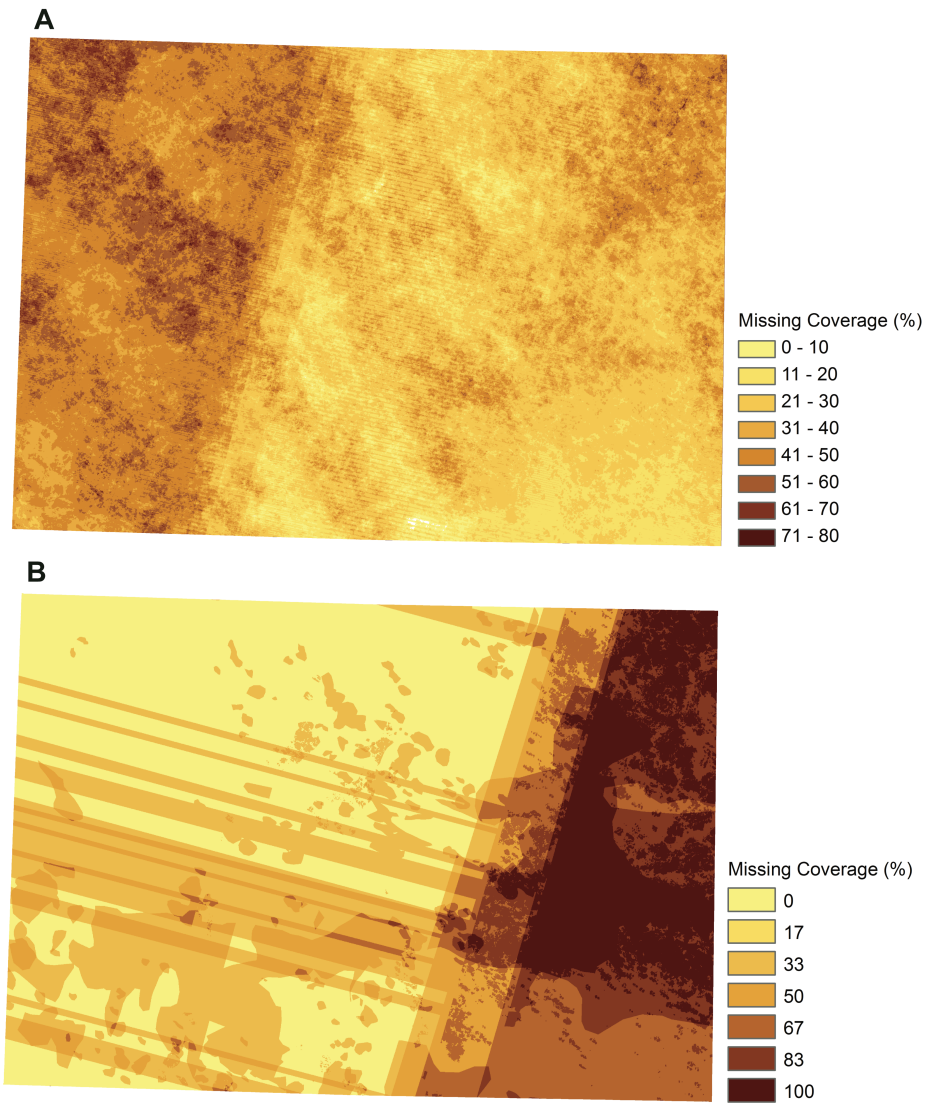

Figure 6. Pixel level relative frequency maps of missing image coverage including cloud and shadow contamination: a) TM/ETM+ missing coverage for 24 years between 1985 and 2011; and b) MSS missing coverage for six years between 1973 and 1992.

Table 2. Lilliefor's normality test for June 1 SCA estimates.

Landsat CDR	Record Length*	Samples (n)	Lilliefor's	Critical-value	p-value	**Decision**
June l SCA – Full Domain	1975-2011	30	0.176	0.158	0.017	Reject
June 1 SCA – Alpine	1975-2011	30	0.160	0.158	0.044	Reject

Decision: The null hypothesis is that SCA estimates come from a normal distribution with an unspecified mean and variance.
Record length*: SCA estimates are not available for all years because of missing imagery or cloud-shadow contamination.

Table 3. Student's two-sample t-test between June 1 SCA estimates.

	Full Domain SCA	Alpine Domain SCA	Total
n	30	30	60
$\sum x$	2.182	9.902	12.084
$\sum x^2$	0.293	5.357	5.650
SS	0.134	2.088	3.216
mean	0.072	0.330	0.201
Full SCA mean - Alpine SCA mean		t	df
-0.257		-6.93*	29

two-tailed significance: $p<0.001$*

differences between sensor-specific spectral and spatial resolutions, as well as frequent cloud cover contamination over mountainous terrain. For MSS images, manual removal of clouds and shadows presents a considerable challenge for operational snow cover mapping at the global scale, although regional mapping efforts may be more feasible. While these limitations do present considerable roadblocks when processing Landsat images for SCA estimation, taking advantage of additional image data from MODIS for example, and/or SNOTEL SWE, may offer viable options for filling in temporal data gaps, identifying transient snow cover anomalies, and increasing cloud-free coverage.

Radiometric calibration across the Landsat missions is a critical requirement for CDR development. Feng et al. (2012) have developed the Landsat-MODIS Consistency Checking System, and present a framework for operational Landsat surface reflectance production. In terms of this multitemporal method, a full atmospheric correction to surface reflectance is not attempted at this time because of operational and computational constraints locally. Instead, a TOA correction is applied that currently excludes optical thickness, atmospheric aerosols, and water vapor corrections common to MODIS products (Vermote and Kotchenova 2008). Moving beyond current constraints into operational Landsat CDR production would likely yield a 'more correct image product' as the benchmark, but regardless, re-processing of image archives can be expected in the future given advancements in algorithm development and computing (Dozier and Frew 2009). At this time, the above TOA method at a minimum provides temporal and radiometric consistency between Landsat sensors and image inputs into Landsat snow

cover CDRs. The prototype Landsat snow cover CDR presented should be accepted as an initial product, but not final in form.

Landsat normalized SCA estimation is based on the assumption that land surface area over a geographically explicit spatial domain constrains and normalizes SCA variance over discrete bi-monthly intervals. The normalized SCA equation proposed also assumes that reliable SCA estimates can be derived independently from the variation in visible image coverage. Cloud-free coverage is not a realistic expectation for Landsat's image archive, image acquisition frequency, or imagery over mountainous terrain. If Landsat's historical image archive is to be used comprehensively in innovative ways, accepting that target land surface variables, in this case mountain SCA, can be derived from partially cloudy images is essential. Currently, Landsat snow cover CDRs exclude SCA underneath clouds although spatial modeling methods for snow cover extrapolation are available using ancillary data, and have shown acceptable performance for images with up to 30% cloud cover obstruction (Seidel and Martinec 2004). Once Landsat snow cover CDRs have been developed for multiple bi-monthly intervals, it may be possible to explore whether implementation of a SCA extrapolation model is operationally feasible, and substantially improves SCA estimation.

The pixel level 'salt and pepper' effect on each frequency map suggests that over time, cloud-shadow contamination is spatially random with greater likelihood of non-randomness directly over mountain peaks. Systematic missing image coverage is largely an artifact of missing Landsat path-row images on historical timescales. More broadly conceived, when missing image coverage is concentrated over specific mountain ranges,

then SCA estimation may have greater uncertainty; however, if missing image coverage is concentrated over lower elevation snow-free land, then SCA estimation may by less influenced by missing image coverage. At this time, Landsat snow cover CDR design and development appears to have few systematic biases other than data driven constraints such as missing imagery. Landsat CDR homogeneity and quality control should remain a high research priority because achieving temporal consistency and spatial accuracy is critical for climate-based study in mountainous terrain.

Landsat snow cover CDRs form the basis for monitoring spatiotemporal variability in mountain SCA, and identifying primary climatic controls on mountain snowpack extent. The SNOTEL network is able to resolve SWE variability at discrete locations, which could be helpful for distinguishing between temporal variability in SWE and SCA. One primary statistical challenge that accompanies Landsat snow cover CDR evaluation is obtaining enough SCA estimates over time to satisfy the assumptions of normality and parametric statistical modeling and inference. It is well known that instrumental ground-based precipitation observations have non-normal distributions largely attributed to spatial variability in precipitation (Jones and Hulme 1996). Landsat SCA estimates are likely to also be non-normal similar to precipitation. This may limit identification of a known SCA mean and standard deviation with the current record. Achieving normality for Landsat CDRs will only come from first, adding more temporal SCA estimates to the probability distribution over longer-timescales, and second, correcting for transient snowfall in SCA estimation.

A comparison between full and alpine domain SCA CDRs suggests that normalized SCA estimates are stationary, but are statistically non-normal. SCA CDRs do show statistically significant covariance in time even though scale parameterization influences the mean and variance. Increasing the spatial extent of the June 1 snow cover CDR to include adjacent regions would likely increase the ability to estimate SCA more continuously during the 1970s and 1980s. The development of longer Landsat snow cover CDRs on past and future timescales will offer greater certainty when determining temporally significant SCA trends.

Multitemporal snow cover mapping in mountainous terrain is now possible dating back to 1973 using Landsat. Snow cover CDR development provides a historical starting point for monitoring fine scale variability in mountain SCA at bi-monthly timescales and beyond. Missing historical Landsat coverage is inherent to the image record, and should be considered a data-driven factor, not a data source limitation. This multitemporal method is operationally executable and grounded in well-validated algorithm selection and performance. Refinements to this multitemporal method should be expected in the future given algorithm advancement, greater computing capacity, additional imagery acquired during the Landsat Data Continuity Mission (LDCM), and the potential for multi-sensor integration between MODIS and Visible Infrared Imaging Radiometer Suite (VIIRS).

Using Landsat to monitor historical changes and trends in mountain snowpack extent through snow cover CDRs is innovative, warranted, and can support climate variability and change study, hydroclimatological modeling and prediction, and

freshwater resource projections under climatic warming. Future work will merge Landsat snow cover CDRs with SNOTEL SWE and surface temperature and precipitation observations to not only identify the temporal climatic controls on mountain SCA, but also enable long-term verses short-term trend detection over the 20th and 21st centuries. This multitemporal method is widely applicable to all mountainous regions where snow cover accumulates and melts annually, and Landsat imagery is available. The proposed method is intended to guide Landsat snow cover CDR development across the western US.

References

Ackerman, S. A., K. I. Strabala, W. P. Menzel, R. A. Frey, C. C. Moeller, and L. E. Gumley. 1998. "Discriminating clear sky from clouds with MODIS." *Journal of Geophysical Research-Atmospheres* no. 103 (D24):32141-32157. doi: 10.1029/1998jd200032.

Barnett, T. P., J. C. Adam, and D. P. Lettenmaier. 2005. "Potential impacts of a warming climate on water availability in snow-dominated regions." *Nature* no. 438 (7066):303-309. doi: 10.1038/nature04141.

Barry, Roger G. 2002. "The role of snow and ice in the global climate system: A review." *Polar Geography* no. 26 (3):235 - 246.

Brown, R. D., and D. A. Robinson. 2011. "Northern Hemisphere spring snow cover variablity and change over 1922-2010 including an assessment of uncertainty." *The Cryosphere* no. 5 (1):219-229. doi: 10.5194/tc-5-219-2011.

Cayan, D. R. 1996. "Interannual climate variability and snowpack in the western United States." *Journal of Climate* no. 9 (5):928-948.

Cayan, D. R., S. A. Kammerdiener, M. D. Dettinger, J. M. Caprio, and D. H. Peterson. 2001. "Changes in the onset of spring in the western United States." *Bulletin of the American Meteorological Society* no. 82 (3):399-415.

Chander, G., and B. Markham. 2003. "Revised Landsat-5 TM radiometric calibration procedures and postcalibration dynamic ranges." *IEEE Transactions on Geoscience and Remote Sensing* no. 41 (11):2674-2677. doi: 10.1109/tgrs.2003.818464.

Chander, G., B. L. Markham, and J. A. Barsi. 2007. "Revised Landsat-5 thematic mapper radiometric calibration." *IEEE Geoscience and Remote Sensing Letters* no. 4 (3):490-494. doi: 10.1109/lgrs.2007.898285.

Chander, G., B. L. Markham, and D. L. Helder. 2009. "Summary of current radiometric calibration coefficients for Landsat MSS, TM, ETM+, and EO-1 ALI sensors." *Remote Sensing of Environment* no. 113 (5):893-903. doi: 10.1016/j.rse.2009.01.007.

Chatfield, C. 2004. *The Analysis of Time Series, an Introduction*. six ed. New York: Chapman and Hall/CRC.

Chavez, P. S. 1996. "Image-based atmospheric corrections revisited and improved." *Photogrammetric Engineering and Remote Sensing* no. 62 (9):1025-1036.

Conover, W. 1980. *Practical nonparameteric statistics*. 2nd ed. New York: John Wiley and Sons.

Coppin, P. R., and M. E. Bauer. 1994. "Processing of multitemporal Landsat TM imagery to optimize extraction of forest cover change features." *IEEE Transactions on Geoscience and Remote Sensing* no. 32 (4):918-927. doi: 10.1109/36.298020.

Derksen, C., and R. Brown. 2012. "Spring snow cover extent reductions in the 2008-2012 period exceeding climate model projections." *Geophysical Research Letters* no. 39. doi: 10.1029/2012GL053387.

Dozier, J. 1984. "Snow reflectance from Landsat-4 Thematic Mapper " *IEEE Transactions on Geoscience and Remote Sensing* no. 22 (3):323-328.

———. 1989. "Spectral signature of alpine snow cover from the Landsat Thematic Mapper." *Remote Sensing of Environment* no. 28:9-22.

Dozier, J., and J. Frew. 1990. "Rapid calculation of terrain parameters for radiation modeling from digital elevation data." *IEEE Transactions on Geoscience and Remote Sensing* no. 28 (5):963-969.

———. 2009. "Computational provenance in hydrologic science: a snow mapping example." *Philosophical Transactions of the Royal Society a-Mathematical Physical and Engineering Sciences* no. 367 (1890):1021-1033. doi: 10.1098/rsta.2008.0187.

Dozier, J., and T. H. Painter. 2004. "Multispectral and hyperspectral remote sensing of alpine snow properties." *Annual Review of Earth and Planetary Sciences* no. 32:465-494. doi: 10.1146/annurev.earth.32.101802.120404.

Hagolle, O., M. Huc, D. V. Pascual, and G. Dedieu. 2010. "A multi-temporal method for cloud detection, applied to FORMOSAT-2, VEN mu S, LANDSAT and SENTINEL-2 images." *Remote Sensing of Environment* no. 114 (8):1747-1755. doi: 10.1016/j.rse.2010.03.002.

Hall, D. K., J. L. Foster, V. V. Salomonson, A. G. Klein, and J. Y. L. Chien. 2001. "Development of a technique to assess snow-cover mapping errors from space." *IEEE Transactions on Geoscience and Remote Sensing* no. 39 (2):432-438.

Hall, D. K., J. L. Foster, D. L. Verbyla, A. G. Klein, and C. S. Benson. 1998. "Assessment of snow-cover mapping accuracy in a variety of vegetation-cover densities in central Alaska." *Remote Sensing of Environment* no. 66 (2):129-137. doi: 10.1016/s0034-4257(98)00051-0.

Hall, D. K., R. E. J. Kelly, G. A. Riggs, A. T. C. Chang, and J. L. Foster. 2002. "Assessment of the relative accuracy of hemispheric-scale snow-cover maps." In *Annals of Glaciology, Vol 34, 2002*, edited by J. G. Winther and R. Solberg, 24-30. Cambridge: Int Glaciological Soc.

Hall, D. K., and J. Martinec. 1985. *Remote Sensing of Ice and Snow*. New York: Chapman and Hall.

Hall, D. K., and G. A. Riggs. 2007. "Accuracy assessment of the MODIS snow products." *Hydrological Processes* no. 21 (12):1534-1547. doi: 10.1002/hyp.6715.

———. 2011. Normalized-Difference Snow Index (NDSI), Encylopedia of Earth Sciences Series. In *Encylopedia of snow, ice and glaciers*, edited by V. P. Singh, P. Singh and U. K. Haritashya: Springer.

Hall, D. K., G. A. Riggs, and V. V. Salomonson. 1995. "Development of methods for mapping global snow cover using moderate resolution imaging spectroradiometer data." *Remote Sensing of Environment* no. 54 (2):127-140. doi: 10.1016/0034-4257(95)00137-p.

Hall, D. K., G. A. Riggs, V. V. Salomonson, N. E. DiGirolamo, and K. J. Bayr. 2002. "MODIS snow-cover products." *Remote Sensing of Environment* no. 83 (1-2):181-194.

Hall, D. K., A. B. Tait, J. L. Foster, A. T. C. Chang, and M. Allen. 2000. "Intercomparison of satellite-derived snow-cover maps." In *Annals of Glaciology, Vol 31, 2000*, edited by K. Steffen, 369-376. Cambridge: Int Glaciological Soc.

Hamlet, A. F., P. W. Mote, M. P. Clark, and D. P. Lettenmaier. 2005. "Effects of temperature and precipitation variability on snowpack trends in the western United States." *Journal of Climate* no. 18 (21):4545-4561.

Huang, C. Q., N. Thomas, S. N. Goward, J. G. Masek, Z. L. Zhu, J. R. G. Townshend, and J. E. Vogelmann. 2010. "Automated masking of cloud and cloud shadow for forest change analysis using Landsat images." *International Journal of Remote Sensing* no. 31 (20):5449-5464. doi: 10.1080/01431160903369642.

Hutchison, K. D., R. L. Mahoney, E. F. Vermote, T. J. Kopp, J. M. Jackson, A. Sei, and B. D. Iisager. 2009. "A Geometry-Based Approach to Identifying Cloud Shadows in the VIIRS Cloud Mask Algorithm for NPOESS." *Journal of Atmospheric and Oceanic Technology* no. 26 (7):1388-1397. doi: 10.1175/2009jtecha1198.1.

Irish, R. R., J. L. Barker, S. N. Goward, and T. Arvidson. 2006. "Characterization of the Landsat-7 ETM+ automated cloud-cover assessment (ACCA) algorithm." *Photogrammetric Engineering and Remote Sensing* no. 72 (10):1179-1188.

Jones, P. D., and M. Hulme. 1996. "Calculating regional climatic time series for temperature and precipitation: Methods and illustrations." *International Journal of Climatology* no. 16 (4):361-377.

Kalnay, E., M. Kanamitsu, R. Kistler, W. Collins, D. Deaven, L. Gandin, M. Iredell, S. Saha, G. White, J. Woollen, Y. Zhu, M. Chelliah, W. Ebisuzaki, W. Higgins, J. Janowiak, K. C. Mo, C. Ropelewski, J. Wang, A. Leetmaa, R. Reynolds, R. Jenne, and D. Joseph. 1996. "The NCEP/NCAR 40-year reanalysis project." *Bulletin of the American Meteorological Society* no. 77 (3):437-471. doi: 10.1175/1520-0477(1996)077<0437:tnyrp>2.0.co;2.

Kane, V. R., A. R. Gillespie, R. McGaughey, J. A. Lutz, K. Ceder, and J. F. Franklin. 2008. "Interpretation and topographic compensation of conifer canopy self-shadowing." *Remote Sensing of Environment* no. 112 (10):3820-3832. doi: 10.1016/j.rse.2008.06.001.

Klein, A. G., D. K. Hall, and G. A. Riggs. 1998. "Improving snow cover mapping in forests through the use of a canopy reflectance model." *Hydrological Processes* no. 12 (10-11):1723-1744.

Knowles, N., M. D. Dettinger, and D. R. Cayan. 2006. "Trends in snowfall versus rainfall in the Western United States." *Journal of Climate* no. 19 (18):4545-4559.

Li, B. L., A. X. Zhu, C. H. Zhou, Y. H. Zhang, T. Pei, and C. Z. Qin. 2008. "Automatic mapping of snow cover depletion curves using optical remote sensing data under conditions of frequent cloud cover and temporary snow." *Hydrological Processes* no. 22 (16):2930-2942. doi: 10.1002/hyp.6891.

Lu, D., H. Ge, S. He, A. Xu, G. Zhou, and H. Du. 2008. "Pixel-based Minnaert correction method for reducing topographic effects on a Landsat 7 ETM+ image." *Photogrammetric Engineering and Remote Sensing* no. 74 (11):1343-1350.

Masek, J. G., E. F. Vermote, N. E. Saleous, R. Wolfe, F. G. Hall, K. F. Huemmrich, F. Gao, J. Kutler, and T. K. Lim. 2006. "A Landsat surface reflectance dataset for North America, 1990-2000." *IEEE Geoscience and Remote Sensing Letters* no. 3 (1):68-72. doi: 10.1109/lgrs.2005.857030.

Meyer, Peter, Klaus I. Itten, Tobias Kellenberger, Stefan Sandmeier, and Ruth Sandmeier. 1993. "Radiometric corrections of topographically induced effects on Landsat TM data in an alpine environment." *ISPRS Journal of Photogrammetry and Remote Sensing* no. 48 (4):17-28.

Minder, J. R., P. W. Mote, and J. D. Lundquist. 2010. "Surface temperature lapse rates over complex terrain: Lessons from the Cascade Mountains." *Journal of Geophysical Research-Atmospheres* no. 115. doi: D1412210.1029/2009jd013493.

Mitchell, J. M. 1976. "The regionalization of climate in the western United States." *Journal of Applied Meteorology* no. 15 (9):920-927.

Mote, P. W., A. F. Hamlet, M. P. Clark, and D. P. Lettenmaier. 2005. "Declining mountain snowpack in western north America." *Bulletin of the American Meteorological Society* no. 86 (1):39-49. doi: 10.1175/bams-86-1-39.

Peterson, T. C., D. R. Easterling, T. R. Karl, P. Groisman, N. Nicholls, N. Plummer, S. Torok, I. Auer, R. Boehm, D. Gullett, L. Vincent, R. Heino, H. Tuomenvirta, O. Mestre, T. Szentimrey, J. Salinger, E. J. Forland, I. Hanssen-Bauer, H. Alexandersson, P. Jones, and D. Parker. 1998. "Homogeneity adjustments of in situ atmospheric climate data: A review." *International Journal of Climatology* no. 18 (13):1493-1517. doi: 10.1002/(sici)1097-0088(19981115)18:13<1493::aid-joc329>3.0.co;2-t.

Pierce, D. W., T. P. Barnett, H. G. Hidalgo, T. Das, C. Bonfils, B. D. Santer, G. Bala, M. D. Dettinger, D. R. Cayan, A. Mirin, A. W. Wood, and T. Nozawa. 2008. "Attribution of Declining Western US Snowpack to Human Effects." *Journal of Climate* no. 21 (23):6425-6444. doi: 10.1175/2008jcli2405.1.

Riggs, G. A., D. K. Hall, and V. V. Salomonson. 2006. "MODIS snow products user guide to collection 5."

Rittger, Karl, Thomas H. Painter, and Jeff Dozier. 2012. "Assessment of methods for mapping snow cover from MODIS." *Advances in Water Resources* (0). doi: 10.1016/j.advwatres.2012.03.002.

Rosenthal, W., and J. Dozier. 1996. "Automated mapping of montane snow cover at subpixel resolution from the Landsat Thematic Mapper." *Water Resources Research* no. 32 (1):115-130.

Salomonson, V. V., and I. Appel. 2004. "Estimating fractional snow cover from MODIS using the normalized difference snow index." *Remote Sensing of Environment* no. 89 (3):351-360. doi: 10.1016/j.rse.2003.10.016.

Seidel, K., F. Ade, and J. Lichtenegger. 1983. "Augmenting landsat mss data with topographic information for enhanced registration and classification " *Ieee Transactions on Geoscience and Remote Sensing* no. 21 (3):252-258.

Seidel, K., and J. Martinec. 2004. *Remote Sensing in Snow Hydrology Runoff Modeling, Effect of Climate Change*. Chichester, UK: Praxis Publishing.

Serreze, M. C., M. P. Clark, R. L. Armstrong, D. A. McGinnis, and R. S. Pulwarty. 1999. "Characteristics of the western United States snowpack from snowpack telemetry (SNOTEL) data." *Water Resources Research* no. 35 (7):2145-2160. doi: 10.1029/1999wr900090.

Smith, J. A., T. L. Lin, and K. J. Ranson. 1980. "The Lambertian assumption and Landsat data." *Photogrammetric Engineering and Remote Sensing* no. 46 (9):1183-1189.

Song, C., C. E. Woodcock, K. C. Seto, M. P. Lenney, and S. A. Macomber. 2001. "Classification and change detection using Landsat TM data: When and how to correct atmospheric effects?" *Remote Sensing of Environment* no. 75 (2):230-244.

Teillet, P. M., B. Guindon, and D. G. Goodenough. 1982. "On the slope-aspect correction of multispectral scanner data." *Canadian Journal of Remote Sensing* no. 8 (2):84-106.

Vermote, E. F., and S. Kotchenova. 2008. "Atmospheric correction for the monitoring of land surfaces." *Journal of Geophysical Research-Atmospheres* no. 113 (D23). doi: D23s9010.1029/2007jd009662.

Vermote, E. F., D. Tanre, J. L. Deuze, M. Herman, and J. J. Morcrette. 1997. "Second Simulation of the Satellite Signal in the Solar Spectrum, 6S: An overview." *IEEE Transactions on Geoscience and Remote Sensing* no. 35 (3):675-686. doi: 10.1109/36.581987.

Warren, S. G. 1982. "Optical-properties of snow." *Reviews of Geophysics* no. 20 (1):67-89. doi: 10.1029/RG020i001p00067.

Westerling, A. L., H. G. Hidalgo, D. R. Cayan, and T. W. Swetnam. 2006. "Warming and earlier spring increase western US forest wildfire activity." *Science* no. 313 (5789):940-943. doi: 10.1126/science.1128834.

Winther, J. G., and D. K. Hall. 1999. "Satellite-derived snow coverage related to hydropower production in Norway: present and future." *International Journal of Remote Sensing* no. 20 (15-16):2991-3008. doi: 10.1080/014311699211570.

Wiscombe, W. J., and S. G. Warren. 1980. "A model for the spectral albedo of snow. 1. pure snow." *Journal of the Atmospheric Sciences* no. 37 (12):2712-2733. doi: 10.1175/1520-0469(1980)037<2712:amftsa>2.0.co;2.

Chapter 3: MODIS Terra Collection 6 Fractional Snow Cover Validation in Mountainous Terrain using Landsat TM and ETM+

Daily swath MODIS Terra Collection 6 (C6) fractional snow cover (FSC) (MOD10_L2) estimates were validated with two-day Landsat TM/ETM+ snow-covered area (SCA) estimates across central Idaho and southwestern Montana, USA. Fourteen cross-sensor snow maps for 2000, 2001, 2002, 2003, 2005, 2007, and 2009 were compared using least-squared regression. Strong spatial and temporal map validation was found between MODIS Terra C6 FSC and Landsat TM/ETM+ SCA, although map disagreements were observed for two dates. High-altitude cirrus cloud contamination during low snow conditions led to disagreement on May 30, 2001. MODIS Terra's spatial resolution limits retrieval of thin-patchy snow cover. Late season transient snowfall between May 22nd and 24th inflated SCA for the Landsat TM/ETM+ map on May 24-25, 2002. Landsat's image acquisition frequency can invoke difficulty when discriminating between transient and resident mountain snow cover for climate data record (CDR) development. Ground-based daily snow telemetry (SNOTEL) snow-water-equivalent (SWE) measurements can be used to verify transient snowfall events. Users of daily MODIS Terra C6 FSC swath products should be aware that FSC estimates in mountainous terrain could be sensitive to local solar illumination and sensor viewing geometry. Cross-sensor interoperability has been confirmed between MODIS Terra and Landsat TM/ETM+ when mapping snow from the visible spectrum. This linear relationship is strong, and supports operational multi-sensor snow cover mapping, specifically CDR development to expand cyrosphere, climate, and hydrological science applications.

Introduction

Successive snow cover accumulation in mountainous terrain during the hemispheric cool-season forms a resident snowpack that melts as springtime solar irradiance and near-surface air temperature increase, and planetary albedo decreases (Barry 2002; Barry 2006; Barry, Fallot, and Armstrong 1995). In arid regions like the western United States, mountain snowpack accumulation and melt contributes approximately 50-70% to the total annually available freshwater resource via snow-fed streamflow (Bales et al. 2006; Barnett, Adam, and Lettenmaier 2005; Cayan 1996). Therefore, documenting how basic (i.e., natural variability) snowpack accumulation and melt processes and patterns vary over multiple spatial and temporal measurement scales, enables identification of localities where mountain snowpack has changed, is changing, and will be susceptible to long-term change triggered by climatic warming. Satellite remote sensing is uniquely positioned to address these questions because a spectrally distinct snow cover signal can be optically retrieved over broad regions and remote mountainous terrain with high confidence (Dozier 1984, 1989; Dozier and Painter 2004; Hall et al. 2001; Hall and Martinec 1985; Hall and Riggs 2007; Hall, Riggs, and Salomonson 1995; Foster et al. 2011; Hall et al. 2012; Rosenthal and Dozier 1996). That said, maximizing the snow cover signal relative to background noise contributed by a mixed land surface response, requires quantifying uncertainty and error in snow cover mapping to ensure that remotely sensed snow algorithms and products are robust and continually improved upon using differing techniques (Dozier and Painter 2004; Dozier et al. 2008; Hall et al. 2001; Hall et al. 1998; Hall, Riggs, et al. 2002; Rittger, Painter, and Dozier 2012; Rosenthal and Dozier 1996;

Antilla, S., and C. 2006; Dobreva and Klein 2011; Hall and Riggs 2011; Metsamaki et al. 2002; Salminen et al. 2009; Pepe et al. 2005). This paper reports on a cross-sensor snow map validation between MODIS Terra and Landsat TM/ETM+ that is intended to assess MODIS Collection 6 (C6) fractional snow cover (FSC) estimate accuracy, and more broadly, summarize the inherent limitations of multispectral sensor-specific mapping capabilities with an eye towards multi-sensor integration for climate data record (CDR) development.

Retrieving multispectral snow cover from satellite platforms over mountainous terrain is challenging from several environmental and observational standpoints (Dozier and Painter 2004; Hall and Martinec 1985; Hall and Riggs 2007; Seidel and Martinec 2004). Throughout the planetary surface-to-atmospheric optical column, fluctuating atmospheric aerosols, variable meteorological conditions, and seasonal change in local solar illumination can produce considerable between image differences at daily to weekly timescales. Decades of research on multispectral snow cover mapping has shown that grain size, cloud cover, forest density, topographic illumination, solar zenith angles, off-nadir viewing angles, and bi-directional reflectance (BDRF) corrections can complicate pixel level snow retrieval (Dozier 1989; Dozier and Frew 1990; Dozier and Painter 2004; Hall, Riggs, et al. 2002; Klein, Hall, and Riggs 1998; Li et al. 2007; Rittger, Painter, and Dozier 2012; Rosenthal and Dozier 1996; Xin et al. 2012; Painter et al. 2009; Schaaf, Wang, and Strahler 2011). Each of these environmental and observational factors is amplified over mountainous terrain, and taken together, results in further between image differences. Retrieving a multispectral snow cover signal can be achieved by using the

normalized difference snow index (NDSI), a spectral band ratioing method (Hall, Riggs, and Salomonson 1995; Hall and Riggs 2011), or spectral mixture analysis (Dozier and Painter 2004; Rosenthal and Dozier 1996; Dozier and Frew 2009; Rittger, Painter, and Dozier 2012), a simultaneous linear equation that separates snow from the unique spectral responses of rock, soils, shadows, and vegetation endmembers. Pixels containing snow are then classified using either 'binary' or 'fractional' decisions. Historically, if a pixel has had greater than 50% (less than 50%) snow cover, then snow has been classified as present (absence) (Dozier and Painter 2004; Hall and Martinec 1985; Seidel and Martinec 2004; Rittger, Painter, and Dozier 2012; Salomonson and Appel 2004, 2006). In comparison, Salomonson and Appel (2004), (2006) developed NDSI FSC models for MODIS Terra and Aqua platforms by using higher resolution Landsat ETM+ 'truth' estimates of snow cover for model calibration. More recently, Rittger et al. (2012) use MODIS Terra snow products MOD10A1 and MOD09GA to compare binary NDSI, fractional NDSI, and MODSCAG (i.e., MODIS snow-covered area and grain size algorithm) methods for snow cover retrieval and classification using Landsat ETM+ for validation.

In this paper, a validation effort is undertaken to examine the accuracy of daily swath MODIS Terra C6 FSC (MOD10_L2) estimates produced from the Salomonson and Appel (2004) model by using Landsat TM/ETM+ binary snow-covered area (SCA) as 'truth' estimates of snow cover. This validation study differs from previous work in that (1) daily swath MODIS Terra FSC estimates originate from C6 re-processing; (2) the temporal validation scale covers the 2000s; and (3) both partially cloudy Landsat TM and

ETM+ images are used for validation. The objective is to determine how well MODIS Terra is retrieving pixel level NDSI FSC for mountainous terrain across the interior northwestern United States during peak spring snowmelt. MODIS Terra and Landsat TM/ETM+ snow cover maps overlap from 2000 to the present. For this study, seven individual years were selected where Landsat TM and ETM+ images provided enough visible coverage during peak spring snowmelt for both cloud-free and partially cloudy conditions. MODIS Terra, Landsat TM, and ETM+ platforms have sun-synchronous orbits with an approximate 30-45 minute image acquisition time lag. MODIS Terra C6 FSC maps selected for comparison reflect snow cover conditions for the same day and approximate time as observed for Landsat. Similar image processing and NDSI classification methods have been used to derive MODIS Terra C6 FSC and Landsat TM/ETM+ binary SCA estimates with two exceptions. First, the MODIS Terra NDSI FSC maps do not include the 283 K land surface temperature threshold criteria employed by previous MODIS snow product collections (Riggs et al. 2006), and second, Landsat TM/ETM+ NDSI binary SCA estimates do not include the normalized difference vegetation index (NDVI) threshold criteria (Klein, Hall, and Riggs 1998). For this validation analysis, MODIS Terra C6 FSC estimates were partitioned into 20 discrete five percent FSC classes, and then the number of Landsat 30-meter pixels classified as snow-covered was summarized for each discrete MODIS 500-meter FSC class. Least-squared regression including a ‘goodness-of-fit’ test was used to assess the linear relationship between MODIS Terra C6 FSC and Landsat TM/ETM+ binary SCA estimates for seven individual years.

Methods

Study Region Description

The geographic domain under investigation covers the mid-latitude mountainous terrain across the interior northwestern United States, specifically, central Idaho and southwestern Montana (Figure 1). Steep vertical relief, and considerable fine-scale topographic variability characterize the regional physiography. The regional vegetation cover and structure is elevationally dependent with low elevation areas containing shrublands that transition into open disjoint evergreen forest stands. Mid-elevations have a mosaic of closed evergreen forests and open sedge-grasslands. High elevation alpine basins contain a mixture of open evergreen forest stands and bare rock (Arno and Hammerly 1984). The regional climate is semi-arid with a peak precipitation maximum during late spring-early summer (Shinker 2010; Mitchell 1976). Maximum snowpack accumulation occurs between early-mid April with peak snowmelt during early June (Cayan 1996). For this validation study and selected time period, snow cover is largely confined to higher elevation regions. Snow cover in low to mid elevation terrain has already melted.

MODIS Terra and Landsat TM/ETM+ Imagery

Daily MODIS Terra swaths, and 16-day Landsat TM and ETM+ path-row images for seven years were used to derive snow cover maps (Table 1). To obtain complete Landsat coverage for the study region, image mosaicking was required between two

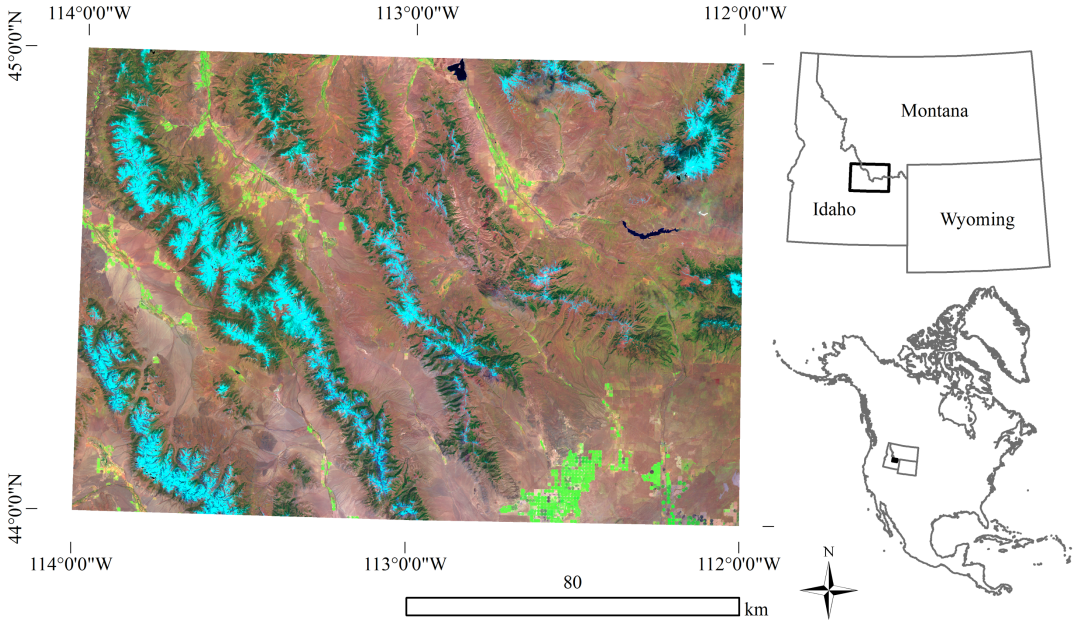

Figure 1. Landsat TM/ETM+ false-color two-day composite (bands 5, 4, and 2) for the central Idaho and southwestern Montana study region on May 27-28, 2003.

Table 1. MODIS Terra C6 FSC and Landsat TM/ETM+ binary SCA map comparison dates.

MODIS Terra Date	UTC Crossing	Landsat Date	UTC Crossing	Landsat Path-Row	Landsat Sensor
June 3, 2000	18:00:00	June 3, 2000	17:55:28	40-29	TM
June 4, 2000	18:45:00	June 4, 2000	18:05:03	39-29	ETM+ (SLC-on)
May 29, 2001	18:45:00	May 29, 2001	18:09:08	40-29	ETM+ (SLC-on)
May 30, 2001	19:25:00	May 30, 2001	17:53:30	39-29	TM
May 24, 2002	19:25:00	May 24, 2002	17:56:05	40-29	TM
May 25, 2002	18:30:00	May 25, 2002	18:01:50	39-29	ETM+ (SLC-on)
May 27, 2003	17:45:00	May 27, 2003	17:54:49	40-29	TM
May 28, 2003	18:30:00	May 28, 2003	18:01:53	39-29	ETM+ (SLC-on)
May 24, 2005	18:35:00	May 24, 2005	18:08:57	40-29	ETM+ (SLC-off)
May 25, 2005	19:15:00	May 25, 2005	18:00:33	39-29	TM
May 30, 2007	18:35:00	May 30, 2007	18:09:37	40-29	ETM+ (SLC-off)
May 31, 2007	19:15:00	May 31, 2007	18:08:27	39-29	TM
May 27, 2009	17:45:00	May 27, 2009	18:07:21	40-29	TM
May 28, 2009	18:30:00	May 28, 2009	18:03:37	39-29	ETM+ (SLC-off)

separate Landsat TM and ETM+ path-rows. This path-row difference resulted in a one-day coverage offset. Landsat TM/ETM+ binary SCA estimates originate from two-day image composites. To account for between sensor image acquisition differences, two-day Landsat TM/ETM+ binary SCA maps were compared with daily MODIS Terra C6 FSC maps for each day contained within the Landsat mosaic. This resulted in two map comparisons per year with a total of fourteen individual comparisons (Table 1). MODIS Terra C6 FSC swaths include MODIS geolocation information (MOD03) and were re-projected to a World Geodetic System (WGS) 1984, Zone 12 Universal Transverse Mercator (UTM) Projection to match Landsat TM and ETM+ image projections. Landsat TM and ETM+ images obtained from the USGS Earth Resources Observation Science (EROS) Data Center have been processed to a standard level of geometric and terrain accuracy (http://landsat.usgs.gov/Landsat_Processing_ Details.php). MODIS Terra C6 FSC and Landsat TM/ETM+ binary SCA maps were compared using a Zone 12 UTM Projection.

MODIS Terra C6 FSC Mapping

A comprehensive description of MODIS Terra snow mapping and classification can be found in Riggs et al. (2006). For this specific study, it is important to note that MODIS Terra Level 1B, MOD02HKM top-of-the-atmosphere (TOA) reflectance products were used. Cloud cover was flagged using the MODIS cloud-mask product MOD35_L2 (Ackerman et al. 1998). Pixel level NDSI FSC estimates were derived using the MODIS Terra NDSI FSC model found in Salomonson and Appel (2004).

Landsat TM/ETM+ Binary SCA Mapping

Landsat TM/ETM+ binary SCA estimates were derived using a similar snow mapping and classification method per Riggs et al. (2006). Because MODIS Terra and Landsat TM and ETM+ sensors have image coverage differences, acquisition frequency, and spatial resolution, additional image processing steps were required to produce snow cover maps in mountainous terrain for Landsat. A detailed image processing and snow cover classification description for Landsat TM and ETM+ can be found in (Crawford et al. 2013), but in short, all evaluated TM and ETM+ images were geo-referenced, converted to TOA reflectance, masked for clouds and shadows, and corrected for local topographic illumination. Using the NDSI algorithm (Hall and Riggs 2011; Hall, Riggs, and Salomonson 1995), pixels having NDSI values > 0.4, band 2 > 0.10, and band 4 > 0.11 were binary classified as > 50% snow-covered.

MODIS Terra C6 FSC and Landsat Binary SCA Map Validation

MODIS Terra C6 FSC and Landsat TM/ETM+ binary SCA maps were subset to the study region. Cloudy MODIS Terra pixels, cloud and shadow Landsat TM/ETM+ pixels, and Landsat ETM+ scan line correction (SLC) SLC-off pixels were excluded from each comparison. For certain daily MODIS Terra C6 FSC maps, pixel level FSC estimates exceed 0.0-1.0. Because snow cover cannot theoretically be greater than 100% in a given pixel, pixel level NDSI FSC estimates beyond 1.0 were truncated to indicate 100% FSC. Next, for each MODIS Terra C6 FSC map, each pixel was assigned into a discrete five percent FSC class covering 0-100% with a total of 20 individual classes. For each MODIS 500-meter FSC class, the sum of 30-meter Landsat pixels classified as snow covered was tallied. It is important to note that a MODIS 500-meter pixel is the

equivalent to approximately 244 Landsat 30-meter pixels. Because MODIS Terra C6 FSC and Landsat TM/ETM+ binary SCA comparisons are exhaustive, and MODIS Terra C6 FSC have discrete class level assignments, the number of possible Landsat 30-meter pixel samples classified with snow cover varied according to the spatial extent of MODIS Terra C6 FSC.

Least-squared regression with a 'goodness-of-fit' test (Draper and Smith 1998) was employed to statistically compare MODIS Terra C6 FSC estimates with Landsat TM/ETM+ 'truth' SCA estimates for each year. First, Landsat TM/ETM+ 'truth' SCA estimates were converted to a percent coverage for each discrete MODIS Terra C6 FSC class by dividing snow-covered pixels by the total number of Landsat pixels behind each MODIS Terra C6 FSC class. Four summary statistics were generated from the 'goodness-of-fit' test including sum of squares due to error (SSE), R-square (R^2), adjusted R-square (adj. R^2), and root mean square error (RSME). In this validation, the central tendency between FSC and SCA estimates within each discrete class was the focus rather than individual pixels. Individual pixels can often have extreme values that result from data retrieval noise that propagate through image processing algorithms. In this least-squared analysis, MODIS Terra C6 FSC was the response variable, and Landsat TM/ETM+ SCA was the independent explanatory variable. SSE measures the total variation in the response variable to model fit. R-square measures how well the model fit explains the variation in the response, and adjusted R-square accounts for residual degrees of freedom and reflects the quality of the fit. RSME is the standard error of the fit and represents the standard deviation of the random component. 'Goodness-of-fit' equations can be found in

Draper and Smith (1998). Residuals were used to assess model error between cross-sensor FSC and SCA estimates. Residuals are the difference between response and predicted response values using an independent explanatory variable.

Results

MODIS Terra C6 FSC and Landsat TM/ETM+ Binary SCA Validation

MODIS Terra C6 FSC and Landsat TM/ETM+ binary SCA estimates have been compared for approximate peak spring snowmelt timing during late May-early June for the mountainous region in central Idaho and southwestern Montana (Figure 1). Fourteen daily snow map comparisons (two per year) between MODIS Terra and Landsat TM/ETM+ span seven years including 2000, 2001, 2002, 2003, 2005, 2007, and 2009. Among these comparison dates, C6 FSC and binary SCA maps possess cloud-free conditions (less than 5% cloud cover)(Figure 2a), partially cloudy conditions (greater than 5% cloud cover)(Figure 2b), and variable snow cover extent (Figure 3). Overall, MODIS Terra C6 FSC and Landsat TM/ETM+ binary SCA estimates show strong, and statistically significant linear agreement in mountainous terrain during peak spring snowmelt over the 2000s; a decade with concurrent MODIS Terra and Landsat TM/ETM+ image coverage.

'Goodness-of-fit' statistics with residuals between discrete MODIS Terra C6 FSC classes and Landsat TM/ETM+ binary SCA 'truth' estimates enabled an examination of MODIS Terra C6 FSC map accuracy and error identification (Table 2, Figure 4). For six out of seven years, and nine out of fourteen daily map comparisons, the adjusted R-squared exceeded 0.95 with a RSME of less than 0.10 (Table 2). For two dates, May 30,

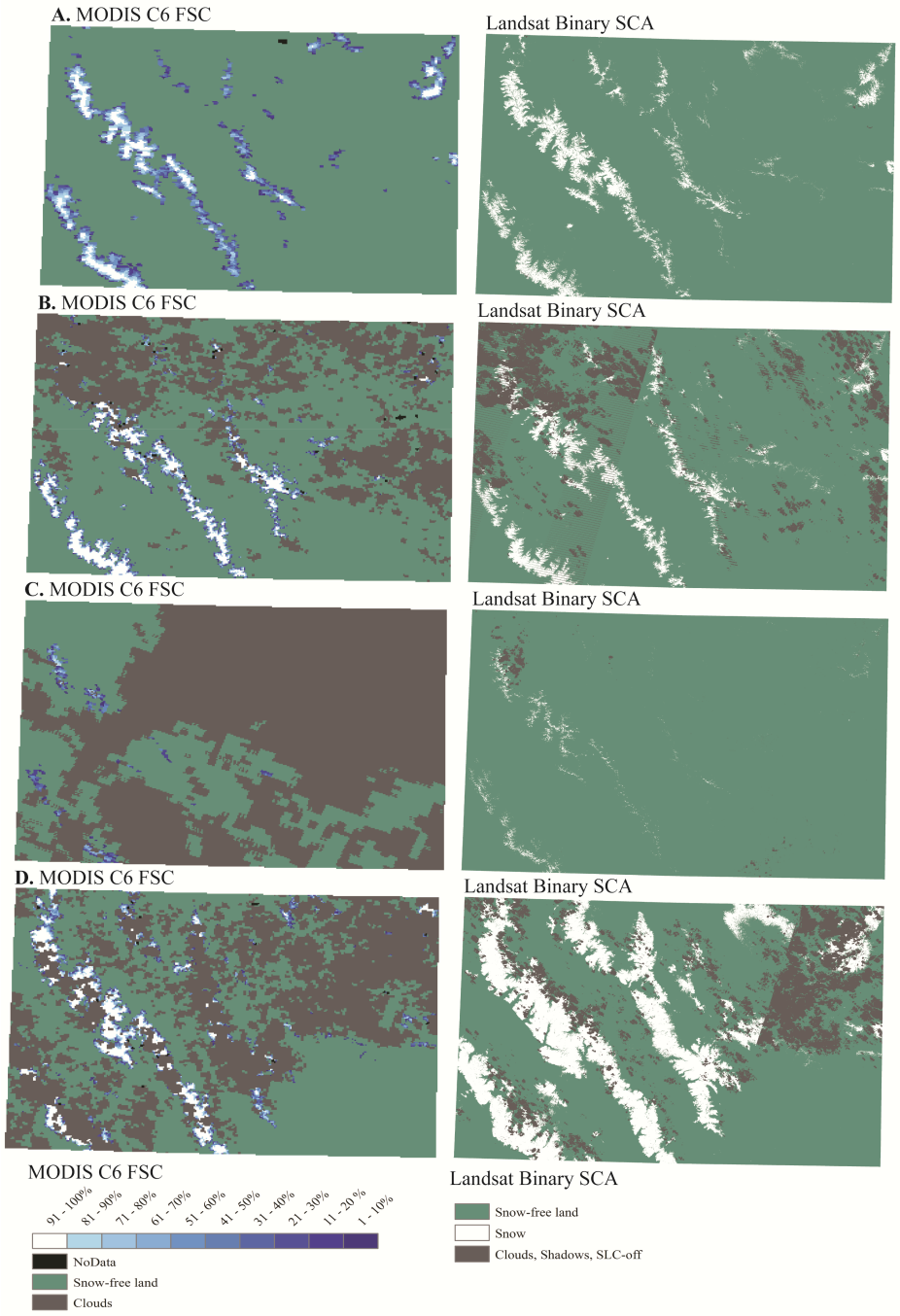

Figure 2. MODIS Terra C6 FSC and Landsat TM/ETM+ binary SCA map comparisons: A) a strong agreement cloud-free example between May 27, 2003 and May 27-28, 2003; B) a strong agreement partially cloudy example between May 24, 2005 and May 24-25, 2005; C) map disagreement between May 30, 2001 and May 29-30, 2001; and D) map disagreement between May 25, 2002 and May 24-25, 2002. Note: the above maps retain their UTM zone 12 projections, but only represent map comparison illustrations.

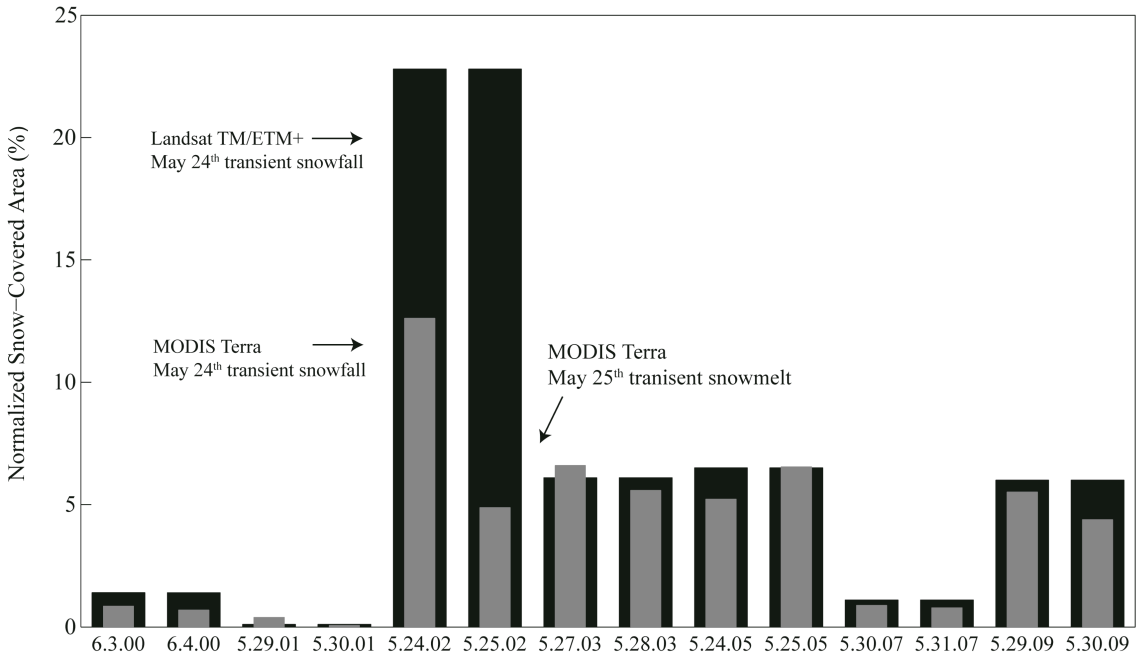

Figure 3. Normalized SCA estimates for Landsat TM/ETM+ (black bars) and MODIS Terra (grey bars) for each daily map comparison. Normalized SCA estimates are the ratio of visible SCA to total area (geographic domain 44°N, 114°W by 45°N, 112°W, see figure 1) minus cloud cover. Note: Daily transient snowfall and snowmelt events responsible for the May 25th map disagreement between Landsat TM/ETM+ and MODIS Terra.

Table 2. MODIS Terra C6 FSC and Landsat TM/ETM+ binary SCA map comparison 'goodness- of-fit' summary statistics.

Comparison Date	MODIS Cloud Cover (%)	Landsat Cloud-Shadow Cover (%)	SSE	R-square	Adj. R-square	RSME
June 3, 2000	0.012	0.047	0.063	0.961	0.959	0.059
June 4, 2000	0.001	0.047	0.043	0.974	0.972	0.049
May 29, 2001	0.135	0.052	0.089	0.946	0.943	0.070
May 30, 2001	0.674	0.052	0.144	0.473	0.415	0.126
May 24, 2002	0.338	0.192	0.017	0.989	0.988	0.031
May 25, 2002	0.408	0.192	0.688	0.585	0.562	0.195
May 27, 2003	0.000	0.047	0.016	0.990	0.989	0.030
May 28, 2003	0.003	0.047	0.031	0.980	0.979	0.042
May 24, 2005	0.279	0.185	0.042	0.974	0.973	0.048
May 25, 2005	0.108	0.185	0.155	0.906	0.901	0.093
May 30, 2007	0.126	0.075	0.019	0.988	0.987	0.032
May 31, 2007	0.056	0.075	0.163	0.865	0.856	0.101
May 27, 2009	0.004	0.057	0.034	0.979	0.978	0.043
May 28, 2009	0.110	0.057	0.031	0.981	0.980	0.041

SSE: sum of squares due to error
R-square: coefficient of determination
Adj. R-square: coefficient of determination adjusted for residual degrees of freedom
RSME: root mean square error

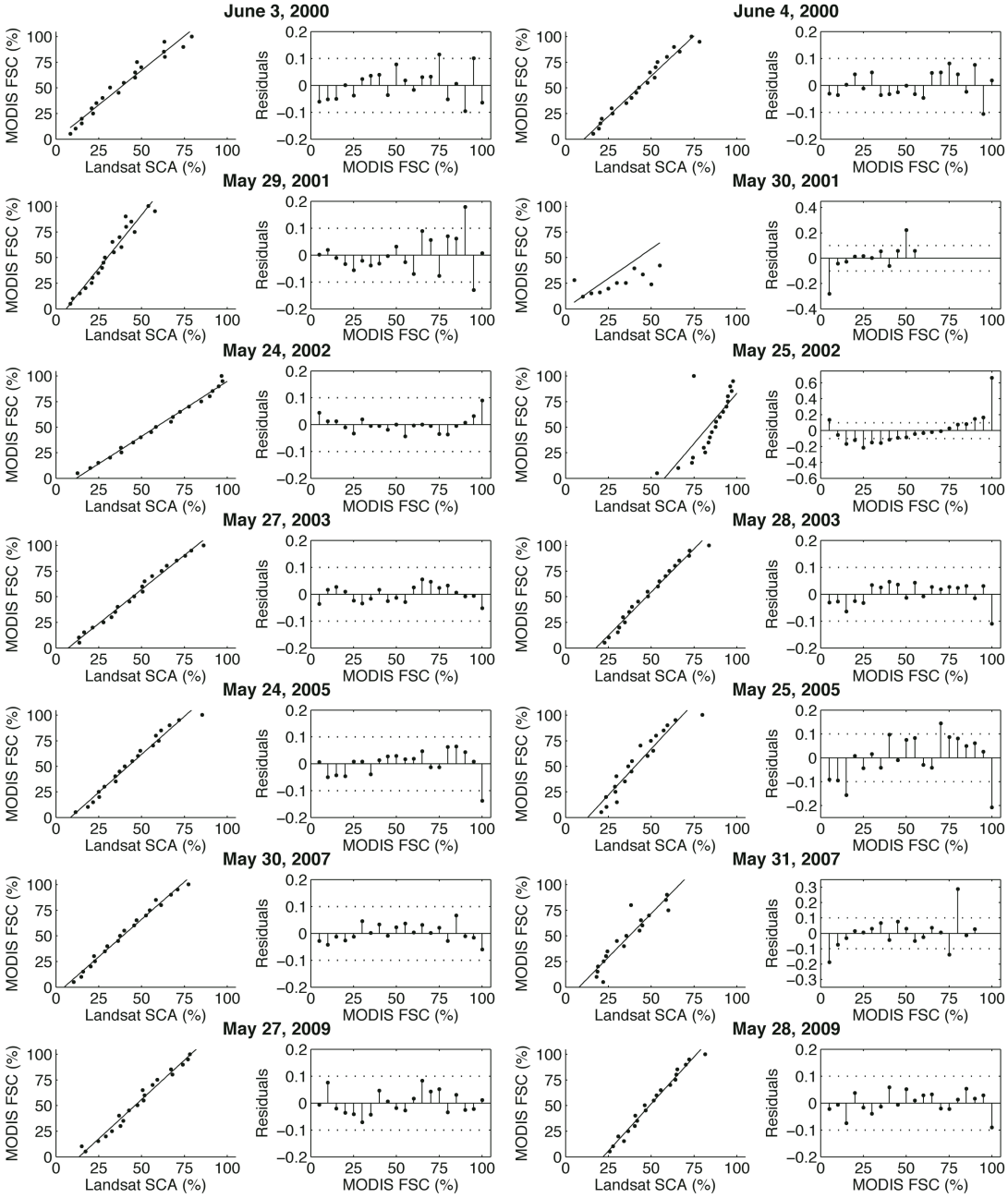

Figure 4. 'Goodness-of-fit' with residuals between MODIS Terra C6 FSC and Landsat TM/ETM+ binary SCA for each map comparison date. Scatterplots and residuals for each date represent individual comparisons between two-day Landsat TM/ETM+ binary SCA estimates and daily MODIS Terra C6 FSC estimates. Dotted lines on residuals plots signify the 0.10 thresholds for allowable error in the Salomonson and Appel (2004) MODIS Terra NDSI FSC model.

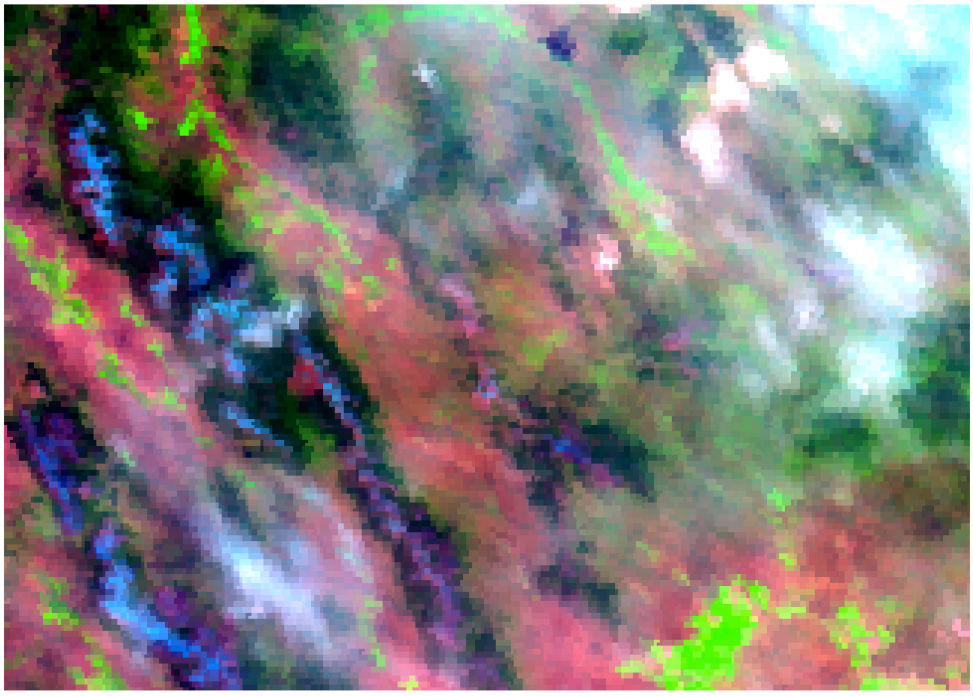

Figure 5. False-color (bands 7, 2, 1) MODIS Terra 1B, MODHKM calibrated radiances (TOA) for May 30, 2001.The MODHKM daily swath has been subset to the study region with a UTM Zone 12 projection and 500 meter nearest neighbor resampling. This MODIS Terra MODHKM swath subset was used to estimate C6 FSC.

2001 and May 25, 2002, MODIS Terra C6 FSC and Landsat TM/ETM+ binary SCA show disagreement (Figure 2c and Figure 2d). Although May 29, 2001 indicates strong agreement during low snow coverage (Table 2, Figure 3), thin high-altitude cirrus clouds coupled with cloud cover concentration over mountain peaks for MODIS Terra on May 30, 2001 (Figure 5), and no change in cloud cover content for the Landsat TM/ETM+ two-day composite, suggests that either visible MODIS Terra C6 FSC coverage is too low or that the MODIS Terra cloud mask (MOD35_L2) is aggressively flagging pixels as cloud covered because thin high altitude cirrus clouds are difficult to discriminate from patchy snow. Correspondingly, May 24, 2002 shows high map agreement between C6 FSC and Landsat TM/ETM+ binary SCA despite the disagreement on May 25, 2002 (Table 2). For May 24-25, 2002, Landsat TM/ETM+ is mapping high snow coverage (Figure 3). Even though both maps show partially cloudy conditions, a closer examination of the Landsat images indicated that greater SCA on May 24, 2002 (i.e., TM path-row 40-29) was a result of late season transient snowfall between May 22nd and 24th that in large part, melted before the ETM+ overpass (path-row 39-29) on May 25, 2002 (Figure 6). Transient snowfall was identified using ground-based daily SNOTEL SWE observations (Figure 6), and by comparing normalized swath MODIS Terra C6 binary SCA and Landsat TM/ETM+ binary SCA estimates between May 24 and May 25, 2002 (Figure 3). The observable difference in Figure 3 between MODIS Terra C6 and Landsat TM/ETM+ normalized SCA on the morning of May 24, 2002 is a function of the image acquisition time lag between sensors, and rapid snowmelt of transient snowfall.

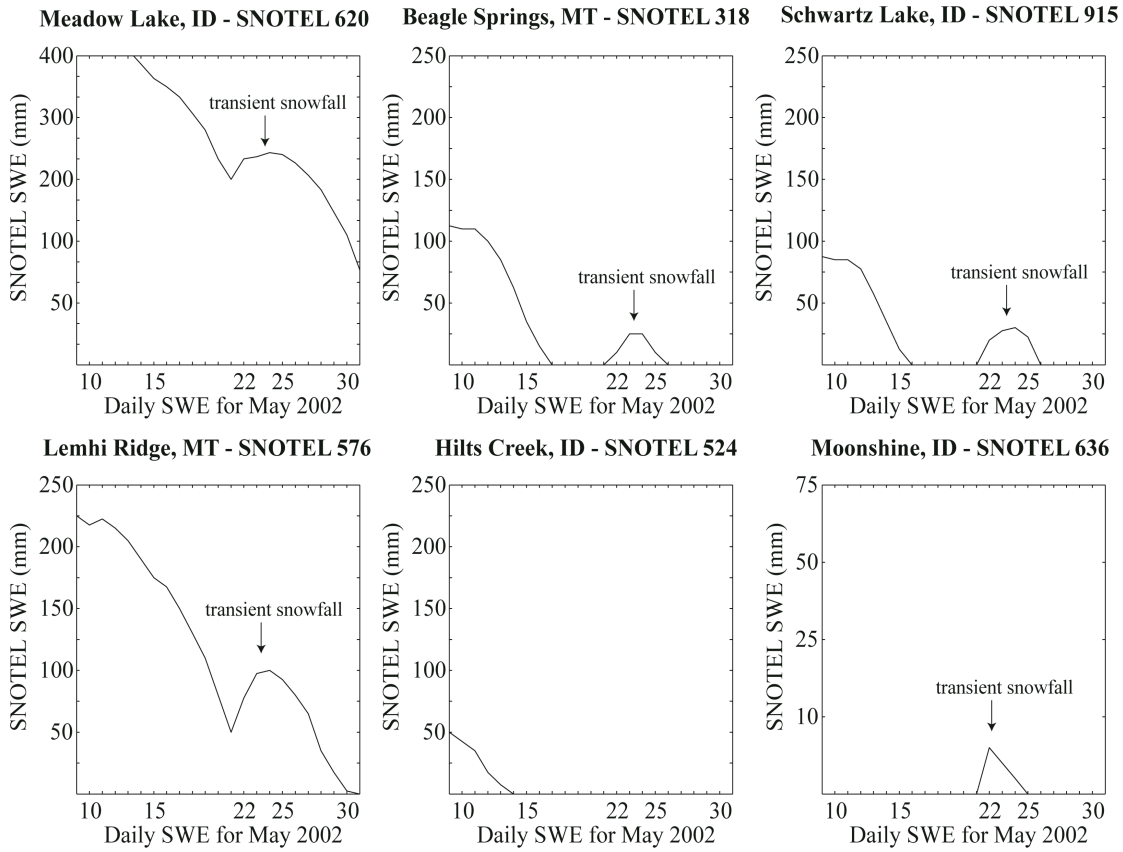

Figure 6. May 10-31, 2002 daily SNOTEL SWE observations for the east-central Idaho-southwestern Montana study region. Six NRCS SNOTEL sites (http://www.wcc.nrcs.usda.gov/snow/) are located within the geographic domain 44-45° N, -114-112° W. Five of six SNOTEL sites show the occurrence of a transient snowfall event between May 22 and 24. Note: SWE amounts on the y-axis vary according to elevation, physiographic setting, and instrument location

Residual analysis for each daily map comparison indicates where MODIS Terra C6 FSC error is concentrated relative to Landsat TM/ETM+ 'truth' SCA estimates (Figure 4). The MODIS Terra C6 NDSI FSC model appears to systematically overestimate FSC in mountainous terrain during late spring snowmelt, especially during lower snow coverage (Figure 4). More specifically, scatterplots and trend lines between MODIS Terra C6 FSC and Landsat TM/ETM+ SCA indicate that when MODIS Terra is estimating 100% FSC, Landsat is only observing ~ 75% SCA. Even so, the residual error for most map comparison dates still falls within the 0.10 margin of MODIS Terra NDSI FSC model RSME (Figure 4). For May 30, 2001 and May 25, 2002, trend lines between MODIS Terra C6 FSC and Landsat TM/ETM+ binary SCA estimates show disagreement in cross-sensor validation during anomalous snow conditions. On May 30, 2001, MODIS Terra C6 FSC classes do not exceed 50% coverage because of extremely low, patchy snow cover. However, on May 25, 2002, Landsat TM/ETM+ binary SCA does not drop below 50% coverage for any MODIS Terra C6 FSC class due to inflated SCA driven by transient snowfall.

Discussion

Similar snow cover retrieval and classification methods were used to produce MODIS Terra C6 FSC and Landsat TM/ETM+ binary SCA estimates during the 2000s. Strong spatial and temporal linear agreement was found between sensor-specific daily snow cover maps with RSME remaining below 10% for each discrete MODIS Terra C6 FSC class. Even though the 283 K temperature screen was excluded from the MODIS Terra snow algorithm, alpine snow coverage was still present during peak spring snowmelt, and

indicates that MODIS Terra C6 is in fact mapping alpine snow cover with validation from Landsat TM/ETM+. This finding addresses Rittger et al. (2012) concern that the MODIS Terra snow algorithm temperature screen could falsely remove snow cover during the melt season. Because snow cover was largely confined to bare rock alpine regions, and landscape vegetation patterns across the study region are a mixed assemblage of open and closed forest, excluding the NDVI criterion from Landsat TM/ETM+ snow mapping likely had little effect on the cross-sensor comparison.

The cross-sensor linear snow map relationship appears insensitive to 'binary' or 'fractional' classification designations. Rittger et al. (2012) point out that a binary presence (absence) classification approach can tend to over- or underestimate snow cover around the snowline periphery in different elevational zones. They suggest that a FSC method enables more accurate snow cover estimates to be derived at the pixel level, and that MODSCAG out performs the Salmonson and Appel (2004) MODIS Terra NDSI model. While MODSCAG may achieve higher snow cover retrieval and classification accuracy over multiple spatial scales as validated by Landsat ETM+, it remains unclear how this method would perform in the temporal domain. This study indicates that daily swath MODIS Terra C6 FSC estimates are both spatially and temporally accurate as validated by Landsat TM and ETM+, and reiterates Salmonson and Appel's (2004) point that NDSI is operationally executable, a trade-off for algorithm complexity, and still, accurate FSC estimates can be generated at less than 10% RSME. Using previous MODIS snow product collections; a number of studies across regional-hemispheric geographic scales have found high MODIS Terra snow map accuracy using Landsat,

passive microwave SWE, and ground-based snow depth observations (Hall et al. 2001; Hall, Kelly, et al. 2002; Hall and Riggs 2007; Hall, Riggs, et al. 2002; Hall et al. 2000; Klein and Barnett 2003). The MODIS Terra C6 snow-mapping algorithm remains robust, and this cross-sensor validation indicates an encouraging improvement in the daily FSC product (MOD10_L2). When estimating 'binary' or 'fractional' snow cover from optical snow properties, producers and users should have awareness that converting from a spectral snow signal to an area measurement is assumed to be plausible and possible. When conducting cross-sensor snow map comparisons, it is crucial to distinguish between whether MODIS Terra or even Landsat Level-2 snow cover maps have been derived from Level-1 TOA or surface reflectance products. These image products are known to possess considerable spectral property differences that can influence pixel level retrieval of land surface properties (Feng et al. 2012; Vermote, El Saleous, and Justice 2002; Vermote and Kotchenova 2008)

It is well established that satellite-based snow map error can arise from differences in retrieval method, classification decisions, and mixed land surface spectral responses (Dozier and Painter 2004; Dozier et al. 2008; Rittger, Painter, and Dozier 2012). However, inherent sensor-specific measurement error during data acquisition has received less attention. Do sensor-specific properties potentially limit efforts to minimize snow map error even with advanced algorithm refinement? Inspection of MODIS Terra C6 and Landsat TM/ETM+ snow cover maps show that spatial resolution exerts a strong influence on the resolvability of fine-scale physiographic snow cover patterns in mountainous terrain. This reality supports a conceptual argument and FSC (binary SCA)

justification for moderate (high) resolution sensors like MODIS Terra and Landsat TM and ETM+. More importantly, MODIS Terra and Landsat TM and ETM+ also have different nadir viewing angles. Li et al. (2007) show that BDRF functions that assume Lambertian scattering can significantly effect snow albedo retrieval at off-nadir viewing angles. Xin et al. (2012) suggest that MODIS Terra consistently underestimates snow cover retrieval underneath dense forest at large viewing angles. Mapping snow underneath dense forest remains a long-standing challenge for visible snow retrieval (Hall et al. 1998; Klein, Hall, and Riggs 1998). Local solar illumination angles vary with time of day, between seasons, and between images (Dozier et al. 2008). This compounds snow albedo retrieval at off-nadir viewing angles, especially in topographically heterogeneous terrain (Dozier et al. 2008; Painter et al. 2009; Schaaf, Wang, and Strahler 2011). Dozier and Warren (1982) find that the infrared brightness temperature of snow can also be dependent on sensor viewing angle. In this study, MODIS Terra C6 appears to slightly overestimate FSC in mountainous terrain during spring snowmelt. This reasoning is based on the fact that not only does spring snow cover increase with elevation, but so does physiographic complexity. Although the MODIS Terra C6 NDSI FSC model exhibits high performance and acceptable FSC estimate accuracy, MODIS Terra may simply be less skillful when estimating FSC in steep mountainous terrain because of spatial resolution distortion due to sensor viewing geometry, variable solar illumination at off-nadir viewing angles, and assumed Lambertian scattering.

Although image processing is intended to reduce or normalize factors effecting pixel level radiance, the accumulated sum of sensor resolution, sensor viewing angle, and

aggregated environmental factors raises important questions about acceptable snow mapping uncertainty and error. This study shows that spatiotemporal snow map accuracy is high between MODIS Terra and Landsat TM/ETM+ despite differences in sensor-specific properties and snow cover classification decisions. More importantly, cross-sensor validation can be useful for establishing the range of inherent measurement confidence when mapping visible snow cover. Cross-sensor validation can also inform whether further snow algorithm refinement and proposed implementation can achieve higher accuracy. Two forward thinking solutions may be to first, focus on image processing algorithm refinement such as correcting for local solar illumination, and second, generate confidence intervals for snow cover estimates using temporal validation as undertaken in this analysis.

While strong spatial and temporal agreement between MODIS Terra C6 FSC and Landsat TM/ETM+ binary SCA was found for most map comparison dates, environmental conditions during time of acquisition and/or image acquisition frequency itself resulted in map disagreement. Map disagreement can be explained from a problem-based scenario. Two potential scenarios when cross-sensor validation can break down between MODIS Terra C6 FSC and Landsat TM/ETM+ SCA is one, when thin-patchy snow during low snow coverage occurs with high altitude cirrus cloud cover contamination, and two, transient snowfall during the spring snowmelt season. On May 30, 2001, the MODIS Terra cloud mask aggressively flagged high altitude cirrus clouds during low snow conditions. With its 500-meter spatial resolution, Hall and Riggs (2007) find that MODIS Terra has difficulty retrieving thin-patchy snow cover. Coupled

together, spectral distinction between thin-patchy snow and high altitude cirrus clouds using NDSI is likely less exact, and a well-known problem (Hall, Riggs, et al. 2002; Irish et al. 2006). High altitude cirrus clouds contain ice crystals that can introduce complications when spectrally distinguishing between optical snow and ice cloud properties.

Although Landsat TM and ETM+ has an acquisition frequency of 16 days, overlap between TM and ETM+ sensors can yield 8-day coverage for certain locations. Landsat's acquisition frequency and swath width remain primary limitations for operational snow cover mapping because image mosaicking is often required to obtain full coverage, and even produces a one-day offset as shown in this study. On May 24-25, 2002, late-season transient snowfall that occurred between May 22nd and 24th drove map disagreement. This snowfall event temporarily increased SCA for May 24th as observed by MODIS Terra and Landsat TM. SNOTEL SWE measurements from five out of six spatially independent sites across the study region showed a brief inflation in daily SWE. On May 25, 2002, transient snow cover melted before the Landsat ETM+ overpass. MODIS Terra also showed a reduction in SCA on May 25, 2002. This scenario points out Landsat's well-known snow cover mapping limitation, but if used in tandem with MODIS Terra and SNOTEL SWE, transient snowfall can be distinguished from resident snow cover.

Operational MODIS Terra snow products since 2000 support snow hydrology science, and many hydrological-based applications. For example, MODIS snow products have been assimilated into a macroscale variable infiltration capacity hydrological model

(Andreadis and Lettenmaier 2006), input into a snowmelt runoff model for water resource management (Butt and Bilal 2011), used to construct snow depletion curves during the melt season (Homan et al. 2011), used to estimate reservoir storage and forecasting (McGuire et al. 2006), and used to examine snowmelt and streamflow timing (Hall et al. 2012). For snow-specific hydrological studies, obtaining best possible results with minimal error is contingent on MODIS Terra snow product accuracy. This study validates daily swath MODIS Terra C6 FSC products, and finds that C6 FSC estimation is accurate in mountainous terrain per Landsat TM and ETM+ even without the 283 K temperature screen. Maintaining a commitment to improve satellite SCA and FSC estimation that includes temporal validation should remain a high priority. Even so, recognizing that sensor resolution, short-term fluctuations in environmental conditions, scaling issues, and product accuracy underpin modeled hydrological processes and patterns is essential (Bloschl 1999).

Conclusion

Daily swath MODIS Terra C6 FSC products (MOD10_L2) during the 2000s have been validated for peak spring snowmelt across central Idaho and southwestern Montana using Landsat TM and ETM+. The MODIS snow algorithm no longer includes the 283 K temperature screen when estimating daily FSC in mountainous terrain. It should be noted that daily swath MODIS Terra C6 FSC estimation could be sensitive to local solar illumination and sensor viewing geometry. Cross-sensor snow map disagreements can occur during high altitude cirrus cloud contamination during thin-patchy snow conditions, as well as transient snowfall during the melt season. The latter scenario points

out MODIS Terra's exceptional operational capacity to track fluctuating snow conditions at the daily timescale. Although Landsat's image acquisition frequency does remain limiting for operational snow cover mapping, several potential contributions have been realized. First, with careful attention towards image processing, NDSI remains a robust snow cover signal that can be exploited for operational FSC and SCA estimation. Second, strong spatial and temporal linear snow map agreement between MODIS Terra and Landsat TM/ETM+ indicates cross-sensor interoperability and confirms that a multi-sensor mapping approach will expand snow cover monitoring through resolution and time. Finally, using MODIS Terra's image acquisition frequency, Landsat's spatial resolution, and Landsat's historical image archive, multi-sensor CDR development is possible for decadal timescales. Visible multi-sensor CDRs are imperative for mountain snowpack extent monitoring in arid regions, and climate and hydrological applications to support freshwater management and forecasting.

References

Ackerman, S. A., K. I. Strabala, W. P. Menzel, R. A. Frey, C. C. Moeller, and L. E. Gumley. 1998. "Discriminating clear sky from clouds with MODIS." *Journal of Geophysical Research-Atmospheres* no. 103 (D24):32141-32157. doi: 10.1029/1998jd200032.

Andreadis, K. M., and D. P. Lettenmaier. 2006. "Assimilating remotely sensed snow observations into a macroscale hydrology model." *Advances in Water Resources* no. 29 (6):872-886. doi: 10.1016/j.advwatres.2005.08.004.

Antilla, S., Metsamaki S., and Derksen C. 2006. A comparison of Finnish SCAmod snow maps and MODIS snow maps in boreal forests in Finland and Manitoba, Canada. Paper read at Geoscience and Remote Sensing Symposium, 2006, IGARRS 2006.

Arno, S.F., and R.P. Hammerly. 1984. *Timberline Mountain and Arctic Forest Frontiers*. Seattle: The Mountaineers.

Bales, R. C., N. P. Molotch, T. H. Painter, M. D. Dettinger, R. Rice, and J. Dozier. 2006. "Mountain hydrology of the western United States." *Water Resources Research* no. 42 (8):13. doi: W0843210.1029/2005wr004387.

Barnett, T. P., J. C. Adam, and D. P. Lettenmaier. 2005. "Potential impacts of a warming climate on water availability in snow-dominated regions." *Nature* no. 438 (7066):303-309. doi: 10.1038/nature04141.

Barry, R. G. 2006. "The status of research on glaciers and global glacier recession: a review." *Progress in Physical Geography* no. 30 (3):285-306. doi: 10.1191/0309133306pp478ra.

Barry, R. G., J. M. Fallot, and R. L. Armstrong. 1995. "Twentieth-century variability in snow-cover conditions and approaches to detecting and monitoring changes: Status and prospects." *Progress in Physical Geography* no. 19 (4):520-532. doi: 10.1177/030913339501900405.

Barry, R. G. 2002. "The role of snow and ice in the global climate system: A review." *Polar Geography* no. 26 (3):235 - 246.

Bloschl, G. 1999. "Scaling issues in snow hydrology." *Hydrological Processes* no. 13 (14-15):2149-2175. doi: 10.1002/(sici)1099-1085(199910)13:14/15<2149::aid-hyp847>3.0.co;2-8.

Butt, M. J., and M. Bilal. 2011. "Application of snowmelt runoff model for water resource management." *Hydrological Processes* no. 25 (24):3735-3747. doi: 10.1002/hyp.8099.

Cayan, D. R. 1996. "Interannual climate variability and snowpack in the western United States." *Journal of Climate* no. 9 (5):928-948.

Crawford, C. J., S. M. Manson, M. E. Bauer, and D. K. Hall. 2013. "Multitemporal snow cover mapping in mountainous terrain for Landsat climate data record development." *Remote Sensing of Environment* no. 135 (0):224-233. doi:10.1016/j.rse.2013.04.004.

Dobreva, I. D., and A. G. Klein. 2011. "Fractional snow cover mapping through artifical neural network analysis of MODIS surface reflectance." *Remote Sensing of Environment* no. 115:3355-3366.

Dozier, J. 1984. "Snow reflectance from Landsat-4 Thematic Mapper " *IEEE Transactions on Geoscience and Remote Sensing* no. 22 (3):323-328.

———. 1989. "Spectral signature of alpine snow cover from the Landsat Thematic Mapper." *Remote Sensing of Environment* no. 28:9-22.

Dozier, J., and J. Frew. 1990. "Rapid calculation of terrain parameters for radiation modeling from digital elevation data." *IEEE Transactions on Geoscience and Remote Sensing* no. 28 (5):963-969.

———. 2009. "Computational provenance in hydrologic science: a snow mapping example." *Philosophical Transactions of the Royal Society a-Mathematical Physical and Engineering Sciences* no. 367 (1890):1021-1033. doi: 10.1098/rsta.2008.0187.

Dozier, J., and T. H. Painter. 2004. "Multispectral and hyperspectral remote sensing of alpine snow properties." *Annual Review of Earth and Planetary Sciences* no. 32:465-494. doi: 10.1146/annurev.earth.32.101802.120404.

Dozier, J., T. H. Painter, K. Rittger, and J. E. Frew. 2008. "Time-space continuity of daily maps of fractional snow cover and albedo from MODIS." *Advances in Water Resources* no. 31 (11):1515-1526. doi: 10.1016/j.advwatres.2008.08.011.

Draper, N.R., and H. Smith. 1998. *Applied Regression Analysis*. 3rd ed. Hoboken, NJ: Wiley-Interscience.

Feng, M., C. Q. Huang, S. Channan, E. F. Vermote, J. G. Masek, and J. R. Townshend. 2012. "Quality assessment of Landsat surface reflectance products using MODIS data." *Computers & Geosciences* no. 38 (1):9-22. doi: 10.1016/j.cageo.2011.04.011.

Foster, J. L., D. K. Hall, J. B. Eylander, G. A. Riggs, S. V. Nghiem, M. Tedesco, E. Kim, P. M. Montesano, R. E. J. Kelly, K. A. Casey, and B. Choudhury. 2011. "A blended global snow product using visible, passive microwave and scatterometer satellite data." *International Journal of Remote Sensing* no. 32 (5):1371-1395. doi: 10.1080/01431160903548013.

Hall, D. K., J. L. Foster, N. E. DiGirolamo, and G. A. Riggs. 2012. "Snow cover, snowmelt timing and stream power in the Wind River Range, Wyoming." *Geomorphology* no. 137 (1):87-93. doi: 10.1016/j.geomorph.2010.11.011.

Hall, D. K., J. L. Foster, V. V. Salomonson, A. G. Klein, and J. Y. L. Chien. 2001. "Development of a technique to assess snow-cover mapping errors from space." *IEEE Transactions on Geoscience and Remote Sensing* no. 39 (2):432-438.

Hall, D. K., J. L. Foster, D. L. Verbyla, A. G. Klein, and C. S. Benson. 1998. "Assessment of snow-cover mapping accuracy in a variety of vegetation-cover densities in central Alaska." *Remote Sensing of Environment* no. 66 (2):129-137.

Hall, D. K., R. E. J. Kelly, G. A. Riggs, A. T. C. Chang, and J. L. Foster. 2002. "Assessment of the relative accuracy of hemispheric-scale snow-cover maps." In *Annals of Glaciology, Vol 34, 2002*, edited by J. G. Winther and R. Solberg, 24-30. Cambridge: Int Glaciological Soc.

Hall, D. K., and J. Martinec. 1985. *Remote Sensing of Ice and Snow*. New York: Chapman and Hall.

Hall, D. K., and G. A. Riggs. 2007. "Accuracy assessment of the MODIS snow products." *Hydrological Processes* no. 21 (12):1534-1547. doi: 10.1002/hyp.6715.

———. 2011. Normalized-Difference Snow Index (NDSI), Encylopedia of Earth Sciences Series. In *Encylopedia of snow, ice and glaciers*, edited by V. P. Singh, P. Singh and U. K. Haritashya: Springer.

Hall, D. K., G. A. Riggs, and V. V. Salomonson. 1995. "Development of methods for mapping global snow cover using moderate resolution imaging spectroradiometer data." *Remote Sensing of Environment* no. 54 (2):127-140. doi: 10.1016/0034-4257(95)00137-p.

Hall, D. K., G. A. Riggs, V. V. Salomonson, N. E. DiGirolamo, and K. J. Bayr. 2002. "MODIS snow-cover products." *Remote Sensing of Environment* no. 83 (1-2):181-194.

Hall, D. K., A. B. Tait, J. L. Foster, A. T. C. Chang, and M. Allen. 2000. "Intercomparison of satellite-derived snow-cover maps." In *Annals of Glaciology, Vol 31, 2000*, edited by K. Steffen, 369-376. Cambridge: Int Glaciological Soc.

Homan, J. W., C. H. Luce, J. P. McNamara, and N. F. Glenn. 2011. "Improvement of distributed snowmelt energy balance modeling with MODIS-based NDSI-derived fractional snow-covered area data." *Hydrological Processes* no. 25 (4):650-660. doi: 10.1002/hyp.7857.

Irish, R. R., J. L. Barker, S. N. Goward, and T. Arvidson. 2006. "Characterization of the Landsat-7 ETM+ automated cloud-cover assessment (ACCA) algorithm." *Photogrammetric Engineering and Remote Sensing* no. 72 (10):1179-1188.

Klein, A. G., and A. C. Barnett. 2003. "Validation of daily MODIS snow cover maps of the Upper Rio Grande River Basin for the 2000-2001 snow year." *Remote Sensing of Environment* no. 86 (2):162-176. doi: 10.1016/s0034-4257(03)00097-x.

Klein, A. G., D. K. Hall, and G. A. Riggs. 1998. "Improving snow cover mapping in forests through the use of a canopy reflectance model." *Hydrological Processes* no. 12 (10-11):1723-1744.

Li, W., K. Stamnes, H. Eide, and R. Spurr. 2007. "Bidirectional reflectance distribution function of snow: corrections for the Lambertian assumption in remote sensing applications." *Optical Engineering* no. 46 (6). doi: 06620110.1117/1.2746334.

McGuire, M., A. W. Wood, A. F. Hamlet, and D. P. Lettenmaier. 2006. "Use of satellite data for streamflow and reservoir storage forecasts in the snake river basin." *Journal of Water Resources Planning and Management-Asce* no. 132 (2):97-110. doi: 10.1061/(asce)0733-9496(2006)132:2(97).

Metsamaki, S., J. Vepsalainen, J. Pulliainen, and Y. Sucksdorff. 2002. "Improved linear interpolation method for the estimation of snow-covered area from optical data." *Remote Sensing of Environment* no. 82 (1):64-78. doi: 10.1016/s0034-4257(02)00025-1.

Mitchell, V.L. 1976. "The regionalization of climate in the western United States." *Journal of Applied Meteorology* no. 15 (9):920-927.

Painter, T. H., K. Rittger, C. McKenzie, P. Slaughter, R. E. Davis, and J. Dozier. 2009. "Retrieval of subpixel snow covered area, grain size, and albedo from MODIS." *Remote Sensing of Environment* no. 113 (4):868-879. doi: 10.1016/j.rse.2009.01.001.

Pepe, M., P. A. Brivio, A. Rampini, F. R. Nodari, and M. Boschetti. 2005. "Snow cover monitoring in alpine regions using ENVISAT optical data." *International Journal of Remote Sensing* no. 26 (21):4661-4667.

Rittger, K., T. H. Painter, and J. Dozier. 2012. "Assessment of methods for mapping snow cover from MODIS." *Advances in Water Resources* (0). doi: 10.1016/j.advwatres.2012.03.002.

Rosenthal, W., and J. Dozier. 1996. "Automated mapping of montane snow cover at subpixel resolution from the Landsat Thematic Mapper." *Water Resources Research* no. 32 (1):115-130.

Salminen, M., J. Pulliainen, S. Metsamaki, A. Kontu, and H. Suokanerva. 2009. "The behaviour of snow and snow-free surface reflectance in boreal forests: Implications to the performance of snow covered area monitoring." *Remote Sensing of Environment* no. 113 (5):907-918. doi: 10.1016/j.rse.2008.12.008.

Salomonson, V. V., and I. Appel. 2004. "Estimating fractional snow cover from MODIS using the normalized difference snow index." *Remote Sensing of Environment* no. 89 (3):351-360. doi: 10.1016/j.rse.2003.10.016.

———. 2006. "Development of the Aqua MODIS NDSI fractional snow cover algorithm and validation results." *IEEE Transactions on Geoscience and Remote Sensing* no. 44 (7):1747-1756. doi: 10.1109/tgrs.2006.876029.

Schaaf, C. B., Z. S. Wang, and A. H. Strahler. 2011. "Commentary on Wang and Zender-MODIS snow albedo bias at high solar zenith angles relative to theory and to in situ observations in Greenland." *Remote Sensing of Environment* no. 115 (5):1296-1300. doi: 10.1016/j.rse.2011.01.002.

Seidel, K., and J. Martinec. 2004. *Remote Sensing in Snow Hydrology Runoff Modeling, Effect of Climate Change*. Chichester, UK: Praxis Publishing.

Shinker, J. J. 2010. "Visualizing spatial heterogeneity of western U.S. climate variability." *Earth Interactions* no. 14. doi: 1010.1175/2010ei323.1.

Vermote, E. F., N. Z. El Saleous, and C. O. Justice. 2002. "Atmospheric correction of MODIS data in the visible to middle infrared: first results." *Remote Sensing of Environment* no. 83 (1-2):97-111. doi: 10.1016/s0034-4257(02)00089-5.

Vermote, E. F., and S. Kotchenova. 2008. "Atmospheric correction for the monitoring of land surfaces." *Journal of Geophysical Research-Atmospheres* no. 113 (D23). doi: D23s9010.1029/2007jd009662.

Xin, Q. C., C. E. Woodcock, J. C. Liu, B. Tan, R. A. Melloh, and R. E. Davis. 2012. "View angle effects on MODIS snow mapping in forests." *Remote Sensing of Environment* no. 118:50-59. doi: 10.1016/j.rse.2011.10.029.

Chapter 4: Evidence for Spring Mountain Snowpack Retreat from a Landsat-Derived Snow Cover Climate Data Record

A Landsat snow cover climate data record (CDR) of visible mountain snow-covered area (SCA) across interior northwestern USA during spring was compared with ground-based snow telemetry (SNOTEL) snow-water-equivalent (SWE) measurements and mean surface temperature and total precipitation observations. Landsat spring SCA on June 1st was positively correlated with May 15th and June 1st SWE, negatively correlated with spring temperatures (April-June), and positively correlated with March precipitation. Using linear regression with predicted residual error sum-of-squares (PRESS) cross-validation, spring SCA was reconstructed (1901-2009) for the mountains of central Idaho and southwestern Montana using instrumental spring surface temperature records. The spring SCA reconstruction shows natural internal variability at interannual to decadal timescales including above average SCA in the 1900s, 1910s, 1940s-1970s, and below average SCA in the 1920s, 1930s, and since the mid 1980s. The reconstruction also reveals a centennial trend towards decreasing spring SCA with estimated losses of -36.2% since 1901. Based on the inferred thermal relationship between temperature and snow, strong evidence emerges for mountain snowpack retreat triggered by spring warming, a signal that includes both feedback and response mechanisms. Expanding snow cover CDRs to include additional operational satellite retrievals will add temporal SCA estimates during other snow accumulation and melt intervals for improved satellite-instrumental climate model calibration. Merging Landsat snow cover CDRs with instrumental climate records is a formidable method to monitor climate-driven changes in western US snowpack extent over 20th and 21st centuries.

1. Introduction

Documenting climate variability and change is dependent on the source of evidence and its observational timescale. While instrumental, proxy, and written historical records provide most of the primary data for climate assessment and interpretation on interannual to centennial timescales, Earth observing satellites and their data retrievals exist as a recent type of climate record since the mid 1960s (Matson and Wiesnet 1981). In 1972, the Landsat mission launched with the Multi-Spectral Scanner (MSS), and since that time, additional platforms have followed including the Thematic Mapper (TM), Enhanced Thematic Mapper Plus (ETM+), and now the Landsat Data Continuity Mission (LDCM). Thus, Landsat's observational timescale possesses key attributes for climate data record (CDR) development. The suite of Landsat platforms includes a continuous period of recurrent multispectral measurements, and with LDCM now retrieving imagery into the next decade; the Landsat record continues to grow on climatically relevant timescales (i.e., beyond the 30 year normal). More specifically, and arguably the most valuable attribute, data users have no cost access to the image archive at the USGS EROS Data Center. Coupled together, these characteristics place Landsat at the core of climate-cyrosphere CDR derivation and study.

Climatic warming poses serious threats to the seasonal cyrosphere (Barry 2002). As Earth's climate system continues to evolve and change, more satellite retrievals are acquired and archived, and future missions are planned, the significance of CDRs increase. Global and regional climate model projections show agreement on the pace of temperature rise in the coming decades (Meehl and Teng 2012; Teng, Buja, and Meehl

2006) even though precipitation models remain less certain regarding the liquid content of snow (Duffy et al. 2006). Successive snow cover accumulation during the cool season followed by spring melt is vital for snow-dominated freshwater systems (Barnett, Adam, and Lettenmaier 2005), but is sensitive to short and long-term temperature change (Barry 2006; Barry 2002; Barry, Fallot, and Armstrong 1995). Across the arid western United States, seasonal mountain snowpack accumulation and melt contributes approximately 50-70% to the total annual freshwater resource thru snow-fed streamflow (Cayan 1996; Redmond and Koch 1991). Several western US studies on snow course and snow telemetry (SNOTEL) snow-water-equivalent (SWE) measurements indicate that mountain snowpack is declining because of warming springtime temperatures (Cayan et al. 2001; Mote et al. 2005; Pierce et al. 2008; Westerling et al. 2006; Hamlet et al. 2005). Yet, satellite-based study on mountain snowpack spatiotemporal variability is insufficient because CDRs do not yet exist for decadal timescales. To achieve this, CDRs derived from Landsat snow-covered area (SCA) estimates since the early 1970s fill this data need, especially for freshwater-sensitive regions of the western US. In response, this paper compares a Landsat derived snow cover CDR (Crawford et al. 2013) with ground-based SNOTEL SWE, and surface temperature and precipitation observations. Landsat SCA is then reconstructed using instrumental climate records to examine longer-term trends in spring snowpack extent.

Merging satellite observations with ground-based instrumental data has been proposed as a means to advance study on seasonal snow properties including extent, duration, depth, and water equivalent at finer spatial scales in mountainous terrain (Bales

et al. 2006; Barry, Fallot, and Armstrong 1995; Frei, Robinson, and Hughes 1999; Robinson 1991). Snow accumulation, distribution, and melt heterogeneity is controlled by physiography, radiation, and energy exchanges, which in total, contributes significantly to snow cover and SWE variation across watershed-basin scales (Elder, Dozier, and Michaelsen 1991; Anderton, White, and Alvera 2004; Cline, Bales, and Dozier 1998). Comparisons between point-based SNOTEL SWE measurements and a continuous mean SWE grid has shown that SNOTEL SWE may not be representative across multiple spatial scales that in part, reflect sampling density and instrument location in areas with disproportionate accumulation and ablation rates (Molotch and Bales 2005). Furthermore, a high proportion of SNOTEL measurements across the western US do not start until the late 1970s (Serreze et al. 1999), and are located in mid elevation zones with little sampling stratification across low and high elevation regions (Bales et al. 2006). This leaves SWE inadequately monitored in many high alpine basins (Nolin 2012). Even so, satellite snow cover retrievals provide continuous spatial observations that can be exploited in the form of CDRs to monitor SCA over mountainous terrain. Adopting this Landsat snow cover CDR approach is especially powerful for identifying watersheds or basins where significant climate-driven changes in mountain snowpack are occurring. Merging satellite CDRs with SNOTEL SWE and instrumental climate records is not a replacement for current modeling efforts, only an additional method to track snow cover (snowpack) accumulation and melt trends on longer timescales. This method is particularly important for understanding alpine snowpack change and streamflow timing (Lundquist and Dettinger 2005; Stewart, Cayan, and Dettinger 2005; McCabe and Clark

2005; Dettinger and Cayan 1995), as well as identifying low elevation zones where temperature-driven phase changes in precipitation are already underway (Knowles, Dettinger, and Cayan 2006; Hall et al. 2012; Nolin and Daly 2006).

Landsat snow cover CDRs have three spatiotemporal dimensions to examine mountain snowpack variability and change that include SCA extent (spatial domain), SCA elevational zonation (vertical domain), and SCA time-series variance (time domain). SCA variability within each of these domains can be directly compared with SNOTEL SWE and surface temperature and precipitation using time-series analysis techniques. This paper uses a Landsat snow cover CDR that has been developed for spring peak snowmelt timing for an interior northwestern USA sub-region, namely the mountains of central Idaho and southwestern Montana (Crawford et al. 2013). The objectives are to (1) statistically compare Landsat SCA with SNOTEL SWE; (2) statistically compare Landsat SCA with surface temperature and precipitation observations; and (3) reconstruct Landsat SCA during 20th and early 21st centuries to document long-term mountain SCA trends during spring melt.

2. Methods

2.1 *Landsat CDR Description and Instrumental Climate Data*

Landsat snow cover CDR coverage is centered over the mountains of central Idaho and southwestern Montana in the interior northwestern USA (Figure 1). This CDR has been derived from the Landsat image archive including MSS, TM, and ETM+ imagery, and includes June 1 SCA (hereinafter spring SCA) as the spring snowmelt target (Crawford et al. 2013). The spring SCA CDR spans 1975-2011 with missing SCA estimates in 1973,

1974, 1978-1982, 1987, and 1988 because of missing image coverage or cloud cover contamination. Specific methods for Landsat data processing and CDR development are outlined in Crawford et al. (2013). SNOTEL SWE measurements for six stations falling within the study region (Figure 1) were collected from the Natural Resource Conservation Service (NRCS) National Water and Climate Center at http://www.wcc.nrcs.usda.gov/snow/. SNOTEL station metadata is summarized in Table 1. The high-resolution (0.5° x 0.5°) Climate Research Unit (CRU), University of East Anglia TS3.1 surface temperature and precipitation grid (Mitchell and Jones 2005) was accessed through http://iridl.ldeo.columbia.edu/, and grid points for the study region were extracted (Figure 1).

2.2 *Study Region Description*

The central Idaho and southwestern Montana mountains are part of the northern Rocky Mountain region, and situated in a mid-latitude continental position with steep vertical relief and fine scale topographic variability. The regional climate is semi-arid with a peak precipitation maximum during spring-early summer (Shinker 2010; Mitchell 1976). For this continental region, maximum snowpack accumulation occurs between early-mid April with peak snowmelt during early June (Cayan 1996). Snow coverage during spring is largely confined to the mid and high elevations. Low elevation zones have already melted out during early spring.

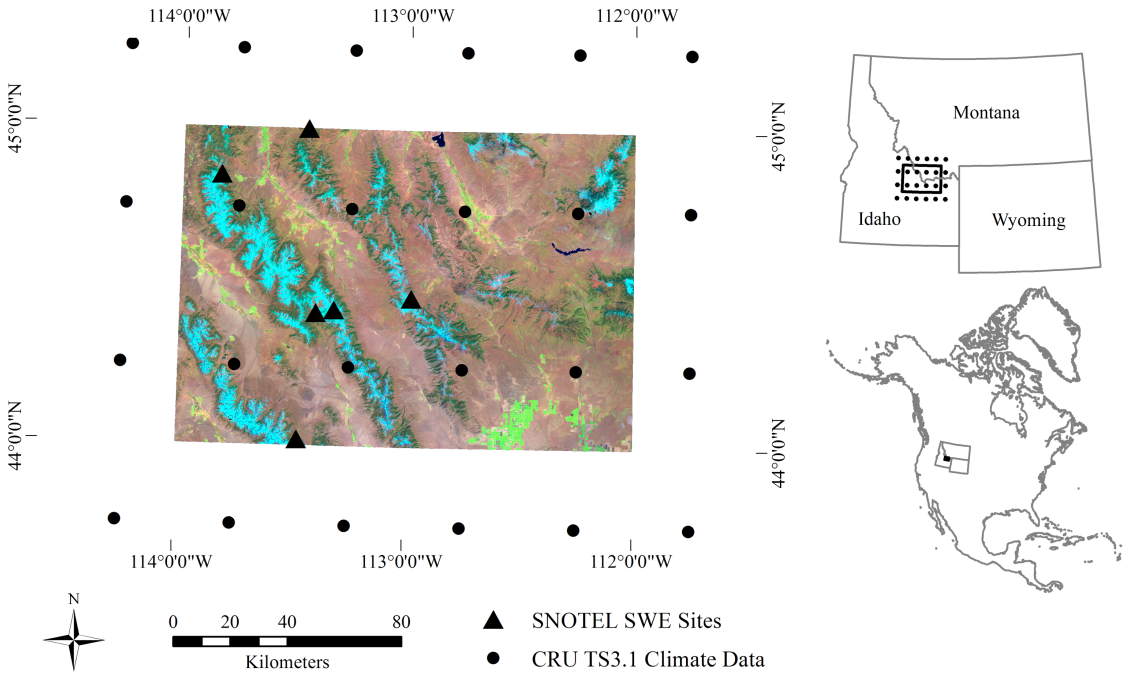

Figure 1. A false-color Landsat TM/ETM+ composite of the interior northwestern USA study region including the mountains of central Idaho and southwestern Montana. This is the spatially explicit domain for the snow cover CDR. The distribution of ground-based instrumental climate records is shown.

2.3 *Landsat SCA – SNOTEL SWE Comparison*

Bi-monthly SNOTEL SWE for April 1, April 15, May 1, May 15, and June 1 for each station were converted into z-scores using the station mean and standard deviation for the period of record. Estimated SWE prior to the start of snow telemetry on the 1st and 15th day of each month were excluded from the analysis. A six-station regional SWE z-score time-series was constructed using the six-station mean and standard deviation. The regional SWE time-series was adjusted for the number of stations because of differing start dates. Spring SCA (i.e., a normalized percentage, see Crawford et al. (2013)) estimates for 1975-2009 were compared with individual station SWE and regional SWE using scatterplots, linear fits, and correlation analysis. The selected time period for comparison was based on time-series overlap and data availability.

2.4 *Landsat SCA Correction*

During the spring snowmelt season, transient snowfall events in mountainous terrain are difficult to distinguish from resident snow cover when satellite image acquisitions are not daily (Li et al. 2008). Since Landsat's image acquisition frequency is 16-18 days, transient snowfall can inflate SCA on the day of Landsat overpass and must be corrected. To correct for transient snowfall, Landsat SCA estimates are converted into z-scores using the SCA mean and standard deviation for the period of record. Positive SCA estimates falling beyond 1.96 (> 95% confidence interval, one-tailed test) standard deviations are flagged as possible anomalies and are subject to further evaluation. Scatterplots between SCA z-scores and regional SNOTEL SWE z-scores are used to identify outliers and the year of occurrence. Once the year has been identified, daily

SNOTEL SWE measurements for stations falling within the CDR geographic domain are inspected for days preceding Landsat's overpass. Transient snowfall is confirmed within 1-3 days if SWE temporarily increases along a seasonally decreasing SWE curve (i.e., snowmelt curve). It is preferable to observe SWE increases at multiple SNOTEL stations within the CDR domain. A Landsat SCA correction is then applied by removing the SCA outliers, deriving a linear equation that relates SCA to regional SWE, and then uses regional SWE to predict resident SCA for years with transient snowfall. This Landsat SCA correction approach mimics the widely used methods in statistical climatology to estimate missing values for in situ climate data (Eischeid et al. 1995; Peterson et al. 1998).

2.5 *Landsat SCA – Surface Temperature and Precipitation Comparison*

Spring SCA estimates for 1975-2009 were compared with mean monthly surface temperature and total monthly precipitation for months January to June using scatterplots, linear fits, and correlation analysis. SCA estimates were also compared with seasonalized mean temperature (i.e., mean) and total accumulated precipitation (i.e., sum). Regional mean temperature and total precipitation time-series were constructed from CRU TS3.1 grid points covering the CDR region that included 0.5° grid points surrounding the CDR boundary to reduced edge effects (Figure 1). The regional mean temperature time-series was calculated using the average of all grid points (Jones and Hulme 1996). The regional precipitation time-series was calculated using unrotated principal component analysis (PCA) to identify the dominant spatial mode of precipitation variability at monthly and

seasonal timescales (Comrie and Glenn 1998). The statistical significance of each correlation coefficient was tested at $p<0.05$ (two-tailed).

2.6 *Landsat SCA Reconstruction and Trend Analysis*

Spring SCA estimates were reconstructed for the CDR region during 1901-2009 using regional CRU TS3.1 instrumental climate records. A stepwise 'leave-one-out' linear regression model with predicted residual error sum-of-squares (PRESS) cross-validation was employed to develop the spring SCA reconstruction (Michaelsen 1987; Wilks 1995). The pool of potential predictor variables included statistically significant monthly and seasonal mean temperature and total precipitation correlations. Because the Landsat spring SCA CDR was continuous only for 1989-2009, this 21-year period was used for model calibration. 'Leave-one-out' validation statistics were generated for each step to assess model skill and accuracy during the calibration period. A Durbin-Watson test assessed model residuals for autocorrelation, and regression residuals were evaluated for trend and randomness using Portmanteau's Q test statistic (Ostrom 1990). The reduction of error (RE) and root-mean-squared error ($RSME_v$) cross-validation statistics determined model construction, fit, and performance (Michaelsen 1987). Error bars were generated for $p=0.10$ and $p=0.90$ (80% confidence level) for the final spring SCA reconstruction to insure the plausibility of SCA estimates given model uncertainty.

Since the Landsat spring SCA CDR was discontinuous with missing SCA estimates in 1973, 1974, 1978-1982, 1987, and 1988, reconstruction model verification was carried out using independent Landsat spring SCA estimates in 1975, 1976, 1977, and 1983-1986. Reconstructed and observed spring SCA estimates having the same z-

score (i.e., reconstructed and observed SCA estimates where scaled to the calibration spring SCA mean and standard deviation) positive (negative) sign were considered 'successful predictions' because of a limited number of verification samples (n=7). An exact binomial probability test was used to distinguish 'successful predictions' from random chance (p=0.5). Finally, reconstructed spring SCA estimates during 1901-2009 were evaluated for trend using a modified Mann-Kendall test (Yue and Wang 2004). This non-parametric technique removes the serial correlation from the time-series, and then uses a Mann-Kendall test to determine whether the trend is statistically significant given an effective sample size. A percent SCA change estimate was also derived for the 1901-2009 reconstruction.

3. Results

3.1 *Landsat SCA – SNOTEL SWE Comparison*

Landsat spring SCA is positively correlated with SNOTEL SWE at individual stations within the CDR region (Table 1). The strongest spring SCA-SWE association corresponds to previous May 15 bi-monthly SWE. SCA correlations are much weaker for preceding bi-monthly SWE intervals and show a varying individual station response. The elevational difference between SNOTEL SWE station measurements, and local scale snowmelt timing, prevents SCA-SWE comparisons later in the snowmelt season. Landsat spring SCA is positively correlated with regional SWE during previous May 15 and current June 1 bi-monthly intervals, respectively (Figure 2). Transient snowfall events during the snowmelt season significantly affect the SCA-SWE linear relationship in time (Figure 2).

Table 1. Landsat spring SCA-SNOTEL SWE correlation coefficients.

SNOTEL Station	Lat./Long.	Elevation (m)	Time Period	(n)	April 1	April 15	May 1	May 15	June 1
Idaho 524	44.02,-113.47	2438	1981-2009	23	0.41*	0.45*	0.62*	0.80*	na
Idaho 620	44.43,-113.32	2852	1982-2009	21	0.11	0.11	0.26	0.52*	0.55*
Idaho 636	44.42,-113.40	2268	1982-2009	23	0.37	0.47*	0.65*	0.81*	na
Idaho 915	44.85,-113.83	2603	1996-2009	13	0.14	0.14	0.32	0.74*	na
Montana 318	44.47,-112.98	2698	1979-2009	23	0.35	0.61*	0.82*	na	na
Montana 576	45.00,-113.45	2469	1976-2009	25	0.36	0.55*	0.76*	na	na

* two-tailed significance ($p<0.05$)
na: no comparison was made because snow had already melted for SNOTEL SWE sites
Note: the time period for analysis is restricted to years with available Landsat SCA estimates

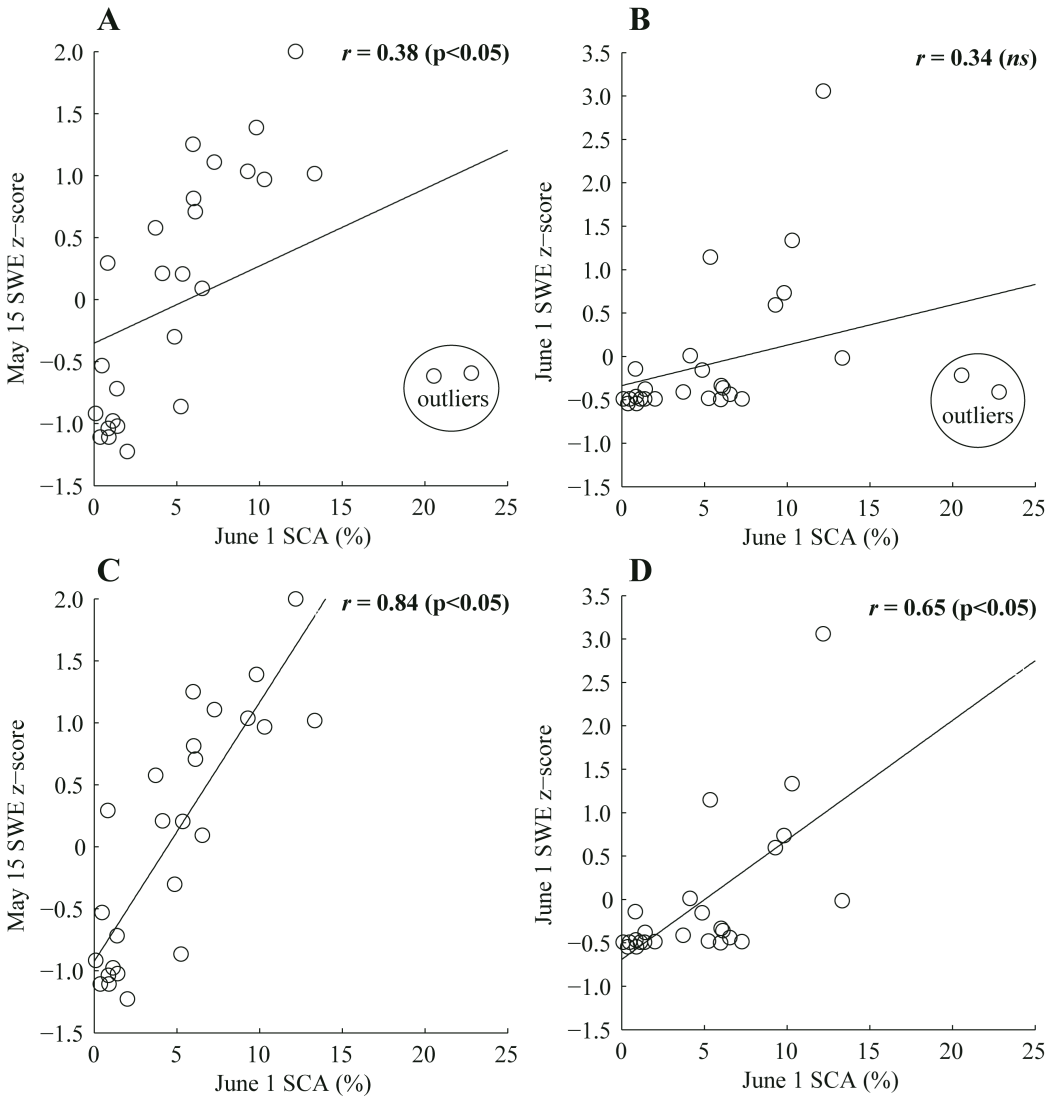

Figure 2. Scatterplots, linear fits, and correlation coefficients between SCA and SNOTEL SWE for 1976-2009: a) June 1 SCA and regional May 15 SWE with 1990 and 2002 transient snowfall outliers; b) June 1 SCA and regional June 1 SWE with 1990 and 2002 transient snowfall outliers; c) June 1 SCA and regional May 15 SWE without outliers; d) June 1 SCA and regional June 1 SWE without outliers. Note the change in SWE z-scores along the y-axis. *NS* indicates no statistical significance.

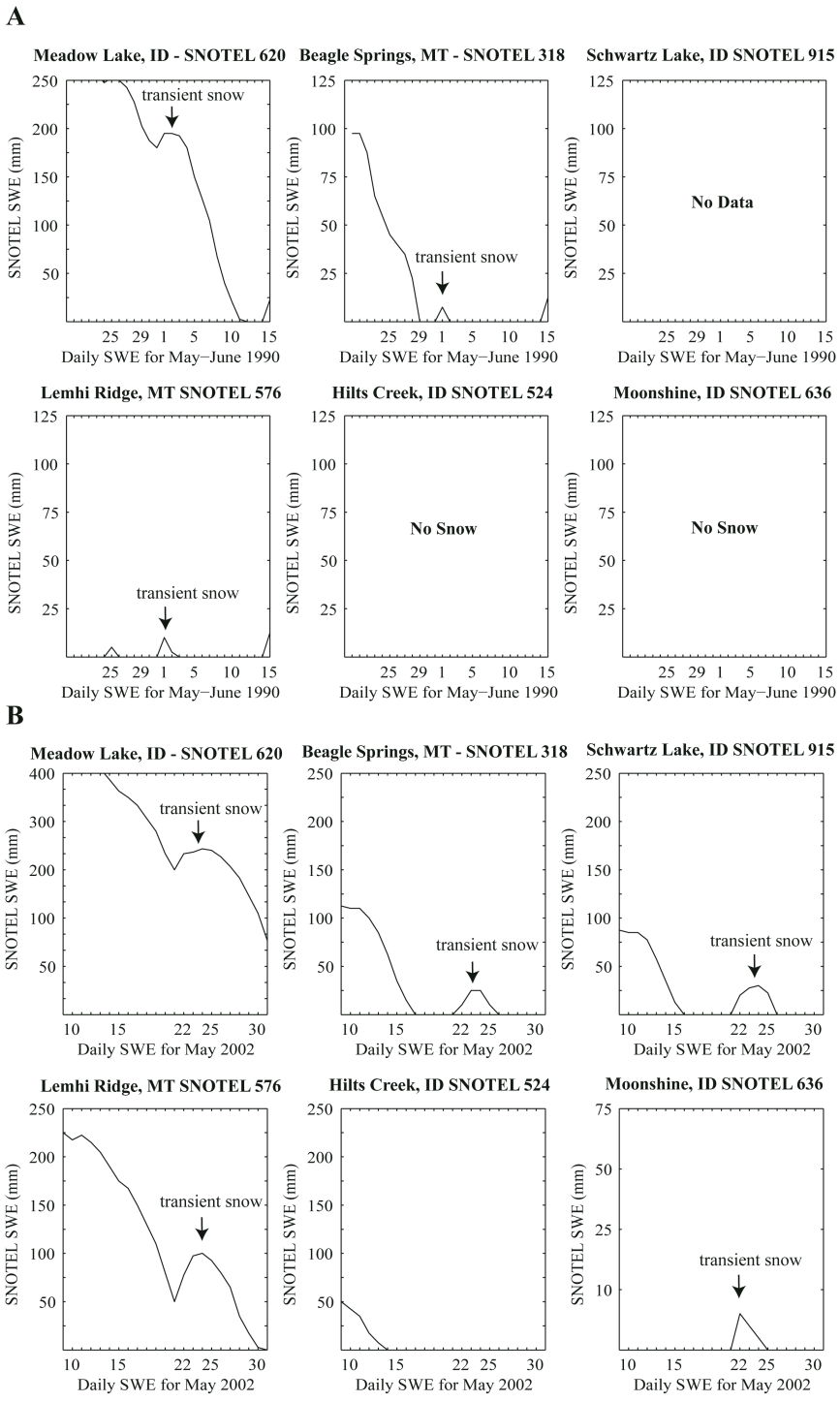

Figure 3. Daily SNOTEL SWE measurements for a) 1990 and b) 2002. Note the temporary increase in daily SWE highlighted by transient snowfall labels. For 1990, Idaho SNOTEL 915 did not have SWE measurements and had already melted for Idaho SNOTEL 524 and 636. Note the change in SWE (mm) along the y-axis.

3.2 *Landsat SCA Correction*

Transient snowfall events inflated Landsat spring SCA estimates, and were identified as statistical outliers in years 1990 and 2002 (Figure 2). Daily SNOTEL SWE measurements preceding Landsat's overpass in 1990 and 2002 showed temporary SWE increases along a continuously decreasing snowmelt curve (Figure 3). For 1990, three SNOTEL stations with available SWE measurements recorded a transient snowfall event between May 31 and June 1. For 2002, five SNOTEL stations recorded a transient snowfall event between May 22 and May 24. Spring SCA estimates for 1990 and 2002 were removed from the CDR, and resident spring SCA was estimated using May 15 regional SWE for 1990 and 2002.

3.3 *Landsat SCA – Surface Temperature and Precipitation Comparison*

Landsat spring SCA is negatively correlated with regional April, May, and June mean temperature (Figure 4). Spring SCA had the strongest inverse response to regional spring mean temperature (April-June) (Figure 4). Spring SCA was also positively correlated with regional March precipitation PC-1 (r=0.38, p<0.05, not shown).

3.4 *Landsat SCA Reconstruction and Trend Analysis*

Landsat spring SCA was reconstructed (1901-2009) for the CDR region using May-June mean temperature (Figure 5a and 5b). May-June mean temperature was the only statistically significant stepwise 'leave-one-out' regression predictor for the 1989-2009 calibration period. The model explained 58% (adj. r^2) of the spring SCA variance with strong PRESS validation statistics (Table 2). Durbin-Watson and Portmanteau Q test statistics indicated no significant autocorrelation, no trend, and pure randomness in the

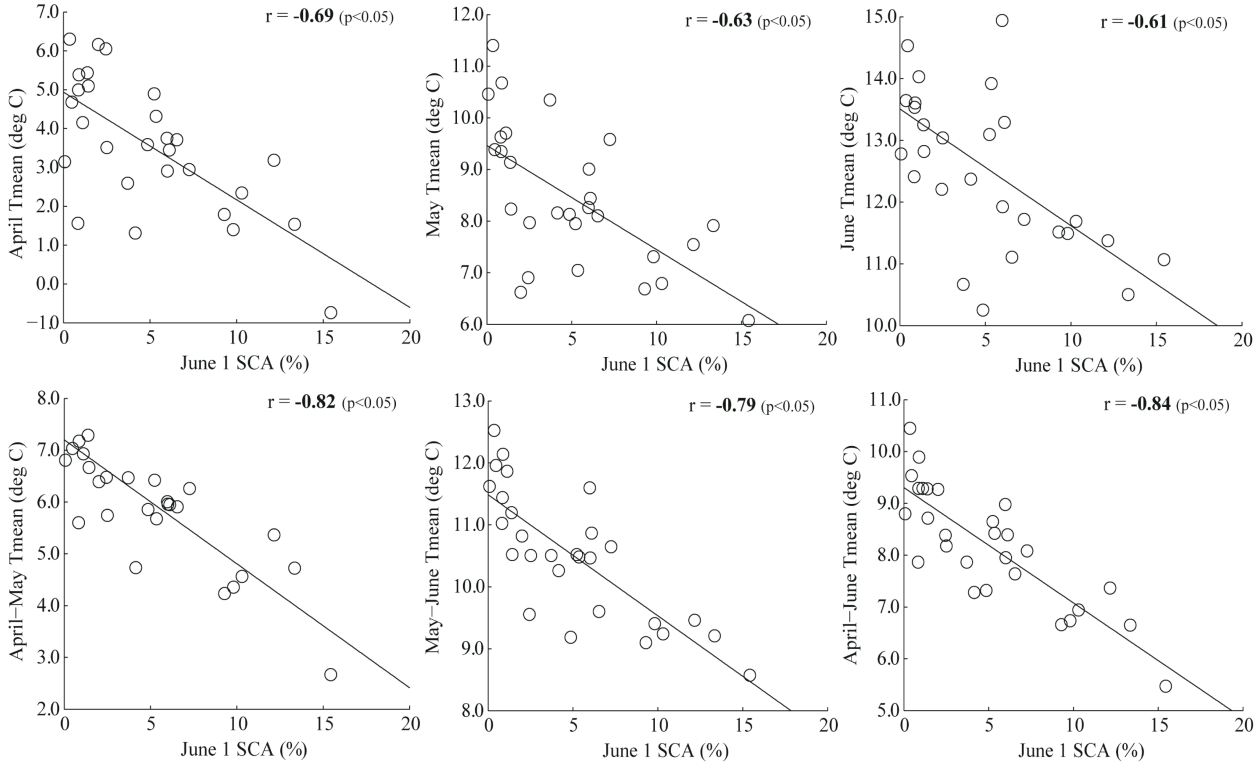

Figure 4. Scatterplots, linear fits, and correlation coefficients between June 1 SCA and spring mean temperature (April-June) for the CDR region. Note the change in monthly and seasonal temperatures (degrees Celsius) along the y-axis.

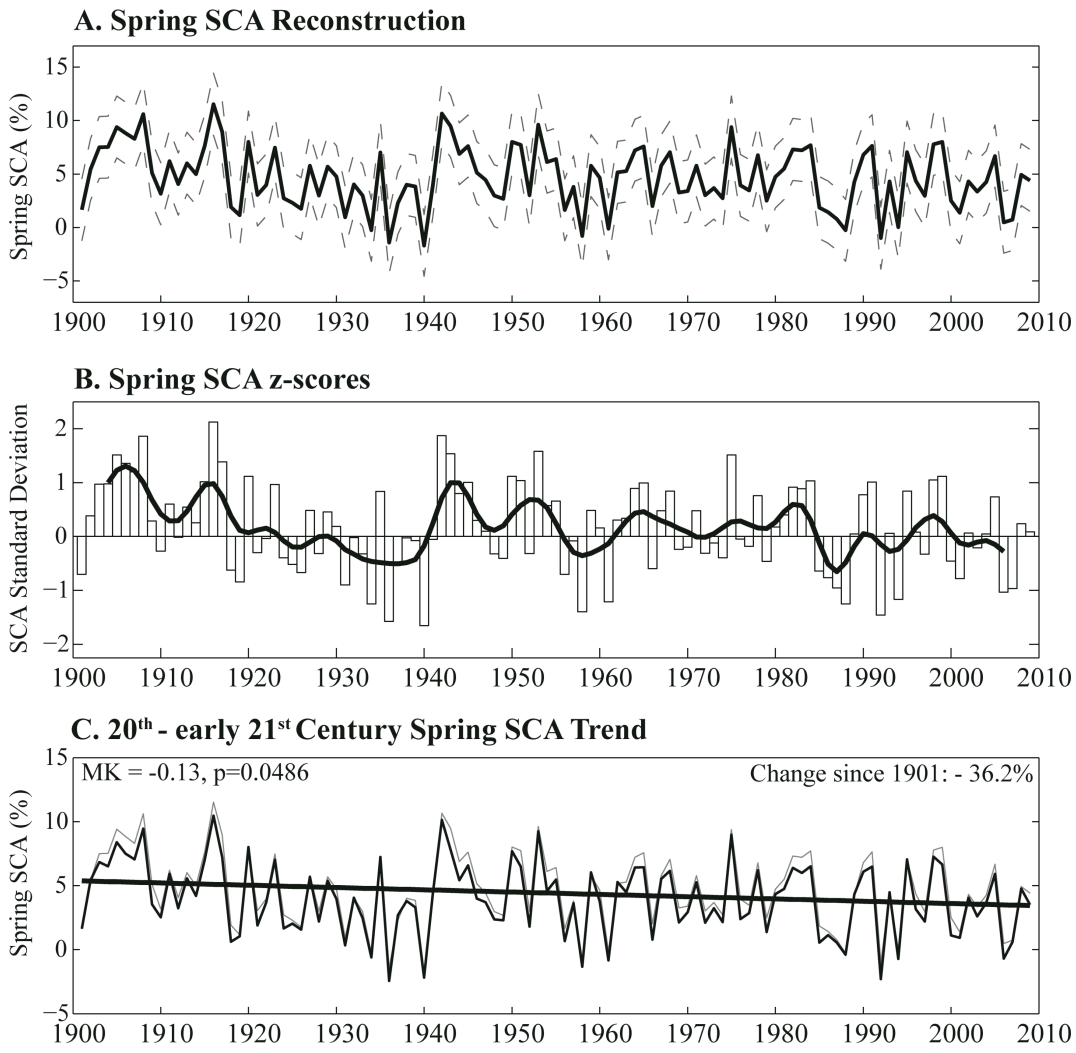

Figure 5. Spring SCA reconstruction for 1901-2009 using instrumental spring mean temperature records: a) SCA reconstruction (black line) with 80% confidence intervals (gray dotted lines); b) normalized SCA scaled to the calibration mean and standard deviation (1989-2009) with a 50% frequency response 9 year binomial filter (black line); c) centennial spring SCA trend with (black line) and without serial autocorrelation (gray line).

Table 2. Spring SCA reconstruction model statistics.

Target		Predictor		Reconstruction	Port. Q	DW
Spring SCA		May-June Tmean*		1901-2009	10.52 (p=0.40)	2.28 (Accept)
PRESS Calibration 1989-2009						
R^2	Adj. R^2	F-stat.	*p*-value	Std. Error	RE	$RSME_v$
0.60	0.58	28.28	<0.001	0.022	0.50	0.023

*CRU TS3.1 regional mean temperature
Port. Q: Portmanteau Q statistic tests whether regression residuals are purely random or white noise.
DW: Durbin-Watson statistic tests for autocorrelation in residuals at lag-1. The null hypothesis states that there is no autocorrelation. The decision is 'Accept' or 'Reject'.
RE: Reduction of error statistic measures reconstruction skill in excess of climatology, and is based on the calibration mean. A positive value > 0 indicates forecast skill.
$RSME_v$: Root mean square error - a 'leave-one-out' PRESS cross-validation statistic.

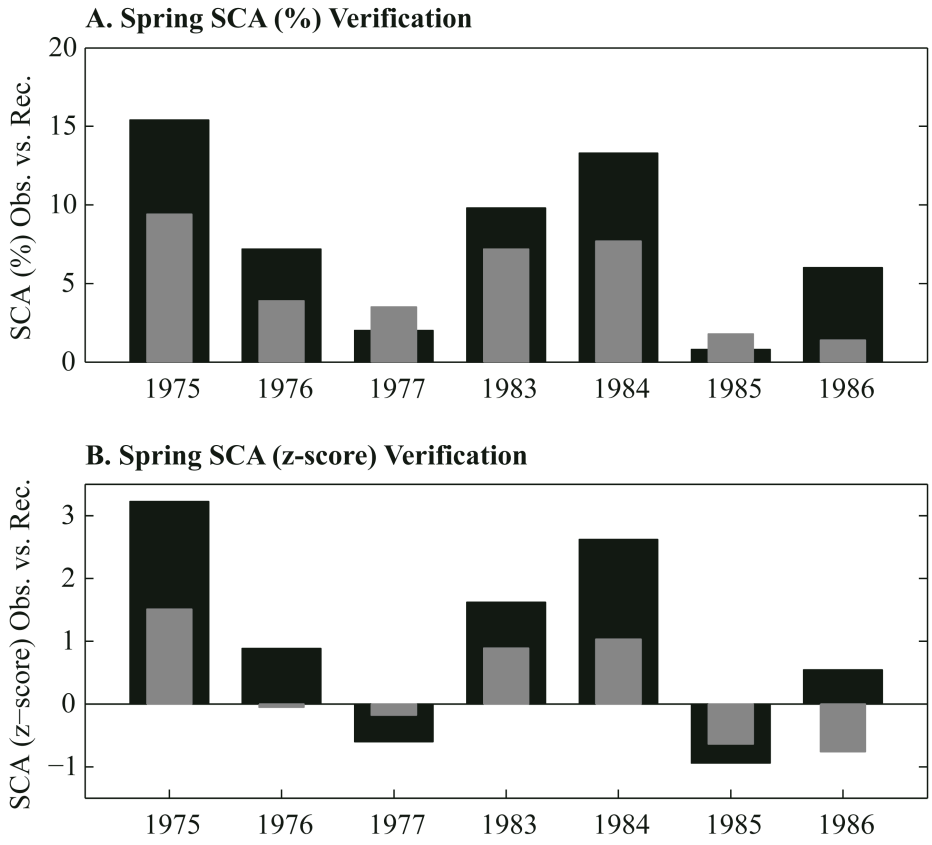

Figure 6. Spring SCA reconstruction model verification for a) percent SCA and b) z-score SCA. Observed Landsat SCA (black bars) and reconstructed SCA (grey bars) using instrumental spring mean temperature.

residuals (Table 2). It is important to note that even though spring mean temperature (April-June) had the highest correlation with spring SCA during 1975-2009, May-June mean temperature produced the most statistically significant spring SCA model for the 1989-2009 calibration.

Reconstructed spring SCA estimates for verification years 1975, 1976, 1977, and 1983-1986 indicated that independently observed spring SCA estimates shared the same sign in five out of seven cases (Figure 6). The probability of same sign occurrence if reconstructed and observed spring SCA estimates are scaled to the calibration mean and variance is p=0.164. The May-June mean temperature model of spring SCA generally underestimated actual SCA outside the calibration period (1989-2009) as observed independently by Landsat. Reconstructed spring SCA during 1901-2009 showed a statistically significant decreasing trend per the Mann-Kendall (MK) test (MK=-0.13, p=0.0486). Based upon the May-June mean temperature model, there has been a -36.2 (%) decrease in spring SCA since 1901 across the central Idaho and southwestern Montana mountains (Figure 5c and Figure 1).

Discussion

The Landsat image archive is an unparalleled satellite database of multispectral observations that can be used to develop CDRs of visible SCA for western US mountain snowpack extent monitoring at fine spatial scales (Crawford et al. 2013). This study merges a Landsat snow cover CDR of spring SCA with ground-based instrumental climate records to extend the available time period for climate-snowpack analysis, specifically resolving natural internal variability and temperature-driven SCA decreases

associated with modern climate change. This method is similar to the approach taken by Robinson (1991) and Frei, Robinson, and Hughes (1999) to merge NOAA Advanced Very High Resolution Radiometer (AVHRR) snow charts with ground-based snow depth measurements. Barry et al. (1995) suggest that better-quality information on spatial and temporal snow cover extent, duration, depth, and water equivalent variability including association to temperature and precipitation improves the ability to assess changing climatic conditions and long-term trends. They point out that no one satellite platform or method is sufficient to provide all the required information, but that integration between multiple satellites and instrumental observations is more comprehensive.

Landsat spring SCA estimates share significant covariance with regionalized SNOTEL SWE observations during the previous and current bi-monthly measurement intervals (i.e., 1st and 15th of each month). When Landsat spring SCA estimates are compared with individual SNOTEL SWE stations, the SCA-SWE relationship appears spatially dependent over time. This suggests that not all SNOTEL SWE stations adequately represent spring SCA variance within a spatially explicit domain. This finding is consistent with Molotch and Bales (2005) and Bales et al. (2006) suggestions that SNOTEL SWE stations do not capture snow ablation heterogeneity well in complex mountainous terrain. This time domain spatial dependence between SCA and SWE may be partly to blame for why snow distribution models perform poorly in certain locations (Erxleben, Elder, and Davis 2002). Equally important to consider, regionalized and individual SNOTEL station SWE during the often-cited April 1 peak mountain snowpack accumulation period for the western US (Cayan 1996) showed weak association to spring

SCA later (i.e., June 1) in the melt season. Anderton et al. (2004) conclude from snow surveys that maximum snow depth and date of snow disappearance could largely explain the spatial patterns in snow ablation, and suggest that melt rates during the snowmelt season are unimportant. In contrast, results obtained here suggests that over time, peak SWE accumulation at the beginning of spring would have little skill when predicting SCA later in the snowmelt season. Moreover, to account for the potential time-dependent relationship between SCA and SWE across mountainous terrain, temporally discrete examination intervals are required to normalize seasonal trend in spatial snow accumulation and melt processes and patterns. This is of particular importance when the objective is to isolate climate driven change in snow cover (snowpack) because multiple accumulation and melt events can occur throughout the snow season (Liston 1999) as shown in 1990 and 2002.

The inverse association between snow and temperature is well established (Barry 2002; Barry, Fallot, and Armstrong 1995; Groisman et al. 1994) including its relationship to orography and sea-level pressure (Sobolowski, Gong, and Ting 2007), sea surface temperatures (McCabe and Dettinger 2002), and atmospheric circulation patterns (Clark, Serreze, and McCabe 2001; Hurrell 1996; McCabe and Legates 1995). This study confirms that below (above) average mountain SCA across the interior northwestern USA has significant linear dependence on warm (cool) spring temperatures. Spring SCA did show a late winter response to March precipitation, but spring temperature was still the overriding signal. Using NOAA AVHRR snow charts, Leathers and Robinson (1993) showed that positive (negative) snow cover extent anomalies over North America are

strongly associated with below (above) normal wintertime surface temperatures. Warming winter temperatures in California since the 1940s have been linked to shifting winter atmospheric circulation patterns over the North Pacific Ocean, and have been suggested as the main driver behind earlier snowmelt runoff in mid elevation basins (Dettinger and Cayan 1995). Groisman et al. (1994) find a strong feedback between spring snow cover extent and northern extratropical land radiative balance. They suggest that 20th century spring warming has been amplified by changes in snow cover extent. More specifically, Stewart et al. (2005) find that earlier streamflow timing across western North America is a response to spring warming, a signal that would be promoted by earlier snowmelt and less SCA during spring. This spring SCA reconstruction in interior northwestern USA supports both of these studies. The weaker SCA response to March precipitation indicates that late winter precipitation contributes to spring SCA variability, but that its interannual predictability is secondary to spring temperature. The nature of this spring SCA temperature response in the continental sub-region of central Idaho and southwestern Montana corroborates high SWE-precipitation ratios (i.e., increased temperature influence) found for Idaho and Montana (Serreze et al. 1999). This continental sub-region and snow cover climatic response falls within alpine and mountain snow classification categories outlined by Sturm, Holmgren, and Liston (1995).

A trend towards decreasing spring SCA during the 20th and early 21st centuries is apparent across the central Idaho and southwestern Montana mountains. Using a spring surface temperature model that is well validated and showed encouraging verification with independent observations, the trend analysis indicates that there has been a -36.2 %

decrease in spring SCA since 1901. On the other hand, natural internal variability in spring SCA is evident on interannual to decadal timescales including above average periods during the decades of 1900s, 1910s, and 1940s-1970s. Periods of below average SCA occur during the 1920s, 1930s, and continue to remain largely below average since the mid-1980s. Hamlet et al. (2005) point out that decadal climate variability associated with Pacific Ocean climate dynamics is not enough to explain warming winter temperatures and decreasing April 1 SWE trends across the western US. Pierce et al. (2008) use an April 1 SWE/precipitation ratio along with simulated climate models to reproduce SWE/precipitation reductions in western US snowpack. Like Hamlet et al. (2005), they find that natural internal climate variability alone cannot explain SWE/precipitation trends. Of more importance, a longer-term centennial trend towards decreasing spring SCA has been identified and is superimposed on natural internal variability; an obvious sign of spring warming. Although Groisman and Easterling (1994) and Kunkel et al. (2007) find that instrumental snow observations are sensitive to measurement inhomogeneities and should be considered carefully when evaluating climatic trends, this spring SCA reconstruction was produced using Landsat and surface temperature records. This temperature-driven trend in spring SCA across central Idaho and southwestern Montana is consistent with declining mountain snowpack SWE documented for the western US (Hamlet et al. 2005; Mote et al. 2005; Pederson et al. 2011; Pierce et al. 2008), decreasing Northern Hemisphere spring snow cover extent (Brown and Robinson 2011; Derksen and Brown 2012), earlier trends towards North American spring snow ablation (Dyer and Mote 2007), earlier disappearance of Arctic

spring snow (Foster 1989), mountain glacier recession (Barry 2006), and summer minimum Arctic sea ice extent (Stroeve et al. 2007).

Conclusion

This Landsat snow cover CDR approach to monitoring SCA in mountainous terrain is sensitive to Landsat's image acquisition frequency, missing historical imagery, and transient snowfall at high elevations during the melt season. Such temporal gaps in SCA estimation currently prevent longer more continuous calibrations with instrumental climate records, which limits model development and increases uncertainty and error. Even though the spring SCA reconstruction presented is based on a short calibration period, acceptable PRESS cross-validation statistics were obtained with a spring mean surface temperature model. Looking forward despite the documented limitations, the SNOTEL SWE network across the western US offers discrete measurement resolution and adequate spatial coverage to anchor bi-monthly Landsat snow cover CDRs including corrections for transient snowfall events that inflate Landsat SCA estimates. Expanding snow cover CDRs to include the Landsat Data Continuity Mission (LDCM), Moderate Resolution Imaging Spectroradiometer (MODIS), and NPP Visible Infrared Imaging Radiometer Suite (VIIRS) retrievals from 2000 on will add to temporal SCA estimation, especially during other accumulation and melt intervals. Satellite-instrumental climate model calibration will certainly improve with additional temporal data acquisitions moving forward. The time-series analysis techniques deployed to reconstruct spring SCA from Landsat is straightforward in concept, design, execution, and provides a formidable statistical method to quantify temperature-driven decreases in SCA across the western

US. Climatic warming induced trends towards decreasing Arctic sea ice and Northern Hemisphere spring snow cover, along with global mountain glacier recession, is also evident in spring mountain SCA. Sustained losses in seasonal SCA are clear, and can be expected to accelerate over the next several decades unless spring surface temperatures stabilize.

References

Anderton, S. P., S. M. White, and B. Alvera. 2004. "Evaluation of spatial variability in snow water equivalent for a high mountain catchment." *Hydrological Processes* no. 18 (3):435-453. doi: 10.1002/hyp.1319.

Bales, R. C., N. P. Molotch, T. H. Painter, M. D. Dettinger, R. Rice, and J. Dozier. 2006. "Mountain hydrology of the western United States." *Water Resources Research* no. 42 (8):13. doi: W0843210.1029/2005wr004387.

Barnett, T. P., J. C. Adam, and D. P. Lettenmaier. 2005. "Potential impacts of a warming climate on water availability in snow-dominated regions." *Nature* no. 438 (7066):303-309. doi: 10.1038/nature04141.

Barry, R. G. 2006. "The status of research on glaciers and global glacier recession: a review." *Progress in Physical Geography* no. 30 (3):285-306. doi: 10.1191/0309133306pp478ra.

Barry, R. G., J. M. Fallot, and R. L. Armstrong. 1995. "Twentieth-century variability in snow-cover conditions and approaches to detecting and monitoring changes: Status and prospects." *Progress in Physical Geography* no. 19 (4):520-532. doi: 10.1177/030913339501900405.

Barry, R. G. 2002. "The role of snow and ice in the global climate system: A review." *Polar Geography* no. 26 (3):235 - 246.

Brown, R. D., and D. A. Robinson. 2011. "Northern Hemisphere spring snow cover variablity and change over 1922-2010 including an assessment of uncertainty." *The Cryosphere* no. 5 (1):219-229. doi: 10.5194/tc-5-219-2011.

Cayan, D. R. 1996. "Interannual climate variability and snowpack in the western United States." *Journal of Climate* no. 9 (5):928-948.

Cayan, D. R., S. A. Kammerdiener, M. D. Dettinger, J. M. Caprio, and D. H. Peterson. 2001. "Changes in the onset of spring in the western United States." *Bulletin of the American Meteorological Society* no. 82 (3):399-415.

Clark, M. P., M. C. Serreze, and G. J. McCabe. 2001. "Historical effects of El Nino and La Nina events on the seasonal evolution of the montane snowpack in the Columbia and Colorado River Basins." *Water Resources Research* no. 37 (3):741-757.

Cline, D. W., R. C. Bales, and J. Dozier. 1998. "Estimating the spatial distribution of snow in mountain basins using remote sensing and energy balance modeling." *Water Resources Research* no. 34 (5):1275-1285.

Comrie, A. C., and E. C. Glenn. 1998. "Principal components-based regionalization of precipitation regimes across the southwest United States and northern Mexico, with an application to monsoon precipitation variability." *Climate Research* no. 10 (3):201-215. doi: 10.3354/cr010201.

Crawford, C. J., S. M. Manson, M. E. Bauer, and D. K. Hall. 2013. "Multitemporal snow cover mapping in mountainous terrain for Landsat climate data record development." *Remote Sensing of Environment* no. 135 (0):224-233. doi:10.1016/j.rse.2013.04.004.

Derksen, C., and R. Brown. 2012. "Spring snow cover extent reductions in the 2008-2012 period exceeding climate model projections." *Geophysical Research Letters* no. 39. doi: 10.1029/2012GL053387.

Dettinger, M. D., and D. R. Cayan. 1995. "Large-scale atmospheric forcing of recent trends toward early snowmelt runoff in California." *Journal of Climate* no. 8 (3):606-623. doi: 10.1175/1520-0442(1995)008<0606:lsafor>2.0.co;2.

Duffy, P. B., R. W. Arritt, J. Coquard, W. Gutowski, J. Han, J. Iorio, J. Kim, L. R. Leung, J. Roads, and E. Zeledon. 2006. "Simulations of present and future climates in the western United States with four nested regional climate models." *Journal of Climate* no. 19 (6):873-895. doi: 10.1175/jcli3669.1.

Dyer, J. L., and T. L. Mote. 2007. "Trends in snow ablation over North America." *International Journal of Climatology* no. 27 (6):739-748. doi: 10.1002/joc.1426.

Eischeid, J. K., C. B. Baker, T. R. Karl, and H. F. Diaz. 1995. "The quality-control of long-term climatological data using objective data-analysis." *Journal of Applied Meteorology* no. 34 (12):2787-2795. doi: 10.1175/1520-0450(1995)034<2787:tqcolt>2.0.co;2.

Elder, K., J. Dozier, and J. Michaelsen. 1991. "Snow accumulation and distrubution in an alpine watershed." *Water Resources Research* no. 27 (7):1541-1552.

Erxleben, J., K. Elder, and R. Davis. 2002. "Comparison of spatial interpolation methods for estimating snow distribution in the Colorado Rocky Mountains." *Hydrological Processes* no. 16 (18):3627-3649. doi: 10.1002/hyp.1239.

Foster, J. L. 1989. "The significance of the date of snow disappearance on the Arctic tundra as a possible indicator of climate change." *Arctic and Alpine Research* no. 21 (1):60-70. doi: 10.2307/1551517.

Frei, A., D. A. Robinson, and M. G. Hughes. 1999. "North American snow extent: 1900-1994." *International Journal of Climatology* no. 19 (14):1517-1534. doi: 10.1002/(sici)1097-0088(19991130)19:14<1517::aid-joc437>3.0.co;2-i.

Groisman, P., and D. R. Easterling. 1994. "Variability and trends of total precipitation and snowfall over the United States and Canada." *Journal of Climate* no. 7:184-205.

Groisman, P. Y., T. R. Karl, R. W. Knight, and G. L. Stenchikov. 1994. "Changes of snow cover, temperature, and radiative heat-balance over the northern-hemisphere." *Journal of Climate* no. 7 (11):1633-1656.

Hall, D. K., J. L. Foster, N. E. DiGirolamo, and G. A. Riggs. 2012. "Snow cover, snowmelt timing and stream power in the Wind River Range, Wyoming." *Geomorphology* no. 137 (1):87-93. doi: 10.1016/j.geomorph.2010.11.011.

Hamlet, A. F., P. W. Mote, M. P. Clark, and D. P. Lettenmaier. 2005. "Effects of temperature and precipitation variability on snowpack trends in the western United States." *Journal of Climate* no. 18 (21):4545-4561.

Hurrell, J. W. 1996. "Influence of variations in extratropical wintertime teleconnections on Northern Hemisphere temperature." *Geophysical Research Letters* no. 23 (6):665-668.

Jones, P. D., and M. Hulme. 1996. "Calculating regional climatic time series for temperature and precipitation: Methods and illustrations." *International Journal of Climatology* no. 16 (4):361-377.

Knowles, N., M. D. Dettinger, and D. R. Cayan. 2006. "Trends in snowfall versus rainfall in the Western United States." *Journal of Climate* no. 19 (18):4545-4559.

Kunkel, K. E., M. A. Palecki, K. G. Hubbard, D. A. Robinson, K. T. Redmond, and D. R. Easterling. 2007. "Trend identification in twentieth-century US snowfall: The challenges." *Journal of Atmospheric and Oceanic Technology* no. 24 (1):64-73. doi: 10.1175/jtech2017.1.

Leathers, D. J., and D. A. Robinson. 1993. "The association between extremes in North-American snow cover extent and United-States temperature." *Journal of Climate* no. 6 (7):1345-1355.

Li, B. L., A. X. Zhu, C. H. Zhou, Y. H. Zhang, T. Pei, and C. Z. Qin. 2008. "Automatic mapping of snow cover depletion curves using optical remote sensing data under conditions of frequent cloud cover and temporary snow." *Hydrological Processes* no. 22 (16):2930-2942. doi: 10.1002/hyp.6891.

Liston, G. E. 1999. "Interrelationships among snow distribution, snowmelt, and snow cover depletion: Implications for atmospheric, hydrologic, and ecologic modeling." *Journal of Applied Meteorology* no. 38 (10):1474-1487. doi: 10.1175/1520-0450(1999)038<1474:iasdsa>2.0.co;2.

Lundquist, J. D., and M. D. Dettinger. 2005. "How snowpack heterogeneity affects diurnal streamflow timing." *Water Resources Research* no. 41 (5):14. doi: W0500710.1029/2004wr003649.

Matson, M., and D. R. Wiesnet. 1981. "New data-base for climate studies." *Nature* no. 289 (5797):451-456. doi: 10.1038/289451a0.

McCabe, G. J., and M. P. Clark. 2005. "Trends and variability in snowmelt runoff in the western United States." *Journal of Hydrometeorology* no. 6 (4):476-482.

McCabe, G. J., and M. D. Dettinger. 2002. "Primary modes and predictability of year-to-year snowpack variations in the western United States from teleconnections with Pacific Ocean climate." *Journal of Hydrometeorology* no. 3 (1):13-25.

McCabe, G. J., and D. R. Legates. 1995. "Relationships between 700 hpa height anomalies and 1 April snowpack accumulations in the western USA " *International Journal of Climatology* no. 15 (5):517-530.

Meehl, G. A., and H. Y. Teng. 2012. "Case studies for initialized decadal hindcasts and predictions for the Pacific region." *Geophysical Research Letters* no. 39. doi: L2270510.1029/2012gl053423.
Michaelsen, J. 1987. "Cross-validation in statistical climate forecast models." *Journal of Applied Meteorology* no. 26:1589-1600.
Mitchell, T. D., and P. D. Jones. 2005. "An improved method of constructing a database of monthly climate observations and associated high-resolution grids." *International Journal of Climatology* no. 25 (6):693-712. doi: 10.1002/joc.1181.
Mitchell, V.L. 1976. "The regionalization of climate in the western United States." *Journal of Applied Meteorology* no. 15 (9):920-927.
Molotch, N. P., and R. C. Bales. 2005. "Scaling snow observations from the point to the grid element: Implications for observation network design." *Water Resources Research* no. 41 (11):16. doi: W1142110.1029/2005wr004229.
Mote, P. W., A. F. Hamlet, M. P. Clark, and D. P. Lettenmaier. 2005. "Declining mountain snowpack in western north America." *Bulletin of the American Meteorological Society* no. 86 (1):39-49. doi: 10.1175/bams-86-1-39.
Nolin, A. W. 2012. "Perspectives on Climate Change, Mountain Hydrology, and Water Resources in the Oregon Cascades, USA." *Mountain Research and Development* no. 32:S35-S46. doi: 10.1659/mrd-journal-d-11-00038.s1.
Nolin, A. W., and C. Daly. 2006. "Mapping "at risk" snow in the Pacific Northwest." *Journal of Hydrometeorology* no. 7 (5):1164-1171. doi: 10.1175/jhm543.1.
Ostrom, C. W. Jr. 1990. *Time Series Analysis, Regression Techiques*. second ed. Vol. 07-009. Newbury Park: Sage Publications.
Pederson, G. T., S. T. Gray, C. A. Woodhouse, J. L. Betancourt, D. B. Fagre, J. S. Littell, E. Watson, B. H. Luckman, and L. J. Graumlich. 2011. "The Unusual Nature of Recent Snowpack Declines in the North American Cordillera." *Science* no. 333 (6040):332-335. doi: 10.1126/science.1201570.
Peterson, T. C., D. R. Easterling, T. R. Karl, P. Groisman, N. Nicholls, N. Plummer, S. Torok, I. Auer, R. Boehm, D. Gullett, L. Vincent, R. Heino, H. Tuomenvirta, O. Mestre, T. Szentimrey, J. Salinger, E. J. Forland, I. Hanssen-Bauer, H. Alexandersson, P. Jones, and D. Parker. 1998. "Homogeneity adjustments of in situ atmospheric climate data: A review." *International Journal of Climatology* no. 18 (13):1493-1517.
Pierce, D. W., T. P. Barnett, H. G. Hidalgo, T. Das, C. Bonfils, B. D. Santer, G. Bala, M. D. Dettinger, D. R. Cayan, A. Mirin, A. W. Wood, and T. Nozawa. 2008. "Attribution of Declining Western US Snowpack to Human Effects." *Journal of Climate* no. 21 (23):6425-6444. doi: 10.1175/2008jcli2405.1.
Redmond, K. T., and R. W. Koch. 1991. "Surface climate and streamflow variablity in the western United-States and their relationship to large-scale circulation indexes." *Water Resources Research* no. 27 (9):2381-2399. doi: 10.1029/91wr00690.
Robinson, D. A. 1991. "Merging operational satellite and historical station snow cover data to monitor climate change." *Global and Planetary Change* no. 90 (1-3):235-240.

Serreze, M. C., M. P. Clark, R. L. Armstrong, D. A. McGinnis, and R. S. Pulwarty. 1999. "Characteristics of the western United States snowpack from snowpack telemetry (SNOTEL) data." *Water Resources Research* no. 35 (7):2145-2160. doi: 10.1029/1999wr900090.

Shinker, J. J. 2010. "Visualizing spatial heterogeneity of western U.S. climate variability." *Earth Interactions* no. 14. doi: 1010.1175/2010ei323.1.

Sobolowski, S., G. Gong, and M. Ting. 2007. "Northern hemisphere winter climate variability: Response to North American snow cover anomalies and orography." *Geophysical Research Letters* no. 34 (16). doi: L1682510.1029/2007gl030573.

Stewart, I. T., D. R. Cayan, and M. D. Dettinger. 2005. "Changes toward earlier streamflow timing across western North America." *Journal of Climate* no. 18 (8):1136-1155. doi: 10.1175/jcli3321.1.

Stroeve, J., M. M. Holland, W. Meier, T. Scambos, and M. Serreze. 2007. "Arctic sea ice decline: Faster than forecast." *Geophysical Research Letters* no. 34 (9). doi: L0950110.1029/2007gl029703.

Sturm, M., J. Holmgren, and G. E. Liston. 1995. "A seasonal snow cover classification-system for local to global applications." *Journal of Climate* no. 8 (5):1261-1283. doi: 10.1175/1520-0442(1995)008<1261:asccs>2.0.co;2.

Teng, H. Y., L. E. Buja, and G. A. Meehl. 2006. "Twenty-first-century climate change commitment from a multi-model ensemble." *Geophysical Research Letters* no. 33 (7). doi: 10.1029/2005GL024766.

Westerling, A. L., H. G. Hidalgo, D. R. Cayan, and T. W. Swetnam. 2006. "Warming and earlier spring increase western US forest wildfire activity." *Science* no. 313 (5789):940-943. doi: 10.1126/science.1128834.

Wilks, D. S. 1995. *Statistical methods in the atmospheric sciences*. Boston: Academic Press.

Yue, S., and C. Y. Wang. 2004. "The Mann-Kendall test modified by effective sample size to detect trend in serially correlated hydrological series." *Water Resources Management* no. 18 (3):201-218. doi: 10.1023/b:warm.0000043140.61082.60.

Chapter 5: Annual and Sub-Annual Precipitation Reconstructions for the Craters of the Moon Lava Complex, Eastern Snake River Plain, USA

Four millennial to multicentennial length tree-ring chronologies were constructed from ancient lower forest border limber pine (*Pinus flexilis*) and Rocky Mountain Douglas fir (*Pseudotsuga menziesii* var. *glauca* (Bessin.) Franco) growing at the Craters of the Moon (COM) on the eastern Snake River Plain (SRP), USA. Standardized limber pine and Douglas fir total ring widths (RW) and Douglas fir sub-annual earlywood (EW), latewood (LW), and adjusted latewood (LW_a) widths share spectral coherence at decadal timescales. A comparison between instrumental climate records and tree-ring widths indicate a summer-winter precipitation response for limber pine RW and Douglas fir LW_a, and an annual precipitation response for Douglas fir RW and EW. Two independent tree-ring precipitation reconstructions (1532-2008) were developed for the eastern SRP using a 'leave-one-out' stepwise multiple regression with cross-validation procedure. During the 1930-2009 calibration, Douglas fir EW was a predictor for annual precipitation (pJuly-June), and limber pine RW and Douglas fir LW_a were predictors for sub-annual summer-winter precipitation (July-March). Models explained between 29-40% of the observed precipitation, exhibited skillful prediction and validation, and passed verification tests with independent data. This climate reconstruction method exploits total and partial tree-ring widths from two species with season-specific climate signals to estimate annual and sub-annual precipitation over the past five centuries. This method improved the resolution of annual and sub-annual drought and pluvial occurrence on the eastern SRP at decadal and multidecadal timescales. Well-documented western US paleodrought and pluvial episodes are captured in these reconstructions.

Introduction

The Craters of the Moon (COM) National Monument is a basaltic-lava complex on the eastern Snake River Plain (SRP) in south central Idaho, USA. The COM has formed over eight eruptive periods during the Holocene, and since the last eruption ~ 2,000 years ago (Owen 2008), limber pine (*Pinus flexilis*) and Rocky Mountain Douglas fir (*Pseudotsuga menziesii* var. *glauca* (Bessin.) Franco.) have established on lava flows and ancient weathered cinder cones. These long-lived trees have survived several hundred meters below the lower forest border on this well-drained porous rock. These limiting growth factors invite the possibility that these arid-site tree-ring widths will yield faithful proxy-records of moisture variability (Fritts 1965) on the eastern SRP, a region with few high-resolution paleoclimate archives. The objectives of this research paper are to compare limber pine and Douglas fir radial growth, identify the climate response window for annual and sub-annual growth increments, and then transform tree-ring widths into estimates of past climate.

The eastern SRP supports agricultural production for local, regional, and national distribution (Marston et al. 2005; Wise 2010). The eastern SRP is also adjacent to the Yellowstone Hydrological Unit where the Snake River system provides an aboveground water source for multiple uses (McGuire et al. 2006; Slaughter and Wiener 2007; Wise 2010). In addition to the Snake River, a large aquifer lies beneath the SRP known as the 'Eastern Snake Plain Aquifer (ESPA)' (Slaughter and Wiener 2007). Many millennia of volcanism in this region have produced porous soils that allow snowmelt surface water and surface irrigation to infiltrate and resupply aquifer water levels

(http://pubs.usgs.gov/ha/ha730/ch_h/H-text8.html). The ESPA is a vital belowground water source that sustains agricultural irrigation during drought, although a 1992 moratorium on consumptive appropriation prohibits ESPA mining and aquifer drawdown (Slaughter and Wiener 2007). The ability for COM tree-ring widths to provide past climate estimates at annual and sub-annual timescales, offers a unique historical reference to establish the timing, amount, and range of moisture infiltration to belowground water resources.

Limber pine, and especially Douglas fir, have and remain reliable proxy-records for past climate estimation across western North America due to their remarkable moisture sensitivity (Fritts 1966, 1974; Gray, Graumlich, and Betancourt 2007; Meko et al. 1993; Meko and Woodhouse 2005; Salzer and Kipfmueller 2005; Stahle et al. 2009; Watson and Luckman 2001). In the broader geographic region surrounding COM, tree-ring widths from these two species have provided estimates of summer Palmer Drought Severity Index (PDSI)(Cook et al. 2004), annual precipitation (Gray, Graumlich, and Betancourt 2007), and annual streamflow (Graumlich et al. 2003; Wise 2010). These reconstructions show that persistent drought has been an important feature of regional climate variability over the last five to eight centuries, but that the 20th century stands out as a wet period relative to the past (Gray and McCabe 2010). While drought magnitude and duration has been a primary investigation for this region thus far, less emphasis has been placed on resolving frequency-dependent precipitation variability at annual and sub-annual timescales.

This paper is divided into two sections. Section one compares radial growth between limber pine ring-width (RW), and Douglas fir ring-width (RW), earlywood-width (EW), latewood-width (LW), and adjusted latewood-width (LW_a), and identifies season-specific climate response windows for standardized tree-ring widths. The objective is to determine whether limber pine and Douglas fir tree-ring widths are significantly correlated in time, share spectral coherence (Hughes and Funkhouser 2003), and have appreciable climate signals. Section two uses limber pine RW, Douglas fir EW, and Douglas fir LW_a to reconstruct past climate. The objective is to estimate annual and sub-annual precipitation on the eastern SRP, and extract the dominant frequencies contributing to the total variance.

Methods

COM Study Area

COM is located in south central Idaho on the eastern SRP (Figure 1). The SRP semi-arid climate is characterized by a winter-dominant moisture regime including snowfall that is directly linked to a shifting seasonal cycle in ocean-atmosphere dynamics between the semi-permanent Aleutian low in the North Pacific Ocean, and the North American ridge over interior western North America (Harman 1991; Mitchell 1976; Mock 1996; Shinker 2010). On average (1981-2010), the COM receives 243 cm of annual snowfall across October-May (http://www.ncdc.noaa.gov/cdo-web/datasets/NORMAL_MLY/stations/GHCND: USC00102260) that translates into a

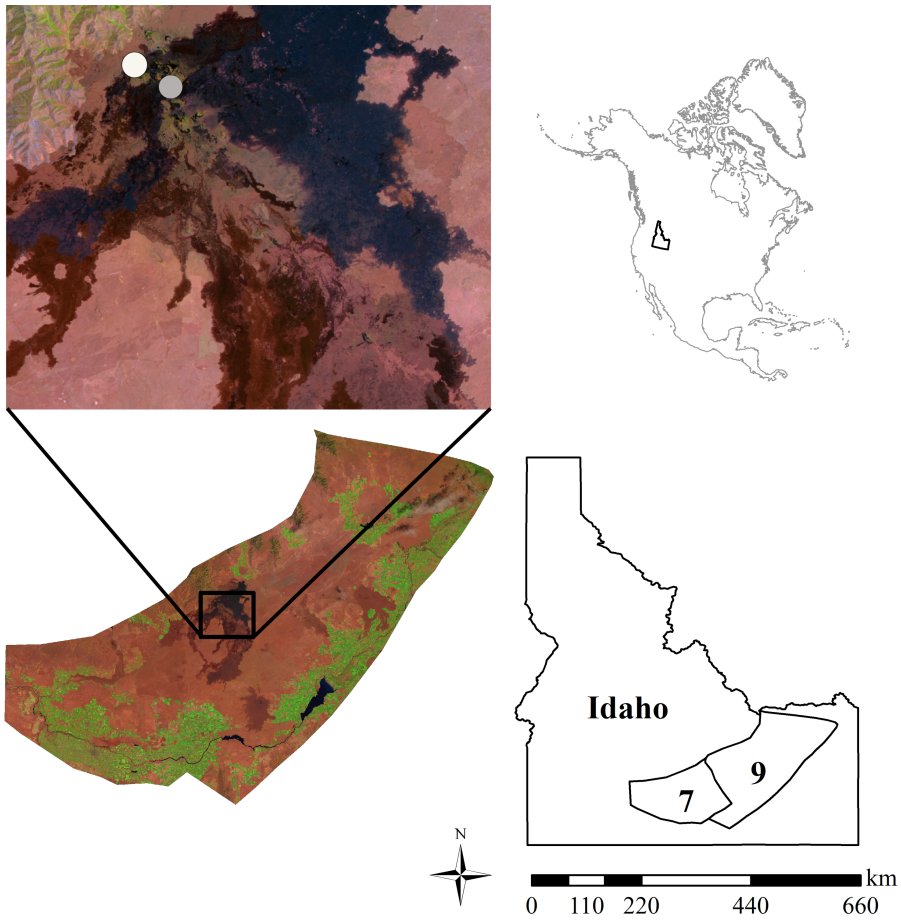

Figure 1. The COM lava complex on the eastern SRP in south central Idaho, USA. Notice that COM is situated between Idaho climate divisions seven (central plains) and nine (upper Snake River Plain). The false-color Landsat image represents the target spatial domain for tree-ring based climate reconstructions. The circles in the upper left panel indicate limber pine (grey) and Douglas fir (white) sample sites.

lower elevation snowpack. The eastern most flank of the SRP receives considerable winter precipitation, but a peak in precipitation also occurs during spring (Mock 1996; Shinker 2010). In summer, large-scale subsidence from both Pacific and continental high-pressure centers limit moisture advection and convection across the eastern SRP. Therefore, much of the available annual hydrological budget for warm season tree-growth is stored in cool season belowground soil moisture reserves. Divisional climatologies along the eastern SRP indicate a subtle west to east winter-spring dominated seasonal precipitation gradient (Figure 2). Because the COM sits between this transitional winter-spring moisture zones, limber pine and Douglas fir tree-ring widths should show elevated sensitivity to seasonal moisture availability.

Site Description and Tree-Ring Data Collection

This volcanic landscape consists of lava fields, ancient craters, and weathered cinder cones (Owen 2008). Soil types at COM ranges from basaltic pebbles with grasses and sagebrush to solid basaltic conglomerates having no vegetation. The limber pine and Douglas fir trees under investigation occupy different ecological niches at COM. Limber pine grows on all types of lava soil conditions, whereas Douglas fir grows almost exclusively on highly weathered soils on north-facing cinder cone slopes (Figure 3).

Tree-ring core specimens were collected from living trees and remnant wood across the COM. Thirty individual open-canopy limber pine and Douglas fir trees were selected for core extraction at approximately 30 cm using an increment borer (Fritts 1976). Cores were processed according to standard techniques and crossdated to an exact calendar year (Stokes and Smiley 1996). Visual crossdating was verified statistically with

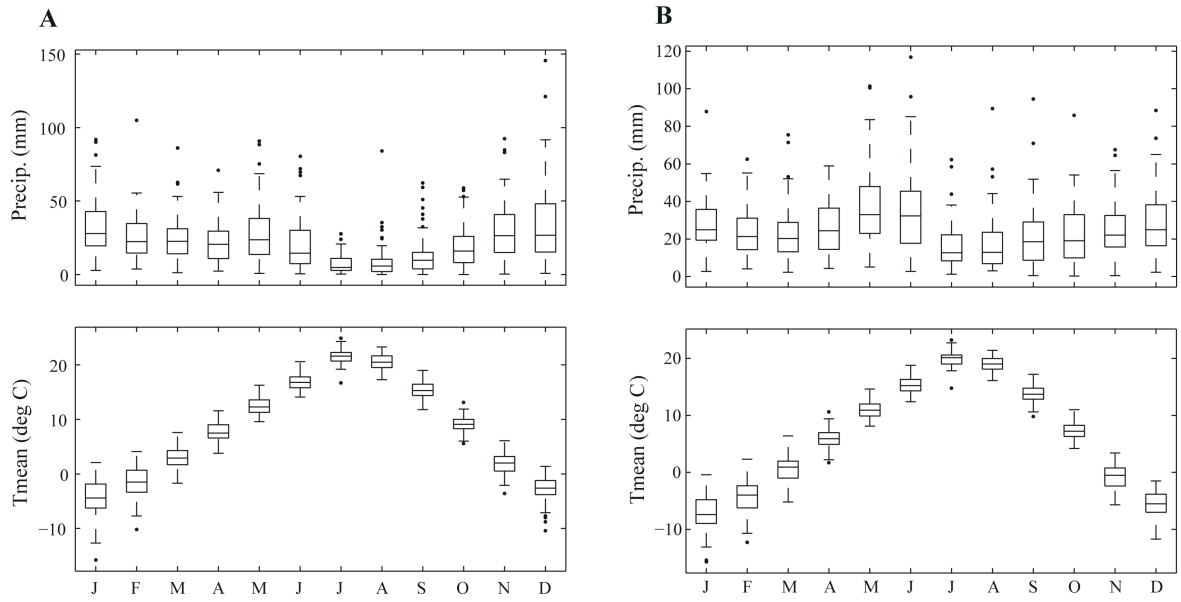

Figure 2. Climatographs for Idaho climate divisions seven (central plains) and nine (upper Snake River Plain): a) central plains annual cycle and b) upper Snake River Plain annual cycle. Temperature and precipitation observations originate from the PRISM climate dataset (Daly et al. 2008), and have been summarized over 1930-2009.

A B

Figure 3. Douglas fir and limber pine trees growing at COM: a) limber pine on a lava flow, and b) Douglas fir on a north facing cider cone slope.

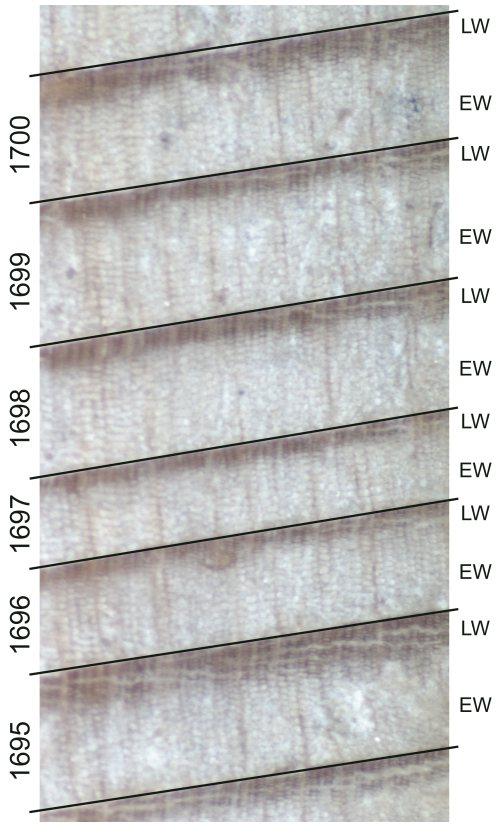

Figure 4. Douglas fir EW and LW boundaries on sample CMF020b from AD 1695-1700. Black lines indicate annual growth increments.

COFECHA (Holmes 1983). Total annual growth increments were measured to the nearest 0.001 mm for limber pine and Douglas fir ring-width. Also, partial earlywood (EW) and latewood (LW) increments were measured for Douglas fir. Partial ring boundaries were delineated at the abrupt transition from light colored (EW) to dark colored wood (LW) (Figure 4). If the EW-LW transition was gradual, boundaries were delineated in the middle of the transition.

Chronology Development

Age-related growth trends associated with tree maturation were removed using a conservative standardization approach (Cook and Kairiukstis 1990). Only tree-ring width series greater than 200 years were used in chronology construction. Before standardization, raw ring-width measurements were power transformed adaptively to reduce population skew, improve curve fits, and minimize trend propagation (Cook and Peters 1997). Variance was stabilized using Briffa's r-bar method (Briffa and Jones 1990). Each tree-ring width series was fit with a horizontal mean line, negative exponential curve, or linear regression line with a negative slope (Cook et al. 1995). Standardized RW, EW, and LW chronologies were estimated using a bi-robust weight mean, and the expected width was divided by the actual width to produce a dimensionless index of average growth. Autoregressive modeling was applied to remove serial autocorrelation, and produce residual indices (Cook 1985). Lastly, an adjusted LW chronology (LW_a) was developed for Douglas fir (Griffin et al. 2011). Thus far, this Douglas fir LW adjustment method has not been attempted outside the Southwestern US. Adjusting for LW's antecedent dependence on EW isolates independent sub-annual

variability contained in LW (Meko and Baisan 2001). We applied this adjustment method using site-level residual indices because age-related growth trends exhibited by individual trees may contain unique patterns that could potentially bias the adjustment (Griffin et al. 2011).

Section One: Radial Growth and Climate Sensitivity

Radial growth between limber pine RW and Douglas fir RW, EW, and LW_a was compared in time and frequency domains over periods where chronologies exhibited an expressed population signal (EPS) greater than 0.85 (Wigley, Briffa, and Jones 1984). Simple correlation analysis was used to calculate the covariance between limber pine and Douglas fir tree-ring widths in time (Hughes and Funkhouser 2003). Magnitude squared coherency (MSC) between tree-ring widths identified frequencies with significant co-spectral power (Hughes and Funkhouser 2003). Because tree-ring width chronologies can retain persistent 'redness' even after autoregressive modeling, differentiating between signal and noise coherence requires the generation of a red noise floor. A red noise floor was constructed using a Monte-Carlo simulation with 10,000 synthetic chronologies having similar means, standard deviations, and spectral properties to the original reference chronology. Tree-ring width climate responses were identified with SEASCORR using instrumental climate records (Meko, Touchan, and Anchukaitis 2011). Domain averaged Parameter-elevation Relationships on Independent Slopes Model (PRISM) climate data (Daly et al. 2008) was extracted for Idaho climate divisions seven (central plains) and nine (upper Snake River plain)(http://www.cefa.dri.edu/Westmap/). The 1930-2009 period was selected for the climate response assessment because station

data prior to 1930 is based primarily on regression estimates from distant climate stations (Eischeid et al. 1995). Monthly, seasonal, and annual correlations were computed for a 14-month window spanning prior August to current September.

Section Two: Tree-Ring Climate Reconstructions

A stepwise 'leave-one-out' linear regression model with cross-validation was used to develop annual and sub-annual reconstructions for Idaho climate divisions seven (central plains) and nine (upper Snake River Plain) (Michaelsen 1987; Wilks 1995). Instrumental climate targets were evaluated for first-order autocorrelation (Meko, Touchan, and Anchukaitis 2011). Specific annual and sub-annual climate reconstruction targets were selected based upon statistically significant tree-ring width-climate correlations, plausible radial growth-climate physiology (Fritts 1976), and significant instrumental climate autocorrelation. Initial reconstruction model development for each annual and sub-annual target originated from a pool of potential tree-ring predictors that included limber pine RW, Douglas fir EW, and Douglas fir LW_a at t-1, t, and t+1.

Tree-ring based reconstructions were intended to retain climatically driven low frequency variability without violating statistical independence and multiple linear regression assumptions. The potential pool of tree-ring predictors was selected from residual indices in order to not mistake biological autocorrelation for climatic persistence. Using 'leave-one-out' stepwise modeling, validation statistics were generated for each step to assess model skill and accuracy during the calibration period. A Durbin-Watson test determined whether there was autocorrelation embedded within model residuals (Ostrom 1990). Regression residuals were evaluated for trend and pure randomness using

a Portmanteau Q test (Ostrom 1990). The reduction of error (RE) and root-mean-squared error ($RSME_v$) cross-validation statistics were used to assess model construction, fit, and performance (Michaelsen 1987). Error bars were generated for p=0.10 and p=0.90 (80% confidence level) for the final annual and sub-annual reconstruction targets to insure the plausibility of climate estimates given model uncertainty (Meko et al. 2007).

Additional reconstruction model verification was undertaken using independently withheld instrumental climate data (Fritts 1991). Two separate calibrations were developed for 1930-1979 (early) and 1960-2009 (late) periods using identical modeling protocols during the 1930-2009 calibration. For two separate verification periods, 1930-1959 and 1980-2008, independently withheld instrumental climate data was compared with tree-ring based estimates using correlation coefficients (*r*), RE, and coefficient of efficiency (CE) statistics (Cook et al. 1999; Fritts 1991).

Simple correlation analysis was used to compare annual and sub-annual climate estimates for 1532-2008. Finally, we identified the dominant frequencies for annual and sub-annual climate estimates using Singular Spectrum Analysis (SSA). SSA is a data-adaptive signal-to-noise enhancement tool that extracts independent, but dominant trends, oscillatory patterns, and noise within a time-series having peak spectral power above a background-level continuous spectrum (Ghil et al. 2002; Vautard and Ghil 1989). SSA is a non-parametric spectral method that uses a specified lag window (*M*) to execute singular value decomposition on the autocovariance matrix to obtain an orthogonal set of basis vectors. Next, the original time-series is decomposed into *M* reconstructed components (RCs) and corresponding *M* normalized eigenvalues. We used an *M* of 15

years, but tested a wide of range *M* values (15-40 years) to insure that SSA estimates were insensitive to lag window choice. RCs accounting for decadal variability (> 10 yrs.) and beyond were retained, and if successive RCs possessed a similar frequency (within 1 yr.), RCs were summed. Based upon Fourier transform, dominant decadal RCs and cumulative variance for each reconstruction target was estimated (Ault and St George 2010). We chose only to evaluate dominant RCs contributing to decadal climate variability because it becomes increasingly difficult to distinguish high-order signals from noise (Ault and St George 2010; Ghil et al. 2002).

Results

Tree-Ring Width Chronologies

Limber pine and Douglas fir trees have survived for many centuries, even greater than 1000 years on the COM lava complex. Median tree age for both species ranged from 342 to 400 years (Table 1). Limber pine is the oldest living tree (1073 yrs.) at COM with several remnant wood samples exceeding 600 years in length. Inter-tree correlations were stronger for Douglas fir widths, and exhibited greater mean sensitivity than limber pine (Table 1). Standardized tree-ring width chronologies for both species contain moderately high first-order autocorrelation indicating some degree of biological persistence from the previous year on the current year's growth (Figure 5). Development of a Douglas fir LW_a chronology indicated a moderately strong linear relationship between LW and antecedent EW. Douglas fir EW was able to explain 58% of LW's variance.

Table 1. COM tree-ring width chronology statistics.

	Location	Elevation (m)	Trees (series)	Chronology Length	Segment Length	*r*	ms	acf	eps>0.85
PIFL RW	43.45, -113.54	1783	30 (60)	937-2009	400	0.501	0.123	0.573	1315-2009
PSME RW	43.46, -113.59	1867	31 (62)	1468-2009	342	0.712	0.148	0.548	1520-2009
PSME EW	43.46, -113.59	1867	31 (62)	1468-2009	342	0.683	0.146	0.557	1520-2009
PSME LW	43.46, -113.59	1867	31 (62)	1468-2009	342	0.589	0.175	0.416	1532-2009

r: inter-series correlation
ms: mean sensitivity (Fritts 1976)
acf: first-order autocorrelation
eps: expressed population signal (Wigley et al. 1984)

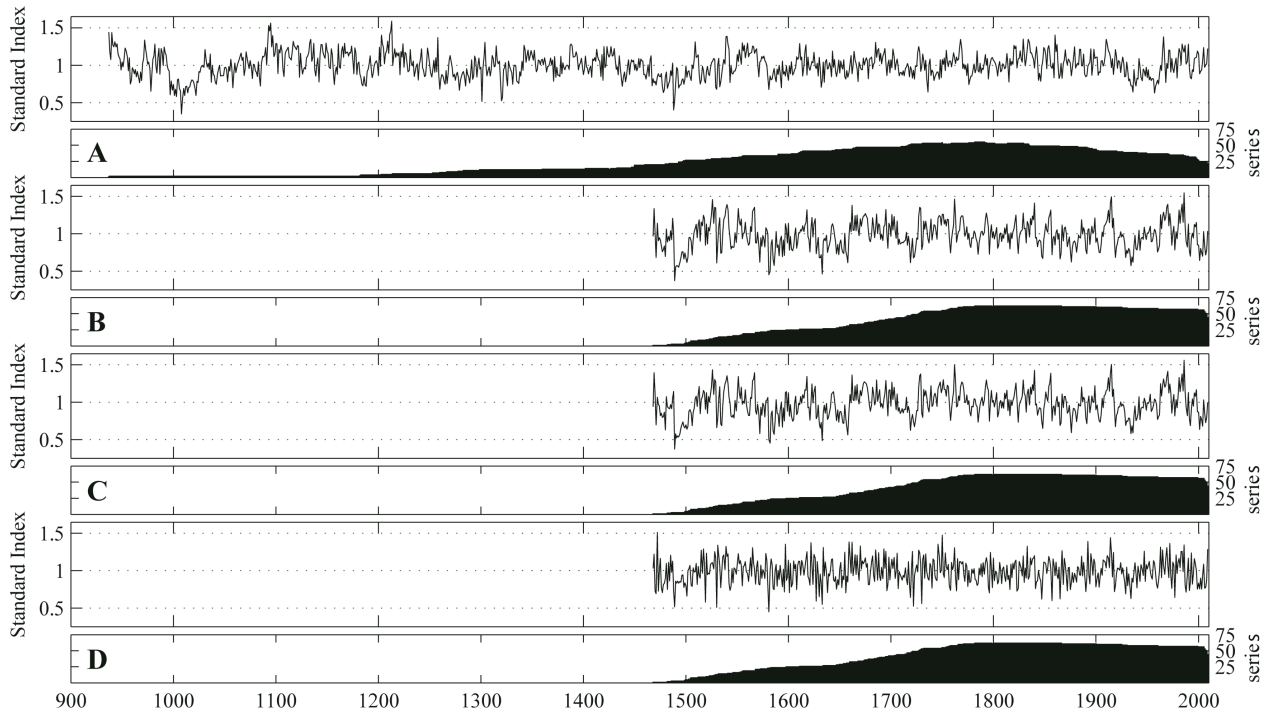

Figure 5. COM tree-ring width chronologies a) limber pine RW; b) Douglas fir RW; c) Douglas fir EW; and d) Douglas fir LW.

Table 2. Time domain correlations between tree-ring width chronologies (1532-2009).

Standardized chronologies				
	Douglas fir RW	Douglas fir EW	Douglas fir LW	
Limber Pine RW	0.36	0.34	0.25	
Residual chronologies				
	Douglas fir RW	Douglas fir EW	Douglas fir LW	Douglas fir LW_a
Limber Pine RW	0.09	0.08	0.16	0.15

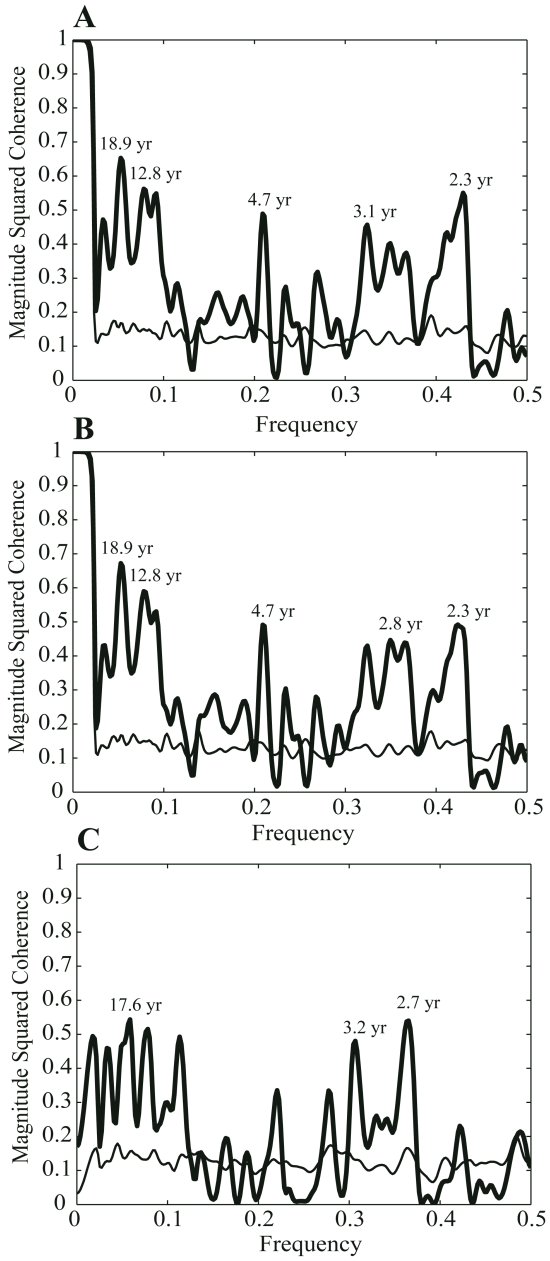

Figure 6. Magnitude squared coherence (thick black line) between limber pine RW and Douglas fir: a) RW, b) EW, and c) LW_a for 1532-2009. The thin black line is the red noise floor.

Section One: Radial Growth and Climate Sensitivity

Despite their close proximity (less than 5 km), limber pine and Douglas fir tree-ring width chronologies are not correlated ($r \sim = 0$) over time. Simple correlation coefficients between limber pine and Douglas fir standardized and residual RW, EW, LW, and LW_a indices can be found in Table 2. MSC between residual limber pine RW and residual Douglas fir RW, EW, and LW_a chronologies indicated significant coherence at decadal frequencies and above (Figure 6).

Limber pine and Douglas fir tree-ring widths at COM are moisture-sensitive. The primary climate variables controlling radial growth are total precipitation at monthly, seasonal, and annual timescales. The secondary climate variable controlling radial growth, which is statistically independent from the primary variable (Meko, Touchan, and Anchukaitis 2011), is mean monthly temperature during the summer season. Limber pine RW positively responds to prior late summer, fall, and early winter precipitation (Figure 7), and strongest seasonal correlation is prior summer-winter total precipitation ($r=0.42$, $p<0.01$). Douglas fir RW and EW have significant positive association to prior early winter and current spring precipitation (Figure 7). Total annual precipitation is the strongest correlation ($r=0.55$, $p<0.01$ and $r=0.52$, $p<0.01$, respectively). Douglas fir LW is positively correlated with prior fall, early winter, and current summer precipitation (Figure 7) with also a strong total annual precipitation correlation ($r=0.58$, $p<0.01$). Douglas fir LW_a is positively correlated with prior fall, early winter, and current summer precipitation. Adjusting for LW's dependence on EW removes the positive spring

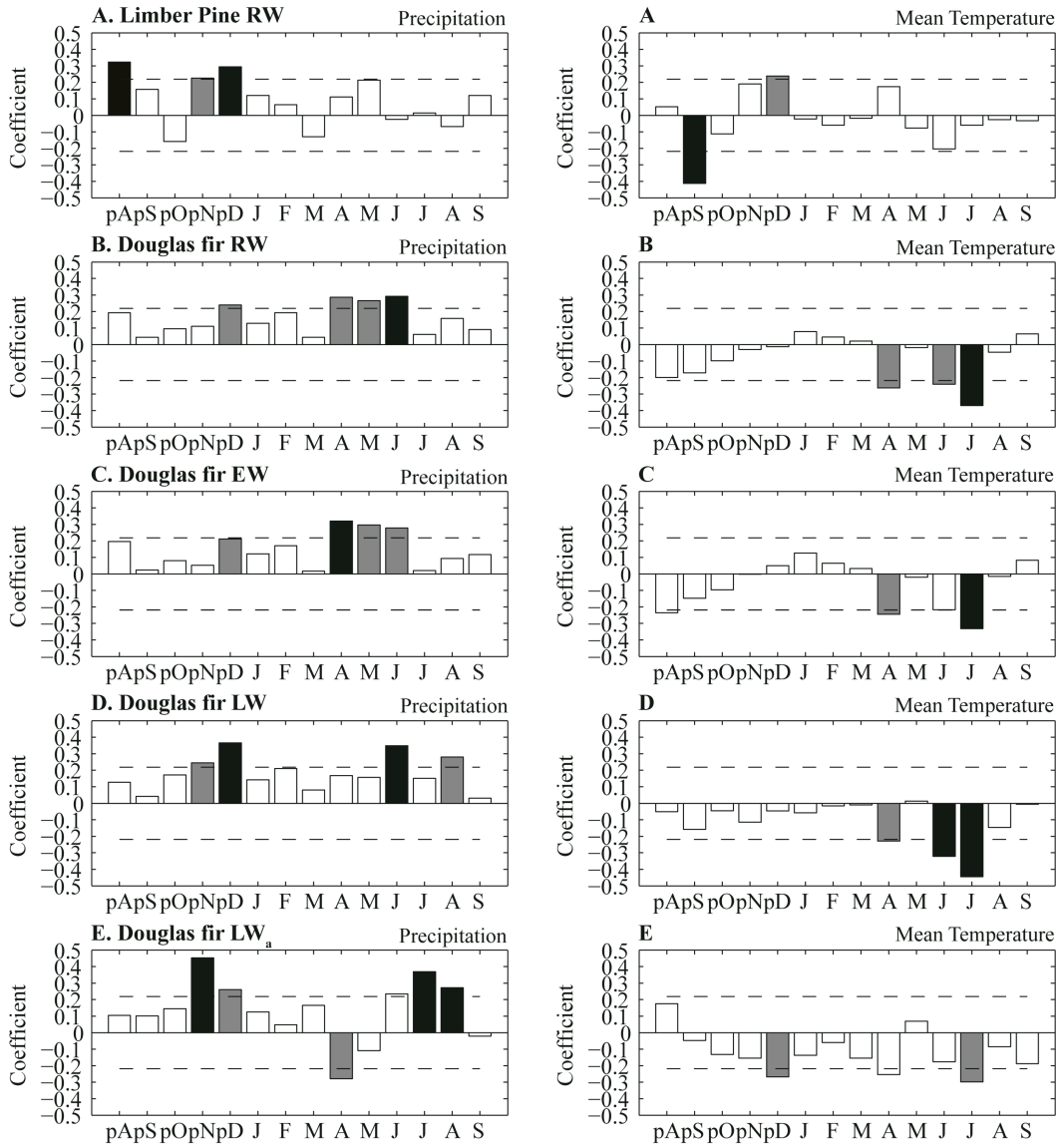

Figure 7. SEASCORR monthly correlations for a 14-month period from prior August to current September between a) limber pine RW, b) Douglas fir RW, c) Douglas fir EW, d) Douglas fir LW, e) Douglas fir LW_a and total precipitation (first column primary variable) and mean temperature (second column secondary variable) for 1930-2009. Monte-Carlo simulations (1000) were used to generate monthly coefficients. Dotted lines indicate 95% confidence intervals. Black bars indicate a non-exceedence probability of $p<0.01$, and grey bars indicate a non-exceedence probability of $p<0.05$.

precipitation response (Figure 7). The strongest seasonal response is prior summer-winter total precipitation ($r=0.46$, $p<0.01$).

Section Two: Tree-Ring Climate Reconstructions

Using COM tree-ring width precipitation signals, and the decadal persistence in observed eastern SRP annual and sub-annual precipitation, independent annual and sub-annual reconstructions were developed. During the 1930-2009 calibration, the first-order autocorrelation for annual and summer-winter precipitation was 0.294 ($p<0.05$) and 0.305 ($p<0.05$), respectively. The annual reconstruction includes the 12-month period from prior July to current June. The sub-annual (i.e., summer-winter) reconstruction includes the 9-month period from current July into the following March. The key difference between these reconstructions is the inclusion (exclusion) of April-June.

Annual and sub-annual summer-winter precipitation reconstructions were developed from Douglas fir EW predictors in year's *t*-1, *t*, and *t*+1, and Douglas fir LW_a and limber pine RW predictors in year *t* (Table 3). For 1930-2009, models explained 37% and 29% (adj. r^2) of the observed annual and summer-winter precipitation variance with 49.6 and 41.0 mm standard error of predictions. Cross-validation statistics indicate that reconstructed estimates are skillful; do not violate the assumptions of least-squared regression, and the regression residuals are randomly distributed around zero and contain no significant trend (Table 3). Time-dependent differences were detected between different calibrations, and model statistics showed sensitivity to the selected period of calibration (Table 4).

Table 3. Annual and sub-annual precipitation reconstruction statistics for Idaho climate divisions seven and nine on the eastern SRP.

Annual Reconstruction

					Press Calibration (1930-2009)						
Target	Predictors	Period	Port. Q	DW	R^2	Adj. R^2	F	*p*-value	Std. Error	RE	$RSME_v$
pJul.-Jun.	PSME EW *t*-1, *t*, *t*+1	1532-2008	7.90 (p=0.63)	2.09 (Accept)	0.40	0.37	16.39	<0.001	49.6	0.32	51.3

Sub-annual Summer-Winter Reconstruction

					Press Calibration (1930-2009)						
Target	Predictors	Period	Port. Q	DW	R^2	Adj. R^2	F	*p*-value	Std. Error	RE	$RSME_v$
Jul.-Mar.	PSME LW_a *t*, PIFL RW *t*	1532-2008	9.25 (p=0.57)	1.73 (Accept)	0.31	0.29	17.01	<0.001	41.0	0.25	41.8

Port. Q: Portmanteau Q statistic tests whether regression residuals are purely random or white noise.
DW: Durbin-Watson statistic tests for autocorrelation in residuals at lag-1. The null hypothesis states that there is no autocorrelation. The decision is 'Accept' or 'Reject'.
RE: Reduction of error statistic measures reconstruction skill in excess of climatology, and is based on the calibration mean. A positive value > 0 indicates forecast skill.
$RSME_v$: Root mean square error - a 'leave-one-out' PRESS cross-validation statistic.

Table 4. Early and late period annual and sub-annual precipitation reconstruction statistics with verification for Idaho climate divisions seven and nine on the eastern SRP.

Annual Reconstruction

					Press Calibration (1930-1979)						
Target	Predictors	Period	Port. Q	DW	R^2	Adj. R^2	F	*p*-value	Std. Error	RE	$RSME_v$
pJul.-Jun.	PSME EW *t*-1, *t*, *t*+1	1532-2008	7.26 (p=0.70)	2.01 (Accept)	0.40	0.36	10.20	<0.001	41.1	0.25	44.0
					Press Calibration (1960-2009)						
pJul.-Jun.	PSME EW *t*-1, *t*, *t*+1	1532-2008	9.26 (p=0.50)	2.29 (Accept)	0.36	0.32	8.40	<0.001	57.3	0.24	59.9

Verification (1930-1959)			Verification (1980-2008)		
r	RE	CE	*r*	RE	CE
0.64**	0.54	0.19	0.60**	0.33	0.27

Sub-annual Summer-Winter Reconstruction

					Press Calibration (1930-1979)						
Target	Predictors	Period	Port. Q	DW	R^2	Adj. R^2	F	*p*-value	Std. Error	RE	$RSME_v$
Jul.-Mar.	PSME LWa *t*, PIFL RW *t*	1532-2008	8.91 (p=0.54)	1.79 (Accept)	0.29	0.26	9.79	<0.001	38.6	0.19	40.1
					Press Calibration (1960-2009)						
Jul.-Mar.	PSME LWa *t*, PIFL RW *t*	1532-2008	6.17 (p=0.79)	1.96 (Accept)	0.39	0.36	14.44	<0.001	41.6	0.30	43.0

Verification (1930-1959)			Verification (1980-2008)		
r	RE	CE	*r*	RE	CE
0.29	0.16	-0.17	0.60**	0.31	0.26

Port. Q: Portmanteau Q statistic tests whether regression residuals are purely random or white noise.
DW: Durbin-Watson statistic tests for autocorrelation in residuals at lag-1. The null hypothesis states that there is no autocorrelation. The decision is 'Accept' or 'Reject'.
RE: Reduction of error statistic measures reconstruction skill in excess of climatology, and is based on the calibration mean. A positive value > 0 indicates forecast skill.
$RSME_v$: Root mean square error - a 'leave-one-out' PRESS cross-validation statistic.
CE: Coefficient of efficiency statistic measures reconstruction skill in excess of climatology, and is based on the verification mean. A positive value > 0 indicates forecast skill.
****:** Statistical significance p<0.01 (two-tailed test)

Two independent verification periods were used to further assess each early and late period calibration. Both annual calibrations passed correlation, RE, and CE verification tests (Table 4). For the sub-annual summer-winter reconstruction, the 1930-1979 calibration passed all three tests, but the 1960-2008 calibration only passed RE, and failed correlation and CE tests (Table 4). Annual and sub-annual precipitation reconstructions only show moderate positive agreement (r=0.38, p<0.01) during 1532-2008. Decadal and multidecadal variability account for 48% and 42% of the variance in the annual and sub-annual precipitation reconstructions, respectively.

Discussion

Section One: Radial Growth and Climate Sensitivity

Ancient lower forest border limber pine and Douglas fir trees growing on the COM lava complex enabled centuries-long annual and sub-annual tree-ring chronology development. For most of the last millennium, it appears as though limber pine has occupied and survived on a range lava site conditions while Douglas fir has been largely confined to north facing cinder cone slopes. Standardized tree-ring widths between species show moderate covariance when biological persistence is retained, and weak covariance when it is removed. This time domain difference indicates that the autocovariance structure of limber pine and Douglas fir radial growth is more similar over decades, than at interannual timescales. Even when first-order autocorrelation is removed from each tree-ring width chronology, co-spectral analysis shows that limber pine RW is coherent with Douglas fir RW, EW, and LW_a at decadal frequencies and above. Lamarche (1974a) and Hughes and Funkhouser (2003) found that decadal and

higher frequency precipitation variability was primarily responsible for the observed frequency-dependent coherence between upper and lower forest border Great Basin Bristlecone pine (*Pinus longeva*). Because COM limber pine and Douglas fir have and continue to grow in the same local climatic envelope, and more or less have equal accessibility to atmospheric moisture inputs, decadal growth coherence across nearly five centuries points to a lower frequency moisture control despite weak interannual association. This higher frequency radial growth mismatch between species likely reflects differences in tree physiology and season-specific climate sensitivity.

Across the southwestern US, recent methodological advancements by Meko and Basian (2001), Stahle et al. (2009), and Griffin et al. (2011) have exploited Douglas fir and Ponderosa pine (*Pinus ponderosa*) sub-annual EW and LW growth increments to fine-tune seasonal precipitation signals embedded within total ring-width. For Douglas fir at the COM, removing the linear dependence on EW produces an adjusted LW record that has a strong connection to precipitation in summer, autumn and early winter, while reducing the influence of spring precipitation. The varying climate responses exhibited by limber pine and Douglas fir at COM may reflect the physiological differences between the two species that influence the timing of radial growth formation, storage of carbon resources, and seasonal climate sensitivity (Fritts 1976). Needle elongation and retention in five-needle pines can last for more than six years, offering a rationale for why climate responses are often observed in seasons prior to growth formation (Kipfmueller and Salzer 2010; Lamarche 1974b; Salzer et al. 2009). Fritts et al's. (1965) Douglas fir study at Mesa Verde found that radial growth was influenced by moisture availability in all

seasons of the prior and current year. Using dendrographs, they were able to conclude that terminal growth and needle elongation (i.e., earlywood formation) was complete by early June, and that latewood formation was a function of needle density and moisture availability during winter and early spring. Given the weak correlations between limber pine and Douglas fir tree-ring widths observed at interannual timescales, species-dependent physiological responses to season-specific precipitation likely contributes to the observed growth differences, especially since the eastern SRP has bimodal precipitation peaks in winter and spring.

Limber pine RW and Douglas fir RW, EW, and LW_a provide faithful high-resolution proxies for accumulated monthly, seasonal, and annual precipitation in the region surrounding COM. Limber pine RW is a proxy for summer-winter precipitation. This late summer into early winter climate response for limber pine is typical for five-needle pines in certain localities of the western US (Kipfmueller and Salzer 2010). Douglas fir RW and EW have very similar precipitation responses, and both serve as proxies for annual precipitation (prior summer through current spring), though the spring season largely drives the annual precipitation signal. This annual precipitation signal corroborates Gray et al. (2007) and Gray and McCabe (2010) who found that Douglas fir ring-width in the Greater Yellowstone region was significantly correlated with previous July-June precipitation. Other studies in the region have only focused on using Douglas fir ring-width as a proxy for summer PDSI (Cook et al. 1999; Cook et al. 2004) or annual streamflow (Graumlich et al. 2003; Wise 2010). By applying the LW adjustment to Douglas fir at COM (Griffin et al. 2011), season-specific precipitation signals can be

partitioned within total ring-width. This result suggests that Douglas fir LW_a may have utility as a centuries-long proxy for summer-winter precipitation elsewhere across the intermountain Northwest.

Section Two: Tree-Ring Climate Reconstructions

Using the annual and sub-annual summer-winter precipitation signals encoded within COM limber pine and Douglas fir tree-ring widths, and the temporal length of each record, we opted to develop precipitation reconstructions for the period 1532-2008. Three independent tree-ring width chronologies (limber pine RW, Douglas-fir EW, and Douglas-fir LW_a) were used to reconstruct precipitation. We exploited annual and sub-annual tree-ring width precipitation signals to develop estimates of annual (pJuly-June) and summer-winter (July-March) precipitation because of the observed first-autocorrelation in the PRISM precipitation data during the calibration period. This instrumental autocorrelation structure reflects seasonal persistence in precipitation, and because COM tree-ring width chronologies still retain lower frequency variability despite autoregressive modeling, we are confident that these tree-ring widths match the observed precipitation autocorrelation. Douglas fir EW was used to predict pJuly-June precipitation, and limber pine RW and Douglas fir LW_a were used to predict summer-winter precipitation (July-March). This reconstruction approach follows a similar rationale to Stahle et al. (2009) who used Douglas fir EW and Douglas fir LW_a to independently reconstruct cool-season (pNovember-May) and early warm-season (July) precipitation for the El Malpais lava complex in New Mexico.

Unlike the bimodal precipitation regime across Southwestern US, precipitation on the eastern SRP is more evenly distributed annually although there are distinctive wet seasons in winter (November-February) and spring (May-June), as well as a summer dry season beginning in July. This annual reconstruction is similar to the approach taken by (Gray, Jackson, and Betancourt 2004), (2007), and Gray and McCabe (2010) to reconstruct annual precipitation in nearby Greater Yellowstone and northeastern Utah regions. The main difference between these reconstructions and previous work in this region is the emphasis on sub-annual radial growth variability and precipitation seasonality. Producing skillfully independent annual and sub-annual summer-winter reconstructions that include (exclude) spring precipitation suggest that future efforts must consider partitioning seasonal precipitation when reconstructing climate from tree-ring widths across the intermountain northwest.

When developing tree-ring based climate reconstructions, quantifying error and uncertainty within model structure is critical for insuring that proxy-based estimates are plausible for subsequent paleoclimatic interpretation (Jones et al. 2009; Meko et al. 2007). Although annual and sub-annual reconstructions only explained between 29-40% of the observed precipitation variance, the standard error of prediction was 49.6 and 41.0 mm, respectively. Much of the cool-season precipitation that falls on the eastern SRP is a snow-rain mix, and is delivered from frontal systems moving eastward through the low elevation corridor (Mock 1996; Whitlock and Bartlein 1993). Yet, SRP summer precipitation is almost exclusively convectional, and driven by local thermal heating, frontogenesis, or the occasional northward fringe of monsoonal flow (Mock 1996;

Whitlock and Bartlein 1993). Given that precipitation can originate from frontal or convectional mechanisms, and that standard error in these tree-ring based estimates is relatively low compared to accumulated totals, much of the uncertainty realistically arises from spatial variability in one or two late fall-winter snowfall events and/or locally confined downpours from convectional activity.

Using an early (late) independent calibration-verification modeling design (Fritts 1991) enabled time-dependent calibration error and uncertainty to be further diagnosed. In 'multivariate space', tree-ring predictors can have difficulty reproducing climatic anomalies, so, if the tree-ring-climate calibration interval covers a period of anomalous climatic conditions, then the possibility that reconstructed estimates will not skillfully exceed the observed climatology outside the calibration period is likely, and remains a dilemma in dendroclimatic calibration. Fritts (1974) notes that high temperatures limit cell formation and division processes differently than low precipitation, so if physiological temperature-induced thresholds are exceeded for arid site conifers, then the dominant precipitation signal can be temporarily dampened at short-term intervals. Although both annual and sub-annual precipitation reconstructions are well validated across 1930-2009, the late period calibration (1960-2008) for summer-winter precipitation did have difficulty verifying against the early period (1930-1959) summer-winter precipitation climatology. The long run of drier than normal years during this period either points to the shifting influence of growing season temperature as a dominant limiting factor on radial growth, or possibly indicates anomalous seasonal precipitation regime.

The moderate positive agreement between annual and sub-annual precipitation reconstructions indicates that when the preceding summer-winter has been 'dry' or 'wet', then the annual timescale also has a tendency to be 'dry' or 'wet' that includes the following spring. For this SRP low elevation airflow corridor (Mitchell 1976; Mock 1996), slower changing sea surface temperatures (SSTs) in the Pacific basin coupled with upper-level atmospheric long waves propagating from far field (Barnston and Livezey 1987; Harman 1991), and/or faster-pace regionally centered land surface-atmospheric processes acting in- or out-of-phase over multiple timescales (Dettinger et al. 1998) likely forces 'persistent' or 'transitional' behavior in seasonal precipitation regimes across the annual cycle.

The annual precipitation reconstruction showed a pronounced 14.3 yr. frequency that accounted for 36% of the total precipitation variance (Figure 8). This 14 yr. spectral peak has been found to be the dominant decadal cool-season precipitation variation (November-April) for western US instrumental precipitation records north of 40°N, and explains 33% of the decadal precipitation anomalies (Cayan et al. 1998; Dettinger et al. 1998). Ault and St. George (2010) find that annual precipitation in the mid-latitudes (40-50°N) varies at timescales between 10-20 yrs., and at the seasonal timescale, they identify a decadal hotspot in autumn precipitation over the central Rockies. A 73.5 yr. mutidecadal frequency is also present in the annual precipitation reconstruction, but accounts for much less of the total variance (Figure 8). Cayan et al. (1998) suggests that precipitation anomalies during certain seasons may contribute more to decadal

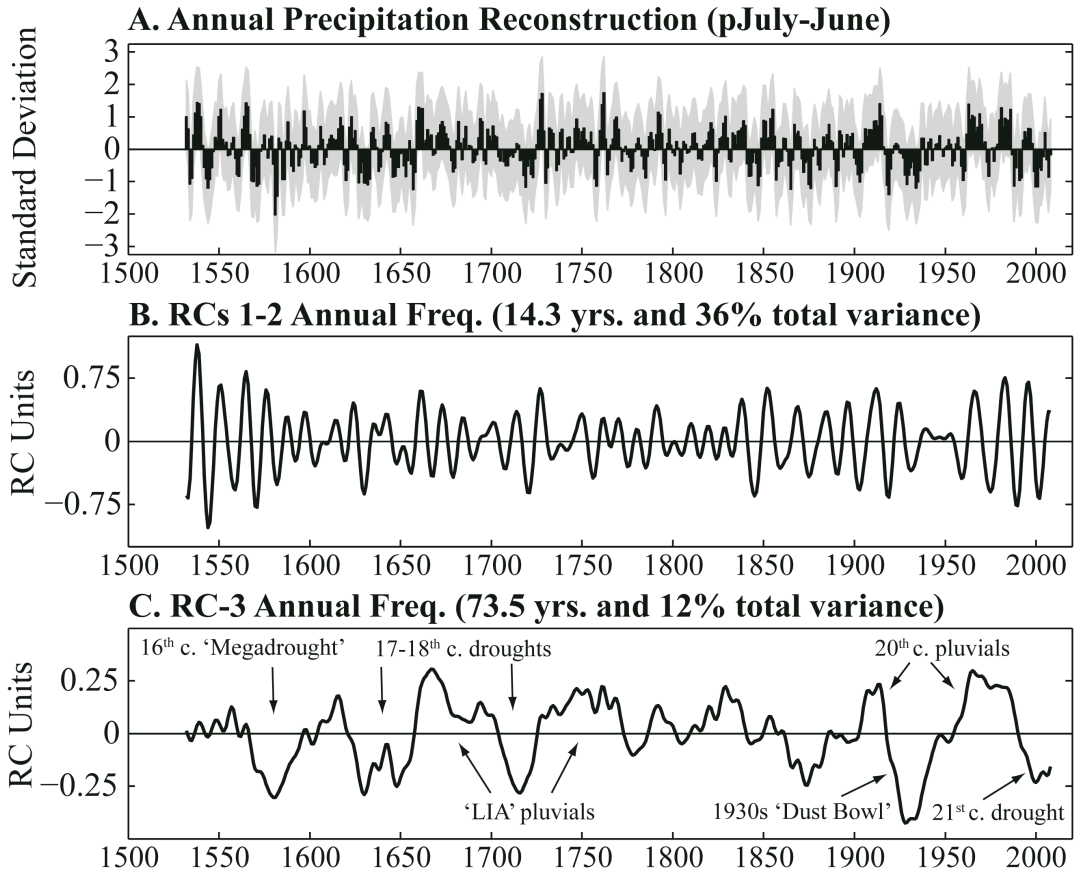

Figure 8. Annual precipitation estimates for the eastern SRP (1532-2008). Tree-ring based estimates have been scaled to match observed precipitation during the calibration period. A) Annual reconstruction with 80% confidence intervals derived from the standard error and t-distribution at probability points 0.10 and 0.90. B) RCs 1 and 2 for annual precipitation. C) RC-3 for annual precipitation. Note, prominent drought and pluvial episodes are well represented at the multidecadal frequency.

variability, often the months with the largest climatological precipitation, but that the largest contributions to decadal variability are not confined to months with peak precipitation maxima.

One of the primary limitations for identifying multidecadal climate variability in instrumental records is the length of the record itself (Mehta et al. 2011). Well-calibrated tree-ring proxies do provide a much longer timeframe to detect lower frequency climate fluctuations than is possible for instrumental climate records (Hughes 2002). The sub-annual summer-winter reconstruction shows a dominant 70.4 yr. multidecadal frequency that explains 21% of the total variance as well as 21.7 and 14.3 yr. frequencies that contribute an additional 22% (Figure 9). Cayan et al. (1998) point out that no one season is the sole source of decadal variability, rather, they suggest more broadly that both winter and summer seasons contribute strongly to decadal fluctuations. Based upon this notion, our sub-annual summer-winter precipitation reconstruction for the eastern SRP realistically captures much of the multidecadal variability embedded within total accumulated precipitation over the annual cycle. Multidecadal climate variability and associated forcing mechanisms has received much attention with interests in long-term drought forecasting (Enfield, Mestas-Nunez, and Trimble 2001; Gray et al. 2003; McCabe and Palecki 2006; McCabe, Palecki, and Betancourt 2004). Much of the work so far has identified lower frequency fluctuations in Atlantic and Pacific Basin SSTs on the order of 30-70 and/or 65-80 yr. timescales that modulate summer rainfall and multidecadal drought over North America

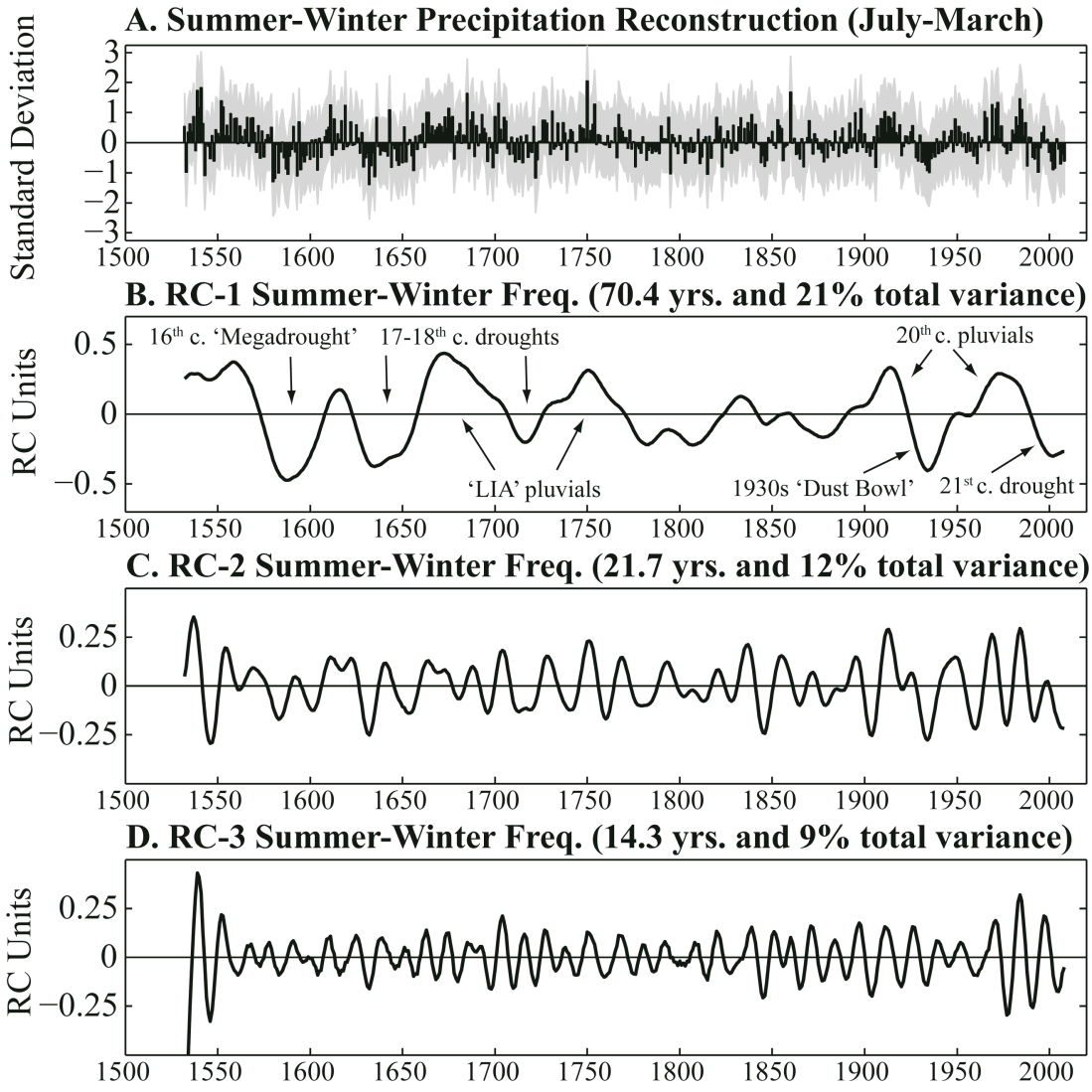

Figure 9. Sub-annual precipitation estimates for the eastern SRP (1532-2008). Tree-ring based estimates have been scaled to match observed precipitation during the calibration period. A) Summer-winter reconstruction with 80% confidence intervals derived from the standard error and t-distribution at probability points 0.10 and 0.90. B) RC-1 for summer-winter precipitation. C) RC-2 for summer-winter precipitation. D) RC-3 for summer-winter precipitation. Note, prominent drought and pluvial episodes are well represented at the multidecadal frequency.

(Enfield, Mestas-Nunez, and Trimble 2001; Gray et al. 2003). The objective of this study is not to link multidecadal summer-winter precipitation variability on the eastern SRP to specific large-scale forcing mechanisms, but draw attention to decadal and multidecadal frequencies that contribute the most to the total variation in precipitation. A dense network of tree-ring records from this region containing similar seasonal precipitation signals and coherent modes of variability will be required before assigning any one forcing mechanism such as El-Nino Southern Oscillation (ENSO), Pacific-Decadal Oscillation (PDO), or Altantic-Multidecadal Oscillation (AMO) to the observed multidecadal variability in precipitation.

Given that tree-ring precipitation reconstructions do exist for certain localities across the western US, we felt it was qualitatively worthwhile to orient these annual and sub-annual reconstructions relative to western US paleoclimate of the past 500 years. If multidecadal precipitation frequencies are selected for interpretation (Figures 8 and 9), both annual and sub-annual summer-winter precipitation reconstructions offer compelling evidence that the late 16th century 'megadrought' (Stahle et al. 2000; Woodhouse and Overpeck 1998) reached northward onto the eastern SRP, and was primarily a summer-winter season phenomena that persisted for several decades between the 1580s and early 1600s. This finding is consistent with Gray et al. (2003) who found in their analysis of fifteen tree-ring reconstructions from the southern and central Rockies that the late 16th century 'megadrought' exhibited widespread synchrony. Interrupted by a brief wet period, another summer-winter multidecadal drought lasting approximately 30 years appears on the eastern SRP between the 1620s and 1650s, and is corroborated by an

annual streamflow reconstruction for upper Snake River system (Wise 2010). For the last half of the 17th century and much of the 18th century, summer-winter precipitation remained above average with only one intervening dry period in the early 1700s. This long run of above average precipitation aligns with high intensity Little Ice Age (LIA) pluvials and Northern Hemispheric cooling (Cook, Esper, and D'Arrigo 2004; Pederson et al. 2006). The early 20th century is marked by a period of above average annual and summer-winter precipitation that directly corresponds to the western US pluvial event (1905-1917) documented by several studies (Cook, Seager, and Miller 2011; Cook et al. 2007; Fye, Stahle, and Cook 2003; Woodhouse et al. 2005). This early 20th century pluvial event appears to be centered on the winter season; instrumental precipitation anomalies on the eastern SRP exceed two standard deviations (Woodhouse et al. 2005). The 1930s 'Dust Bowl' is distinct in both reconstructions, and has been widely documented in many precipitation, streamflow, and PDSI reconstructions regionally (Graumlich et al. 2003; Gray, Graumlich, and Betancourt 2007; Wise 2010) and across the northwestern US (Cook et al. 1999; Cook et al. 2007; Cook et al. 2004; Fye, Stahle, and Cook 2003).

These precipitation reconstructions indicate that the 1960s-early 1980s were anomalously wet, and possibly suggests a more regionally confined late 20th century pluvial (Gray, Jackson, and Betancourt 2004). These reconstructions also indicate that precipitation on eastern SRP since the late 1980s is near or approaching pre-instrumental deficits with the current drought centered on the 2000s. This early 21st century drought still does not exceed the multidecadal droughts of the past 500 years, although if

precipitation remains below average for the next decade, this drought could rival 'megadroughts' of the past. Similar decadal and multidecadal precipitation frequencies dominate both precipitation reconstructions with annual precipitation showing stronger decadal behavior with inclusion of spring, while sub-annual summer-winter precipitation exhibits stronger multidecadal variability. This suggests that multidecadal drought (pluvial) episodes on the eastern SRP cannot occur without deficits (surpluses) in summer-winter precipitation.

Conclusion

Tree-ring width records from ancient lower forest border arid-site conifers growing on basaltic-lava at the COM offer high-resolution centuries-long proxy-records for annual and sub-annual precipitation on the eastern SRP. Limber pine RW and Douglas fir RW, EW, and LW_a show decadal coherence and weak interannual association. The interannual growth difference originates from tree physiology and season-specific precipitation sensitivity. Adjusting for Douglas fir's LW dependence on antecedent EW (Griffin et al. 2011) removed Douglas fir's EW positive spring precipitation signal, and enhanced the late fall-early winter and summer precipitation signals encoded with Douglas fir LW. As a result, precipitation signals in limber pine RW and Douglas fir LW_a align across summer, fall, and winter seasons. Since Douglas fir RW and EW both contained annual precipitation signals driven primarily by the spring season, Douglas fir EW was the preferred proxy for annual precipitation given its independence from Douglas fir LW_a.

This COM tree-ring case study finds that decadal and multidecadal precipitation frequencies account for nearly half of the total variation in moisture availability on the

eastern SRP. Variability in summer-winter precipitation contributes substantially to multidecadal drought (pluvial) occurrence. These precipitation reconstructions are consistent with western US paleoclimate during the past 500 years, and capture well-documented drought and pluvial episodes. Nevertheless, this study points out that isolating sub-annual precipitation variability in tree-ring widths and then extracting dominant frequencies over paleo-timescales may be helpful for identifying large-scale mechanisms forcing natural internal decadal and multidecadal climate variability. As this study has demonstrated, tree-ring based climate reconstructions could continue to benefit from a more detailed season-specific focus that exploits both annual and sub-annual tree-ring widths across multiple species similar to ongoing work in the Southwestern US (Griffin et al. 2011; Stahle et al. 2009). This study provides a method to improve paleo-drought (pluvial) resolution on long-timescales across the intermountain Northwest and elsewhere, but a more spatially dense tree-ring proxy network is required before this season-specific method can be fully realized.

References

Ault, T. R., and S. St George. 2010. "The Magnitude of Decadal and Multidecadal Variability in North American Precipitation." *Journal of Climate* no. 23 (4):842-850. doi: 10.1175/2009jcli3013.1.

Barnston, A. G., and R. E. Livezey. 1987. "Classification, Seasonality and Persistence of Low-Frequency Atmospheric Circulation Patterns." *Monthly Weather Review* no. 115 (6):1083-1126.

Briffa, K. R., and P. D. Jones. 1990. "Basic chronology statistics." In *Methods of Dendrochronology: Applications in the Environmental Sciences*, edited by E. R. Cook and L. A. Kairiukstis, 137-152. Dordrecht: Kluwer Academic Publishers/IIASA.

Cayan, D. R., M. D. Dettinger, H. F. Diaz, and N. E. Graham. 1998. "Decadal variability of precipitation over western North America." *Journal of Climate* no. 11 (12):3148-3166. doi: 10.1175/1520-0442(1998)011<3148:dvopow>2.0.co;2.

Cook, B. I., R. Seager, and R. L. Miller. 2011. "On the Causes and Dynamics of the Early Twentieth-Century North American Pluvial." *Journal of Climate* no. 24 (19):5043-5060. doi: 10.1175/2011jcli4201.1.

Cook, E. R. 1985. *A time series analysis approach to tree ring standardization*. Disseration, University of Arizona, Tucson.

Cook, E. R., K. R. Briffa, D. M. Meko, D. A. Graybill, and G. Funkhouser. 1995. "The segment length curse in long tree-ring chronology development for paleoclimatic studies." *Holocene* no. 5 (2):229-237.

Cook, E. R., J. Esper, and R. D. D'Arrigo. 2004. "Extra-tropical Northern Hemisphere land temperature variability over the past 1000 years." *Quaternary Science Reviews* no. 23 (20-22):2063-2074. doi: 10.1016/j.quaascirev.2004.08.013.

Cook, E. R., and L. A. Kairiukstis. 1990. *Methods of Dendrochronology: Applications in the Environmental Sciences*. Dordrecht: Kluwer Academic Publishers/IIASA.

Cook, E. R., D. M. Meko, D. W. Stahle, and M. K. Cleaveland. 1999. "Drought reconstructions for the continental United States." *Journal of Climate* no. 12 (4):1145-1162.

Cook, E. R., and K. Peters. 1997. "Calculating unbiased tree-ring indices for the study of climate and environmental change." *The Holocene* no. 7:361-370.

Cook, E. R., R. Seager, M. A. Cane, and D. W. Stahle. 2007. "North American drought: Reconstructions, causes, and consequences." *Earth-Science Reviews* no. 81 (1-2):93-134. doi: 10.1016/j.earscirev.2006.12.002.

Cook, E. R., C. A. Woodhouse, C. M. Eakin, D. M. Meko, and D. W. Stahle. 2004. "Long-term aridity changes in the western United States." *Science* no. 306 (5698):1015-1018. doi: 10.1126/science.1102586.

Daly, C., M. Halbleib, J. I. Smith, W. P. Gibson, M. K. Doggett, G. H. Taylor, J. Curtis, and P. P. Pasteris. 2008. "Physiographically sensitive mapping of climatological temperature and precipitation across the conterminous United States." *International Journal of Climatology* no. 28 (15):2031-2064. doi: 10.1002/joc.1688.

Dettinger, M. D., D. R. Cayan, H. F. Diaz, and D. M. Meko. 1998. "North-south precipitation patterns in western North America on interannual-to-decadal timescales." *Journal of Climate* no. 11 (12):3095-3111.

Eischeid, J. K., C. B. Baker, T. R. Karl, and H. F. Diaz. 1995. "The quality-control of long-term climatological data using objective data-analysis." *Journal of Applied Meteorology* no. 34 (12):2787-2795. doi: 10.1175/1520-0450(1995)034<2787:tqcolt>2.0.co;2.

Enfield, D. B., A. M. Mestas-Nunez, and P. J. Trimble. 2001. "The Atlantic multidecadal oscillation and its relation to rainfall and river flows in the continental US." *Geophysical Research Letters* no. 28 (10):2077-2080. doi: 10.1029/2000gl012745.

Fritts, H. C. 1965. "Tree-Ring Characteristics Along a Vegetation Gradient in Northern Arizona." *Ecology* no. 46:394-401.

———. 1976. *Tree Rings and Climate*. Caldwell, New Jersey: The Blackburn Press.
———. 1991. *Reconstructing Large-Scale Climatic Patterns from Tree-Ring Data, A Diagnostic Analysis*. Tucson: The University of Arizona Press.
Fritts, H. C., D. G. Smith, J. W. Cardis, and C. A. Budelsky. 1965. "Tree-ring characteristics along a vegetation gradient in northern Arizona." *Ecology* no. 46 (4):394-401.
Fritts, H. C. 1966. "Growth-rings of trees: their correlation with climate." *Science* no. 154 (3752):973-979.
———. 1974. "Relationships of ring widths in arid-site conifers to variations in monthly temperature and precipitation." *Ecological Monographs* no. 44 (4):411-440.
Fye, F. K., D. W. Stahle, and E. R. Cook. 2003. "Paleoclimatic analogs to twentieth-century moisture regimes across the United States." *Bulletin of the American Meteorological Society* no. 84 (7):901-909.
Ghil, M., M. R. Allen, M. D. Dettinger, K. Ide, D. Kondrashov, M. E. Mann, A. W. Robertson, A. Saunders, Y. Tian, F. Varadi, and P. Yiou. 2002. "Advanced spectral methods for climatic time series." *Reviews of Geophysics* no. 40 (1). doi: 100310.1029/2000rg000092.
Graumlich, L. J., M. F. J. Pisaric, L. A. Waggoner, J. S. Littell, and J. C. King. 2003. "Upper Yellowstone River flow and teleconnections with Pacific basin climate variability during the past three centuries." *Climatic Change* no. 59 (1-2):245-262. doi: 10.1023/a:1024474627079.
Gray, S. T., J. L. Betancourt, C. L. Fastie, and S. T. Jackson. 2003. "Patterns and sources of multidecadal oscillations in drought-sensitive tree-ring records from the central and southern Rocky Mountains." *Geophysical Research Letters* no. 30 (6). doi: 131610.1029/2002gl016154.
Gray, S. T., L. J. Graumlich, and J. L. Betancourt. 2007. "Annual precipitation in the Yellowstone National Park region since AD 1173." *Quaternary Research* no. 68 (1):18-27. doi: 10.1016/j.yqres.2007.02.002.
Gray, S. T., S. T. Jackson, and J. L. Betancourt. 2004. "Tree-ring based reconstructions of interannual to decadal scale precipitation variability for northeastern Utah since 1226 AD." *Journal of the American Water Resources Association* no. 40 (4):947-960. doi: 10.1111/j.1752-1688.2004.tb01058.x.
Gray, S. T., and G. J. McCabe. 2010. "A combined water balance and tree ring approach to understanding the potential hydrologic effects of climate change in the central Rocky Mountain region." *Water Resources Research* no. 46. doi: W0551310.1029/2008wr007650.
Griffin, D., D. M. Meko, R. Touchan, S. W. Leavitt, and C. A. Woodhouse. 2011. "Latewood chronology development for summer-moisture reconstruction in the US Southwest." *Tree-Ring Research* no. 67 (2):87-101.
Harman, J. R. 1991. *Synoptic Climatology of the Westerlies: Process and Patterns*. Washington D.C.: Assocation of American Geographers.
Holmes, R. L. 1983. "Computer-assisted quality control in tree ring dating and measuring." *Tree Ring Bulletin* no. 43:69-78.

Hughes, M. K., and G. Funkhouser. 2003. "Frequency-dependent climate signal in upper and lower forest border tree rings in the mountains of the Great Basin." *Climatic Change* no. 59 (1-2):233-244.

Hughes, M.K. 2002. "Dendrochronology in climatology - The state of the art." *Dendrochronologia v20* no. n1-2:95-116 Journal Code Dendrochronologia.

Jones, P. D., K. R. Briffa, T. J. Osborn, J. M. Lough, T. D. van Ommen, B. M. Vinther, J. Lutherbacher, E. R. Wahl, F. W. Zwiers, M. E. Mann, G. A. Schmidt, C. M. Ammann, B. M. Buckley, K. M. Cobb, J. Esper, H. Goosse, N. Graham, E. Jansen, T. Kiefer, C. Kull, M. Kuttel, E. Mosley-Thompson, J. T. Overpeck, N. Riedwyl, M. Schulz, A. W. Tudhope, R. Villalba, H. Wanner, E. Wolff, and E. Xoplaki. 2009. "High-resolution palaeoclimatology of the last millennium: a review of current status and future prospects." *Holocene* no. 19 (1):3-49. doi: 10.1177/0959683608098952.

Kipfmueller, K. F., and M. W. Salzer. 2010. "Linear trend and climate response of five-needle pines in the western United States related to treeline proximity." *Canadian Journal of Forest Research-Revue Canadienne De Recherche Forestiere* no. 40 (1):134-142. doi: 10.1139/x09-187.

Lamarche, V. C. 1974a. "Frequency-Dependent Relationships between Tree-Ring Series along an Ecological Gradient and Some Dendroclimatic Implications." *Tree-Ring Bulletin* no. 34:1-20.

Lamarche, V. C., Jr. 1974b. "Paleoclimatic Inferences from Long Tree-Ring Records: Intersite comparison shows climatic anomalies that may be linked to features of the general circulation." *Science (New York, N.Y.)* no. 183 (4129):1043-8. doi: 10.1126/science.183.4129.1043.

Marston, R. A., J. D. Mills, D. R. Wrazien, B. Bassett, and D. K. Splinter. 2005. "Effects of Jackson Lake Dam on the Snake River and its floodplain, Grand Teton National Park, Wyoming, USA." *Geomorphology* no. 71 (1-2):79-98. doi: 10.1016/j.geomorph.2005.03.005.

McCabe, G. J., and M. A. Palecki. 2006. "Multidecadal climate variability of global lands and oceans." *International Journal of Climatology* no. 26 (7):849-865. doi: 10.1002/joc.1289.

McCabe, G. J., M. A. Palecki, and J. L. Betancourt. 2004. "Pacific and Atlantic Ocean influences on multidecadal drought frequency in the United States." *Proceedings of the National Academy of Sciences of the United States of America* no. 101 (12):4136-4141. doi: 10.1073/pnas.0306738101.

McGuire, M., A. W. Wood, A. F. Hamlet, and D. P. Lettenmaier. 2006. "Use of satellite data for streamflow and reservoir storage forecasts in the snake river basin." *Journal of Water Resources Planning and Management-Asce* no. 132 (2):97-110. doi: 10.1061/(asce)0733-9496(2006)132:2(97).

Mehta, V., G. Meehl, L. Goddard, J. Knight, A. Kumar, M. Latif, T. Lee, A. Rosati, and D. Stammer. 2011. "Decadal climate predictability and prediction: Where are we?" *Bulletin of the American Meteorological Society* no. 92 (5):637-640. doi: 10.1175/2010bams3025.1.

Meko, D., E. R. Cook, D. W. Stahle, C. W. Stockton, and M. K. Hughes. 1993. "Spatial patterns of tree-growth anomalies in the United-States and Southeastern Canada." *Journal of Climate* no. 6 (9):1773-1786.

Meko, D. M., and C. H. Baisan. 2001. "Pilot study of latewood-width of conifers as an indicator of variability of summer rainfall in the North American Monsoon Region." *International Journal of Climatology* no. 21 (6):697-708. doi: 10.1002/joc.646.

Meko, D. M., R. Touchan, and K. J. Anchukaitis. 2011. "Seascorr: A MATLAB program for identifying the seasonal climate signal in an annual tree-ring time series." *Computers & Geosciences*. doi: 10.1016/j.cageo.2011.01.013.

Meko, D. M., and C. A. Woodhouse. 2005. "Tree-ring footprint of joint hydrologic drought in Sacramento and Upper Colorado river basins, western USA." *Journal of Hydrology* no. 308 (1-4):196-213. doi: 10.1016/j.jhydrol.2004.11.003.

Meko, D. M., C. A. Woodhouse, C. A. Baisan, T. Knight, J. J. Lukas, M. K. Hughes, and M. W. Salzer. 2007. "Medieval drought in the upper Colorado River Basin." *Geophysical Research Letters* no. 34 (10):5. doi: L1070510.1029/2007gl029988.

Michaelsen, J. 1987. "Cross-validation in statistical climate forecast models." *Journal of Applied Meteorology* no. 26:1589-1600.

Mitchell, V.L. 1976. "The regionalization of climate in the western United States." *Journal of Applied Meteorology* no. 15 (9):920-927.

Mock, C. J. 1996. "Climatic controls and spatial variations of precipitation in the western United States." *Journal of Climate* no. 9 (5):1111-1125.

Ostrom, C. W. Jr. 1990. *Time Series Analysis, Regression Techiques*. second ed. Vol. 07-009. Newbury Park: Sage Publications.

Owen, D.E. 2008. Geology of Craters of the Moon. Craters of the Moon National Monument and Preserve: Craters of the Moon Natural History Association.

Pederson, G. T., S. T. Gray, D. B. Fagre, and L. J. Graumlich. 2006. "Long-duration drought variability and impacts on ecosystem services: A case study from Glacier National Park, Montana." *Earth Interactions* no. 10:28. doi: 4.

Salzer, M. W., M. K. Hughes, A. G. Bunn, and K. F. Kipfmueller. 2009. "Recent unprecedented tree-ring growth in bristlecone pine at the highest elevations and possible causes." *Proceedings of the National Academy of Sciences of the United States of America* no. 106 (48):20348-20353. doi: 10.1073/pnas.0903029106.

Salzer, M. W., and K. F. Kipfmueller. 2005. "Reconstructed temperature and precipitation on a millennial timescale from tree-rings in the Southern Colorado Plateau, USA." *Climatic Change* no. 70 (3):465-487. doi: 10.1007/s10584-005-5922-3.

Shinker, J. J. 2010. "Visualizing spatial heterogeneity of western U.S. climate variability." *Earth Interactions* no. 14. doi: 1010.1175/2010ei323.1.

Slaughter, R. A., and J. D. Wiener. 2007. "Water, adaptation, and property rights on the snake and Klamath Rivers." *Journal of the American Water Resources Association* no. 43 (2):308-321. doi: 10.1111/j.1752-1688.2007.00024.x.

Stahle, D. W., M. K. Cleaveland, H. D. Grissino-Mayer, R. D. Griffin, F. K. Fye, M. D. Therrell, D. J. Burnette, D. M. Meko, and J. V. Diaz. 2009. "Cool- and Warm-Season Precipitation Reconstructions over Western New Mexico." *Journal of Climate* no. 22 (13):3729-3750. doi: 10.1175/2008jcli2752.1.

Stahle, D. W., E. R. Cook, M. K. Cleaveland, M. D. Therrell, D. M. Meko, H. D. Grissino-Mayer, E. Watson, and B. H. Luckman. 2000. "Tree-ring data document 16th century megadrought over North America." *EOS, Transactions, American Geophysical Union* no. 81 (12):121-132.

Stokes, M. A., and T. J. Smiley. 1996. *An Introduction to Tree-Ring Dating*. Tucson, Arizona: The University of Arizona Press.

Vautard, R., and M. Ghil. 1989. "Singular spectrum analysis in nonlinear dynamics, with applications to paleoclimatic time-series." *Physica D* no. 35 (3):395-424. doi: 10.1016/0167-2789(89)90077-8.

Watson, E., and B. H. Luckman. 2001. "Dendroclimatic reconstruction of precipitation for sites in the southern Canadian Rockies." *Holocene* no. 11 (2):203-213.

Whitlock, C., and P. J. Bartlein. 1993. "Spatial variations of Holocene climatic-change in the Yellowstone Region." *Quaternary Research* no. 39 (2):231-238.

Wigley, T. M. L., K. R. Briffa, and P. D. Jones. 1984. "On the average value of correlated time series, with applications in dendroclimatology and hydrometeorology." *Journal of Climate and Applied Meteorology* no. 23:201-213.

Wilks, D. S. 1995. *Statistical methods in the atmospheric sciences*. Boston: Academic Press.

Wise, E. K. 2010. "Tree ring record of streamflow and drought in the upper Snake River." *Water Resources Research* no. 46. doi: W1152910.1029/2010wr009282.

Woodhouse, C. A., K. E. Kunkel, D. R. Easterling, and E. R. Cook. 2005. "The twentieth-century pluvial in the western United States." *Geophysical Research Letters* no. 32 (7). doi: L0770110.1029/2005gl022413.

Woodhouse, C. A., and J. T. Overpeck. 1998. "2000 years of drought variability in the central United States." *Bulletin of the American Meteorological Society* no. 79 (12):2693-2714. doi: 10.1175/1520-0477(1998)079<2693:yodvit>2.0.co;2.

Chapter 6: Conclusion

6.1 Summary of Chapter Conclusions

As outlined in chapter one, chapters two-five represent individual research papers that focused on original methods with case study examples that included a subset of specific research questions. The following paragraphs in this section provide a summary of individual chapter objectives and conclusions.

The objective of chapter two was to propose a multitemporal method to map snow cover in mountainous terrain from the Landsat image archive for CDR development. This method included image processing algorithms, a standardized SCA equation, statistical evaluation of a SCA probability distribution, and a quality control assessment. Image processing algorithms selected for Landsat snow cover mapping originated from decades of published work and validation; however, the proposed multitemporal method is original in design because it includes pixel-level cloud and shadow masking, and wavelength dependent corrections for topographic illumination. The normalized SCA equation is a ratio calculation, and was derived to standardize SCA given missing Landsat imagery and cloud cover contamination. The equation assumes no change in land surface area, only a change in SCA or image coverage. Two snow cover CDRs were constructed for full and alpine spatial domains using elevation as an independent control. Both snow cover CDRs were statistically evaluated to determine whether the SCA probability distribution was normal. Lilliefor's test concluded that 30 years of SCA (1975-2011) exhibited a non-normal distribution, and a t-test indicated that mean SCA is sensitive to scale. Corrections for transient snowfall and inclusion of more temporal SCA

estimates should improve attempts to achieve the normality required for parametric statistical inference. Even so, independently controlled SCA variance between CDRs shared strong significant correlation suggesting that the proposed equation produces a stationary SCA time-series. A quality control assessment indicated that the main factor capable of introducing systematic biases into Landsat snow cover CDRs is missing historical imagery. As it stands, this multitemporal method provides a formidable approach to map snow cover in mountainous terrain for Landsat CDR development. Application of this multitemporal method to adjacent mountainous regions will increase statistical confidence.

The objective of chapter three was to validate daily snow maps between MODIS Terra and Landsat TM and ETM+ during spring snowmelt in mountainous terrain. During the 2000s, MODIS Terra C6 FSC and Landsat binary SCA estimates showed strong spatial and temporal map agreement. However, two main factors contributed to a breakdown in snow map validation, high altitude cirrus clouds and transient snowfall. MODIS Terra has difficulty retrieving thin patchy snow, and FSC estimates are sensitive to sensor viewing geometry and solar illumination. Landsat's image acquisition frequency limits snow cover mapping; there is difficulty when distinguishing between transient snowfall and resident snow cover. Despite this issue, daily SNOTEL SWE measurements provided a viable solution to detect transient snowfall events during spring snowmelt. This validation study showed encouraging improvements for MODIS Terra C6 FSC mapping in mountainous terrain, and indicates that the multitemporal method used to derive Landsat SCA maps performs with high confidence. This validation

confirms the robustness of NDSI when retrieving a spectral snow cover signal, and supports cross-sensor interoperability between MODIS Terra and Landsat TM/ETM+ for multi-sensor snow cover CDR development.

The objective of chapter four was to compare the Landsat snow cover CDR derived from the method in chapter two, with ground-based SNOTEL SWE, and temperature and precipitation observations. Instrumental climate records were then used to reconstruct spring mountain SCA during 20th and early 21st centuries. Landsat spring SCA during 1975-2009 showed significant positive correlations with SNOTEL SWE in May and June. This comparison was helpful for identifying SCA outliers and correcting annual SCA anomalies driven by transient snowfall. Landsat spring SCA also showed significant negative association to spring mean temperature, and positive association to March precipitation. Reconstructed spring SCA (1901-2009) exhibited natural internal variability on interannual to decadal timescales. A modified Mann-Kendall trend analysis revealed a centennial trend towards decreasing spring mountain SCA with estimated losses since 1901 at -36.2%. This trend in spring SCA is consistent with widespread documentation on warming springtime temperatures and cryosphere retreat at regional to continental scales.

The objective of chapter five was to use moisture-sensitive lower forest border tree-ring records from the Craters of the Moon National Monument to reconstruct annual and sub-annual precipitation on the eastern SRP. Limber pine RW and Douglas fir RW, EW, and LW showed very weak correlations in time, but shared spectral coherency at decadal frequencies and beyond. Monthly, seasonal, and annual precipitation was the

dominant climate signals encoded within limber pine and Douglas fir tree-ring widths. Independent annual and sub-annual precipitation reconstructions spanning the past 500 years were developed for the eastern SRP using COM tree-ring widths. Singular spectrum analysis showed that annual precipitation (pJuly-June) exhibited significant decadal variability with the inclusion of spring precipitation (April-June), whereas summer thru winter precipitation (July-March) showed multidecadal variability. Both decadal and multidecadal frequencies account for nearly half of the total variance in precipitation. Drought and pluvial episodes documented elsewhere across the western US over the past 500 years are present in these precipitation reconstructions. By improving sub-annual precipitation resolution, strong evidence emerges that prolonged dry (wet) conditions cannot occur without deficits (surpluses) in summer thru winter precipitation. Substantial swings between wet and dry intervals did occur over the 20th and early 21st centuries on the eastern SRP, although tree-ring reconstructions do show that modern precipitation change is still within the range of pre-instrumental climate variability.

6.2 General Conclusions

This dissertation research project asked one central question: Is NRM snowpack undergoing significant decline in response to warming surface temperatures? Even though the research undertaken here is confined to a limited spatial domain, the main conclusion is that spring NRM SCA is decreasing in response to warming spring temperatures during the modern period. It is important to note that spring SCA variability is apparent on interannual to decadal timescales, and strongly suggest that an internal forcing mechanism(s) also exert control(s) on variability. The centennial trend towards

decreasing spring SCA during the modern period is consistent with other key cyrosphere indicators (Barnett, Adam, and Lettenmaier 2005; Barry 2006; Barry, Fallot, and Armstrong 1995; Brown and Robinson 2011; Cayan et al. 2001; Derksen and Brown 2012; Dyer and Mote 2007; Groisman et al. 1994; Hamlet et al. 2005; Mote et al. 2005; Pederson et al. 2011; Stroeve et al. 2007), and is a clear 'signature' of modern warming. Stepping back, another main conclusion is reached regarding historical satellite retrievals and statistical methods used to tackle this question. The Landsat image archive possesses the timescale necessary for satellite CDR development, and furthermore, Landsat CDRs can be reliably compared with ground-based instrumental climate records using time-series theory and analysis techniques. This methodological approach is broadly applicable to all mountainous regions where snow accumulates and melts on seasonal timescales.

Moisture-sensitive tree-ring records from the COM lava complex enabled annual and sub-annual precipitation to be skillfully reconstructed for the eastern SRP. Independently constructed lower forest limber pine and Douglas fir sub-annual tree-ring chronologies were helpful for isolating seasonal precipitation variability at decadal and multidecadal timescales. Well-known paleo-drought (pluvial) episodes across the western US are captured in these precipitation reconstructions (Cook, Seager, and Miller 2011; Cook et al. 1999; Cook et al. 2007; Cook et al. 2004; Fye, Stahle, and Cook 2003; Graumlich et al. 2003; Gray, Graumlich, and Betancourt 2007; Gray, Jackson, and Betancourt 2004; Gray and McCabe 2010; Stahle et al. 2000; Stahle et al. 2007; Wise 2010; Woodhouse et al. 2005; Woodhouse and Overpeck 1998), and show that

substantial swings between wet and dry conditions has occurred on eastern SRP during the modern period. Because the eastern SRP is largely a cool-season dominated precipitation regime, tree-ring reconstructions of precipitation indicate that both summer and winter season precipitation deficits (surpluses) define moisture anomalies on decadal and multidecadal timescales. Although a snow-specific target was not reconstructed, cool-season precipitation offers a surrogate for lower elevation snowpack change. For the NRM region, this methodological approach to sub-annual tree-ring chronology development improved seasonal precipitation resolution on paleo-timescales.

6.3 Future Research

The research proposed and conducted during this dissertation project was successful at garnering a number of funding awards that enabled significant paleoclimate tree-ring data collection, and time spent to develop a method for deviation of satellite CDRs for mountain snowpack study. This dissertation work draws a blueprint, and lays the necessary groundwork to apply this thread of research elsewhere across the NRMs, and more broadly, the American West. Over the next three years, the snow cover CDR work described in this dissertation will continue and expand along a latitudinal gradient to include five more independent monitoring regions from the southwestern to northwestern US. This snow cover CDR work will also include two additional satellite platforms, MODIS Terra and VIIRS, for improved operational mountain snowpack monitoring and analysis. Additional tree-ring preparation, chronology development, and statistical analyses for the NRM region are underway for other lower and upper forest border sites collected during dissertation fieldwork. The main objectives for these lower forest border

collections are to continue with sub-annual chronology development to support additional paleo-precipitation reconstructions on seasonal, spatial, and temporal scales. The main objective for upper forest border collections is to reconstruct warm season temperature variability over the past millennium.

References

Barnett, T. P., J. C. Adam, and D. P. Lettenmaier. 2005. "Potential impacts of a warming climate on water availability in snow-dominated regions." *Nature* no. 438 (7066):303-309. doi: 10.1038/nature04141.

Barry, R. G. 2006. "The status of research on glaciers and global glacier recession: a review." *Progress in Physical Geography* no. 30 (3):285-306. doi: 10.1191/0309133306pp478ra.

Barry, R. G., J. M. Fallot, and R. L. Armstrong. 1995. "Twentieth-century variability in snow-cover conditions and approaches to detecting and monitoring changes: Status and prospects." *Progress in Physical Geography* no. 19 (4):520-532. doi: 10.1177/030913339501900405.

Brown, R. D., and D. A. Robinson. 2011. "Northern Hemisphere spring snow cover variablity and change over 1922-2010 including an assessment of uncertainty." *The Cryosphere* no. 5 (1):219-229. doi: 10.5194/tc-5-219-2011.

Cayan, D. R., S. A. Kammerdiener, M. D. Dettinger, J. M. Caprio, and D. H. Peterson. 2001. "Changes in the onset of spring in the western United States." *Bulletin of the American Meteorological Society* no. 82 (3):399-415.

Cook, B. I., R. Seager, and R. L. Miller. 2011. "On the Causes and Dynamics of the Early Twentieth-Century North American Pluvial." *Journal of Climate* no. 24 (19):5043-5060. doi: 10.1175/2011jcli4201.1.

Cook, E. R., D. M. Meko, D. W. Stahle, and M. K. Cleaveland. 1999. "Drought reconstructions for the continental United States." *Journal of Climate* no. 12 (4):1145-1162.

Cook, E. R., R. Seager, M. A. Cane, and D. W. Stahle. 2007. "North American drought: Reconstructions, causes, and consequences." *Earth-Science Reviews* no. 81 (1-2):93-134. doi: 10.1016/j.earscirev.2006.12.002.

Cook, E. R., C. A. Woodhouse, C. M. Eakin, D. M. Meko, and D. W. Stahle. 2004. "Long-term aridity changes in the western United States." *Science* no. 306 (5698):1015-1018. doi: 10.1126/science.1102586.

Derksen, C., and R. Brown. 2012. "Spring snow cover extent reductions in the 2008-2012 period exceeding climate model projections." *Geophysical Research Letters* no. 39. doi: 10.1029/2012GL053387.

Dyer, J. L., and T. L. Mote. 2007. "Trends in snow ablation over North America." *International Journal of Climatology* no. 27 (6):739-748. doi: 10.1002/joc.1426.

Fye, F. K., D. W. Stahle, and E. R. Cook. 2003. "Paleoclimatic analogs to twentieth-century moisture regimes across the United States." *Bulletin of the American Meteorological Society* no. 84 (7):901-909.

Graumlich, L. J., M. F. J. Pisaric, L. A. Waggoner, J. S. Littell, and J. C. King. 2003. "Upper Yellowstone River flow and teleconnections with Pacific basin climate variability during the past three centuries." *Climatic Change* no. 59 (1-2):245-262. doi: 10.1023/a:1024474627079.

Gray, S. T., L. J. Graumlich, and J. L. Betancourt. 2007. "Annual precipitation in the Yellowstone National Park region since AD 1173." *Quaternary Research* no. 68 (1):18-27. doi: 10.1016/j.yqres.2007.02.002.

Gray, S. T., S. T. Jackson, and J. L. Betancourt. 2004. "Tree-ring based reconstructions of interannual to decadal scale precipitation variability for northeastern Utah since 1226 AD." *Journal of the American Water Resources Association* no. 40 (4):947-960. doi: 10.1111/j.1752-1688.2004.tb01058.

Gray, S. T., and G. J. McCabe. 2010. "A combined water balance and tree ring approach to understanding the potential hydrologic effects of climate change in the central Rocky Mountain region." *Water Resources Research* no. 46. doi: W0551310.1029/2008wr007650.

Groisman, P. Y., T. R. Karl, R. W. Knight, and G. L. Stenchikov. 1994. "Changes of snow cover, temperature, and radiative heat-balance over the northern-hemisphere." *Journal of Climate* no. 7 (11):1633-1656.

Hamlet, A. F., P. W. Mote, M. P. Clark, and D. P. Lettenmaier. 2005. "Effects of temperature and precipitation variability on snowpack trends in the western United States." *Journal of Climate* no. 18 (21):4545-4561.

Mote, P. W., A. F. Hamlet, M. P. Clark, and D. P. Lettenmaier. 2005. "Declining mountain snowpack in western north America." *Bulletin of the American Meteorological Society* no. 86 (1):39-49. doi: 10.1175/bams-86-1-39.

Pederson, G. T., S. T. Gray, C. A. Woodhouse, J. L. Betancourt, D. B. Fagre, J. S. Littell, E. Watson, B. H. Luckman, and L. J. Graumlich. 2011. "The Unusual Nature of Recent Snowpack Declines in the North American Cordillera." *Science* no. 333 (6040):332-335. doi: 10.1126/science.1201570.

Stahle, D. W., E. R. Cook, M. K. Cleaveland, M. D. Therrell, D. M. Meko, H. D. Grissino-Mayer, E. Watson, and B. H. Luckman. 2000. "Tree-ring data document 16th century megadrought over North America." *EOS, Transactions, American Geophysical Union* no. 81 (12):121-132.

Stahle, D. W., F. K. Fye, E. R. Cook, and R. D. Griffin. 2007. "Tree-ring reconstructed megadroughts over North America since AD 1300." *Climatic Change* no. 83 (1-2):133-149. doi: 10.1007/s10584-006-9171.

Stroeve, J., M. M. Holland, W. Meier, T. Scambos, and M. Serreze. 2007. "Arctic sea ice decline: Faster than forecast." *Geophysical Research Letters* no. 34 (9). doi: L0950110.1029/2007gl029703.

Wise, E. K. 2010. "Tree ring record of streamflow and drought in the upper Snake River." *Water Resources Research* no. 46. doi: W1152910.1029/2010wr009282.

Woodhouse, C. A., K. E. Kunkel, D. R. Easterling, and E. R. Cook. 2005. "The twentieth-century pluvial in the western United States." *Geophysical Research Letters* no. 32 (7). doi: L0770110.1029/2005gl022413.
Woodhouse, C. A., and J. T. Overpeck. 1998. "2000 years of drought variability in the central United States." *Bulletin of the American Meteorological Society* no. 79 (12):2693-2714. doi: 10.1175/1520-0477(1998)079<2693:yodvit>2.0.co;2.

Complete Dissertation References

Ackerman, S. A., K. I. Strabala, W. P. Menzel, R. A. Frey, C. C. Moeller, and L. E. Gumley. 1998. "Discriminating clear sky from clouds with MODIS." *Journal of Geophysical Research-Atmospheres* no. 103 (D24):32141-32157. doi: 10.1029/1998jd200032.

Anderton, S. P., S. M. White, and B. Alvera. 2004. "Evaluation of spatial variability in snow water equivalent for a high mountain catchment." *Hydrological Processes* no. 18 (3):435-453. doi: 10.1002/hyp.1319.

Andreadis, K. M., and D. P. Lettenmaier. 2006. "Assimilating remotely sensed snow observations into a macroscale hydrology model." *Advances in Water Resources* no. 29 (6):872-886. doi: 10.1016/j.advwatres.2005.08.004.

Antilla, S., Metsamaki S., and Derksen C. 2006. A comparison of Finnish SCAmod snow maps and MODIS snow maps in boreal forests in Finland and Manitoba, Canada. Paper read at Geoscience and Remote Sensing Symposium, 2006, IGARRS 2006.

Arno, S.F., and R.P. Hammerly. 1984. *Timberline Mountain and Arctic Forest Frontiers*. Seattle: The Mountaineers.

Ault, T. R., and S. St George. 2010. "The Magnitude of Decadal and Multidecadal Variability in North American Precipitation." *Journal of Climate* no. 23 (4):842-850. doi: 10.1175/2009jcli3013.1.

Bales, R. C., N. P. Molotch, T. H. Painter, M. D. Dettinger, R. Rice, and J. Dozier. 2006. "Mountain hydrology of the western United States." *Water Resources Research* no. 42 (8):13. doi: W0843210.1029/2005wr004387.

Barnett, T. P., J. C. Adam, and D. P. Lettenmaier. 2005. "Potential impacts of a warming climate on water availability in snow-dominated regions." *Nature* no. 438 (7066):303-309. doi: 10.1038/nature04141.

Barnston, A. G., and R. E. Livezey. 1987. "Classification, Seasonality and Persistence of Low-Frequency Atmospheric Circulation Patterns." *Monthly Weather Review* no. 115 (6):1083-1126.

Barry, R. G. 1981. *Mountain Weather and Climate*. New York: Methuen.

———. 1992. "Mountain climatology and past and potential future climatic changes in mountainous regions - A review." *Mountain Research and Development* no. 12 (1):71-86.

Barry, R. G., J. M. Fallot, and R. L. Armstrong. 1995. "Twentieth-century variability in snow-cover conditions and approaches to detecting and monitoring changes: Status and prospects." *Progress in Physical Geography* no. 19 (4):520-532. doi: 10.1177/030913339501900405.

Barry, R. G. 2002. "The role of snow and ice in the global climate system: A review." *Polar Geography* no. 26 (3):235 - 246.

Barry, R. G. 2006. "The status of research on glaciers and global glacier recession: a review." *Progress in Physical Geography* no. 30 (3):285-306. doi: 10.1191/0309133306pp478ra.

Beniston, M. 2003. "Climatic change in mountain regions: A review of possible impacts." *Climatic Change* no. 59 (1-2):5-31.

Bloschl, G. 1999. "Scaling issues in snow hydrology." *Hydrological Processes* no. 13 (14-15):2149-2175. doi: 10.1002/(sici)1099-1085(199910)13:14/15<2149::aid-hyp847>3.0.co;2-8.

Briffa, K. R., and P. D. Jones. 1990. "Basic chronology statistics." In *Methods of Dendrochronology: Applications in the Environmental Sciences*, edited by E. R. Cook and L. A. Kairiukstis, 137-152. Dordrecht: Kluwer Academic Publishers/IIASA.

Brown, R. D., and D. A. Robinson. 2011. "Northern Hemisphere spring snow cover variablity and change over 1922-2010 including an assessment of uncertainty." *The Cryosphere* no. 5 (1):219-229. doi: 10.5194/tc-5-219-2011.

Butt, M. J., and M. Bilal. 2011. "Application of snowmelt runoff model for water resource management." *Hydrological Processes* no. 25 (24):3735-3747. doi: 10.1002/hyp.8099.

Cayan, D. R. 1996. "Interannual climate variability and snowpack in the western United States." *Journal of Climate* no. 9 (5):928-948.

Cayan, D. R., M. D. Dettinger, H. F. Diaz, and N. E. Graham. 1998. "Decadal variability of precipitation over western North America." *Journal of Climate* no. 11 (12):3148-3166. doi: 10.1175/1520-0442(1998)011<3148:dvopow>2.0.co;2.

Cayan, D. R., S. A. Kammerdiener, M. D. Dettinger, J. M. Caprio, and D. H. Peterson. 2001. "Changes in the onset of spring in the western United States." *Bulletin of the American Meteorological Society* no. 82 (3):399-415.

Chander, G., and B. Markham. 2003. "Revised Landsat-5 TM radiometric calibration procedures and postcalibration dynamic ranges." *IEEE Transactions on Geoscience and Remote Sensing* no. 41 (11):2674-2677. doi: 10.1109/tgrs.2003.818464.

Chander, G., B. L. Markham, and J. A. Barsi. 2007. "Revised Landsat-5 thematic mapper radiometric calibration." *IEEE Geoscience and Remote Sensing Letters* no. 4 (3):490-494. doi: 10.1109/lgrs.2007.898285.

Chander, G., B. L. Markham, and D. L. Helder. 2009. "Summary of current radiometric calibration coefficients for Landsat MSS, TM, ETM+, and EO-1 ALI sensors." *Remote Sensing of Environment* no. 113 (5):893-903. doi: 10.1016/j.rse.2009.01.007.

Chatfield, C. 2004. *The Analysis of Time Series, an Introduction*. six ed. New York: Chapman and Hall/CRC.

Chavez, P. S. 1996. "Image-based atmospheric corrections revisited and improved." *Photogrammetric Engineering and Remote Sensing* no. 62 (9):1025-1036.

Clark, M. P., M. C. Serreze, and G. J. McCabe. 2001. "Historical effects of El Nino and La Nina events on the seasonal evolution of the montane snowpack in the Columbia and Colorado River Basins." *Water Resources Research* no. 37 (3):741-757.

Cline, D. W., R. C. Bales, and J. Dozier. 1998. "Estimating the spatial distribution of snow in mountain basins using remote sensing and energy balance modeling." *Water Resources Research* no. 34 (5):1275-1285.

Comrie, A. C., and E. C. Glenn. 1998. "Principal components-based regionalization of precipitation regimes across the southwest United States and northern Mexico, with an application to monsoon precipitation variability." *Climate Research* no. 10 (3):201-215. doi: 10.3354/cr010201.

Conover, W. 1980. *Practical nonparameteric statistics*. 2nd ed. New York: John Wiley and Sons.

Cook, B. I., R. Seager, and R. L. Miller. 2011. "On the Causes and Dynamics of the Early Twentieth-Century North American Pluvial." *Journal of Climate* no. 24 (19):5043-5060. doi: 10.1175/2011jcli4201.1.

Cook, E. R. 1985. *A time series analysis approach to tree ring standardization*. Disseration, University of Arizona, Tucson.

Cook, E. R., K. R. Briffa, D. M. Meko, D. A. Graybill, and G. Funkhouser. 1995. "The segment length curse in long tree-ring chronology development for paleoclimatic studies." *Holocene* no. 5 (2):229-237.

Cook, E. R., J. Esper, and R. D. D'Arrigo. 2004. "Extra-tropical Northern Hemisphere land temperature variability over the past 1000 years." *Quaternary Science Reviews* no. 23 (20-22):2063-2074. doi: 10.1016/j.quaascirev.2004.08.013.

Cook, E. R., and L. A. Kairiukstis. 1990. *Methods of Dendrochronology: Applications in the Environmental Sciences*. Dordrecht: Kluwer Academic Publishers/IIASA.

Cook, E. R., D. M. Meko, D. W. Stahle, and M. K. Cleaveland. 1999. "Drought reconstructions for the continental United States." *Journal of Climate* no. 12 (4):1145-1162.

Cook, E. R., and K. Peters. 1997. "Calculating unbiased tree-ring indices for the study of climate and environmental change." *The Holocene* no. 7:361-370.

Cook, E. R., R. Seager, M. A. Cane, and D. W. Stahle. 2007. "North American drought: Reconstructions, causes, and consequences." *Earth-Science Reviews* no. 81 (1-2):93-134. doi: 10.1016/j.earscirev.2006.12.002.

Cook, E. R., C. A. Woodhouse, C. M. Eakin, D. M. Meko, and D. W. Stahle. 2004. "Long-term aridity changes in the western United States." *Science* no. 306 (5698):1015-1018. doi: 10.1126/science.1102586.

Coppin, P. R., and M. E. Bauer. 1994. "Processing of multitemporal Landsat TM imagery to optimize extraction of forest cover change features." *IEEE Transactions on Geoscience and Remote Sensing* no. 32 (4):918-927. doi: 10.1109/36.298020.

Crawford, C. J., S. M. Manson, M. E. Bauer, and D. K. Hall. 2013. "Multitemporal snow cover mapping in mountainous terrain for Landsat climate data record development." *Remote Sensing of Environment* no. 135 (0):224-233. doi:10.1016/j.rse.2013.04.004.

Daly, C., D. R. Conklin, and M. H. Unsworth. 2010. "Local atmospheric decoupling in complex topography alters climate change impacts." *International Journal of Climatology* no. 30 (12):1857-1864. doi: 10.1002/joc.2007.

Daly, C., M. Halbleib, J. I. Smith, W. P. Gibson, M. K. Doggett, G. H. Taylor, J. Curtis, and P. P. Pasteris. 2008. "Physiographically sensitive mapping of climatological temperature and precipitation across the conterminous United States." *International Journal of Climatology* no. 28 (15):2031-2064. doi: 10.1002/joc.1688.

Derksen, C., and R. Brown. 2012. "Spring snow cover extent reductions in the 2008-2012 period exceeding climate model projections." *Geophysical Research Letters* no. 39. doi: 10.1029/2012GL053387.

Dettinger, M. D., and D. R. Cayan. 1995. "Large-scale atmospheric forcing of recent trends toward early snowmelt runoff in California." *Journal of Climate* no. 8 (3):606-623. doi: 10.1175/1520-0442(1995)008<0606:lsafor>2.0.co;2.

Dettinger, M. D., D. R. Cayan, H. F. Diaz, and D. M. Meko. 1998. "North-south precipitation patterns in western North America on interannual-to-decadal timescales." *Journal of Climate* no. 11 (12):3095-3111.

Dobreva, I. D., and A. G. Klein. 2011. "Fractional snow cover mapping through artifical neural network analysis of MODIS surface reflectance." Remote Sensing of Environment no. 115:3355-3366.

Dozier, J. 1984. "Snow reflectance from Landsat-4 Thematic Mapper " *IEEE Transactions on Geoscience and Remote Sensing* no. 22 (3):323-328.

———. 1989. "Spectral signature of alpine snow cover from the Landsat Thematic Mapper." *Remote Sensing of Environment* no. 28:9-22.

Dozier, J., and J. Frew. 1990. "Rapid calculation of terrain parameters for radiation modeling from digital elevation data." *IEEE Transactions on Geoscience and Remote Sensing* no. 28 (5):963-969.

———. 2009. "Computational provenance in hydrologic science: a snow mapping example." *Philosophical Transactions of the Royal Society a-Mathematical Physical and Engineering Sciences* no. 367 (1890):1021-1033. doi: 10.1098/rsta.2008.0187.

Dozier, J., and T. H. Painter. 2004. "Multispectral and hyperspectral remote sensing of alpine snow properties." *Annual Review of Earth and Planetary Sciences* no. 32:465-494. doi: 10.1146/annurev.earth.32.101802.120404.

Dozier, J., T. H. Painter, K. Rittger, and J. E. Frew. 2008. "Time-space continuity of daily maps of fractional snow cover and albedo from MODIS." *Advances in Water Resources* no. 31 (11):1515-1526. doi: 10.1016/j.advwatres.2008.08.011.

Draper, N.R., and H. Smith. 1998. *Applied Regression Analysis*. 3rd ed. Hoboken, NJ: Wiley-Interscience.

Duffy, P. B., R. W. Arritt, J. Coquard, W. Gutowski, J. Han, J. Iorio, J. Kim, L. R. Leung, J. Roads, and E. Zeledon. 2006. "Simulations of present and future climates in the western United States with four nested regional climate models." *Journal of Climate* no. 19 (6):873-895. doi: 10.1175/jcli3669.1.

Dyer, J. L., and T. L. Mote. 2007. "Trends in snow ablation over North America." *International Journal of Climatology* no. 27 (6):739-748. doi: 10.1002/joc.1426.

Eischeid, J. K., C. B. Baker, T. R. Karl, and H. F. Diaz. 1995. "The quality-control of long-term climatological data using objective data-analysis." *Journal of Applied Meteorology* no. 34 (12):2787-2795. doi: 10.1175/1520-0450(1995)034<2787:tqcolt>2.0.co;2.

Elder, K., J. Dozier, and J. Michaelsen. 1991. "Snow accumulation and distrubution in an alpine watershed." *Water Resources Research* no. 27 (7):1541-1552.

Enfield, D. B., A. M. Mestas-Nunez, and P. J. Trimble. 2001. "The Atlantic multidecadal oscillation and its relation to rainfall and river flows in the continental US." *Geophysical Research Letters* no. 28 (10):2077-2080. doi: 10.1029/2000gl012745.

Erxleben, J., K. Elder, and R. Davis. 2002. "Comparison of spatial interpolation methods for estimating snow distribution in the Colorado Rocky Mountains." *Hydrological Processes* no. 16 (18):3627-3649. doi: 10.1002/hyp.1239.

Feng, M., C. Q. Huang, S. Channan, E. F. Vermote, J. G. Masek, and J. R. Townshend. 2012. "Quality assessment of Landsat surface reflectance products using MODIS data." *Computers & Geosciences* no. 38 (1):9-22. doi: 10.1016/j.cageo.2011.04.011.

Foster, J. L., D. K. Hall, J. B. Eylander, G. A. Riggs, S. V. Nghiem, M. Tedesco, E. Kim, P. M. Montesano, R. E. J. Kelly, K. A. Casey, and B. Choudhury. 2011. "A blended global snow product using visible, passive microwave and scatterometer satellite data." *International Journal of Remote Sensing* no. 32 (5):1371-1395. doi: 10.1080/01431160903548013.

Foster, J. L. 1989. "The significance of the date of snow disappearance on the Arctic tundra as a possible indicator of climate change." *Arctic and Alpine Research* no. 21 (1):60-70. doi: 10.2307/1551517.

Frei, A., D. A. Robinson, and M. G. Hughes. 1999. "North American snow extent: 1900-1994." *International Journal of Climatology* no. 19 (14):1517-1534. doi: 10.1002/(sici)1097-0088(19991130)19:14<1517::aid-joc437>3.0.co;2-i.

Fritts, H. C. 1965. "Tree-Ring Characteristics Along a Vegetation Gradient in Northern Arizona." *Ecology* no. 46:394-401.

———. 1976. *Tree Rings and Climate*. Caldwell, New Jersey: The Blackburn Press.

———. 1991. *Reconstructing Large-Scale Climatic Patterns from Tree-Ring Data, A Diagnostic Analysis*. Tucson: The University of Arizona Press.

Fritts, H. C., D. G. Smith, J. W. Cardis, and C. A. Budelsky. 1965. "Tree-ring characteristics along a vegetation gradient in northern Arizona." *Ecology* no. 46 (4):394-401.

Fritts, H. C. 1966. "Growth-rings of trees: their correlation with climate." *Science* no. 154 (3752):973-979.

———. 1974. "Relationships of ring widths in arid-site conifers to variations in monthly temperature and precipitation." *Ecological Monographs* no. 44 (4):411-440.

Fye, F. K., D. W. Stahle, and E. R. Cook. 2003. "Paleoclimatic analogs to twentieth-century moisture regimes across the United States." *Bulletin of the American Meteorological Society* no. 84 (7):901-909.

Ghil, M., M. R. Allen, M. D. Dettinger, K. Ide, D. Kondrashov, M. E. Mann, A. W. Robertson, A. Saunders, Y. Tian, F. Varadi, and P. Yiou. 2002. "Advanced spectral methods for climatic time series." *Reviews of Geophysics* no. 40 (1). doi: 100310.1029/2000rg000092.

Graumlich, L. J., M. F. J. Pisaric, L. A. Waggoner, J. S. Littell, and J. C. King. 2003. "Upper Yellowstone River flow and teleconnections with Pacific basin climate variability during the past three centuries." *Climatic Change* no. 59 (1-2):245-262. doi: 10.1023/a:1024474627079.

Gray, S. T., J. L. Betancourt, C. L. Fastie, and S. T. Jackson. 2003. "Patterns and sources of multidecadal oscillations in drought-sensitive tree-ring records from the central and southern Rocky Mountains." *Geophysical Research Letters* no. 30 (6). doi: 131610.1029/2002gl016154.

Gray, S. T., L. J. Graumlich, and J. L. Betancourt. 2007. "Annual precipitation in the Yellowstone National Park region since AD 1173." *Quaternary Research* no. 68 (1):18-27. doi: 10.1016/j.yqres.2007.02.002.

Gray, S. T., S. T. Jackson, and J. L. Betancourt. 2004. "Tree-ring based reconstructions of interannual to decadal scale precipitation variability for northeastern Utah since 1226 AD." *Journal of the American Water Resources Association* no. 40 (4):947-960. doi: 10.1111/j.1752-1688.2004.tb01058.x.

Gray, S. T., and G. J. McCabe. 2010. "A combined water balance and tree ring approach to understanding the potential hydrologic effects of climate change in the central Rocky Mountain region." *Water Resources Research* no. 46. doi: W0551310.1029/2008wr007650.

Griffin, D., D. M. Meko, R. Touchan, S. W. Leavitt, and C. A. Woodhouse. 2011. "Latewood chronology development for summer-moisture reconstruction in the US Southwest." *Tree-Ring Research* no. 67 (2):87-101.

Groisman, P., and D. R. Easterling. 1994. "Variability and trends of total precipitation and snowfall over the United States and Canada." *Journal of Climate* no. 7:184-205.

Groisman, P. Y., T. R. Karl, R. W. Knight, and G. L. Stenchikov. 1994. "Changes of snow cover, temperature, and radiative heat-balance over the northern-hemisphere." *Journal of Climate* no. 7 (11):1633-1656.

Hagolle, O., M. Huc, D. V. Pascual, and G. Dedieu. 2010. "A multi-temporal method for cloud detection, applied to FORMOSAT-2, VEN mu S, LANDSAT and SENTINEL-2 images." *Remote Sensing of Environment* no. 114 (8):1747-1755. doi: 10.1016/j.rse.2010.03.002.

Hall, D. K., J. L. Foster, N. E. DiGirolamo, and G. A. Riggs. 2012. "Snow cover, snowmelt timing and stream power in the Wind River Range, Wyoming." *Geomorphology* no. 137 (1):87-93. doi: 10.1016/j.geomorph.2010.11.011.

Hall, D. K., J. L. Foster, V. V. Salomonson, A. G. Klein, and J. Y. L. Chien. 2001. "Development of a technique to assess snow-cover mapping errors from space." *IEEE Transactions on Geoscience and Remote Sensing* no. 39 (2):432-438.

Hall, D. K., J. L. Foster, D. L. Verbyla, A. G. Klein, and C. S. Benson. 1998. "Assessment of snow-cover mapping accuracy in a variety of vegetation-cover densities in central Alaska." *Remote Sensing of Environment* no. 66 (2):129-137. doi: 10.1016/s0034-4257(98)00051-0.

Hall, D. K., R. E. J. Kelly, G. A. Riggs, A. T. C. Chang, and J. L. Foster. 2002. "Assessment of the relative accuracy of hemispheric-scale snow-cover maps." In *Annals of Glaciology, Vol 34, 2002*, edited by J. G. Winther and R. Solberg, 24-30. Cambridge: Int Glaciological Soc.

Hall, D. K., and J. Martinec. 1985. *Remote Sensing of Ice and Snow*. New York: Chapman and Hall.

Hall, D. K., and G. A. Riggs. 2007. "Accuracy assessment of the MODIS snow products." *Hydrological Processes* no. 21 (12):1534-1547. doi: 10.1002/hyp.6715.

———. 2011. Normalized-Difference Snow Index (NDSI), Encylopedia of Earth Sciences Series. In *Encylopedia of snow, ice and glaciers*, edited by V. P. Singh, P. Singh and U. K. Haritashya: Springer.

Hall, D. K., G. A. Riggs, and V. V. Salomonson. 1995. "Development of methods for mapping global snow cover using moderate resolution imaging spectroradiometer data." *Remote Sensing of Environment* no. 54 (2):127-140. doi: 10.1016/0034-4257(95)00137-p.

Hall, D. K., G. A. Riggs, V. V. Salomonson, N. E. DiGirolamo, and K. J. Bayr. 2002. "MODIS snow-cover products." *Remote Sensing of Environment* no. 83 (1-2):181-194.

Hall, D. K., A. B. Tait, J. L. Foster, A. T. C. Chang, and M. Allen. 2000. "Intercomparison of satellite-derived snow-cover maps." In *Annals of Glaciology, Vol 31, 2000*, edited by K. Steffen, 369-376. Cambridge: Int Glaciological Soc.

Hamlet, A. F., P. W. Mote, M. P. Clark, and D. P. Lettenmaier. 2005. "Effects of temperature and precipitation variability on snowpack trends in the western United States." *Journal of Climate* no. 18 (21):4545-4561.

Harman, J. R. 1991. *Synoptic Climatology of the Westerlies: Process and Patterns*. Washington D.C.: Assocation of American Geographers.

Heyerdahl, E. K., P. Morgan, and J. P. Riser. 2008. "Multi-season climate synchronized historical fires in dry forests (1650-1900), northern Rockies, USA." *Ecology* no. 89 (3):705-716.

Holmes, R. L. 1983. "Computer-assisted quality control in tree ring dating and measuring." *Tree Ring Bulletin* no. 43:69-78.

Homan, J. W., C. H. Luce, J. P. McNamara, and N. F. Glenn. 2011. "Improvement of distributed snowmelt energy balance modeling with MODIS-based NDSI-derived fractional snow-covered area data." *Hydrological Processes* no. 25 (4):650-660. doi: 10.1002/hyp.7857.

Huang, C. Q., N. Thomas, S. N. Goward, J. G. Masek, Z. L. Zhu, J. R. G. Townshend, and J. E. Vogelmann. 2010. "Automated masking of cloud and cloud shadow for forest change analysis using Landsat images." *International Journal of Remote Sensing* no. 31 (20):5449-5464. doi: 10.1080/01431160903369642.

Hughes, M. K., and C. M. Ammann. 2009. "The future of the past-an earth system framework for high resolution paleoclimatology: editorial essay." *Climatic Change* no. 94 (3-4):247-259. doi: 10.1007/s10584-009-9588-0.

Hughes, M. K., and G. Funkhouser. 2003. "Frequency-dependent climate signal in upper and lower forest border tree rings in the mountains of the Great Basin." *Climatic Change* no. 59 (1-2):233-244.

Hughes, M.K. 2002. "Dendrochronology in climatology - The state of the art." *Dendrochronologia v20* no. n1-2:95-116 Journal Code Dendrochronologia.

Hurrell, J. W. 1996. "Influence of variations in extratropical wintertime teleconnections on Northern Hemisphere temperature." *Geophysical Research Letters* no. 23 (6):665-668.

Hutchison, K. D., R. L. Mahoney, E. F. Vermote, T. J. Kopp, J. M. Jackson, A. Sei, and B. D. Iisager. 2009. "A Geometry-Based Approach to Identifying Cloud Shadows in the VIIRS Cloud Mask Algorithm for NPOESS." *Journal of Atmospheric and Oceanic Technology* no. 26 (7):1388-1397. doi: 10.1175/2009jtecha1198.1.

Irish, R. R., J. L. Barker, S. N. Goward, and T. Arvidson. 2006. "Characterization of the Landsat-7 ETM+ automated cloud-cover assessment (ACCA) algorithm." *Photogrammetric Engineering and Remote Sensing* no. 72 (10):1179-1188.

Jones, P. D., and M. Hulme. 1996. "Calculating regional climatic time series for temperature and precipitation: Methods and illustrations." *International Journal of Climatology* no. 16 (4):361-377.

Jones, P. D., K. R. Briffa, T. J. Osborn, J. M. Lough, T. D. van Ommen, B. M. Vinther, J. Lutherbacher, E. R. Wahl, F. W. Zwiers, M. E. Mann, G. A. Schmidt, C. M. Ammann, B. M. Buckley, K. M. Cobb, J. Esper, H. Goosse, N. Graham, E. Jansen, T. Kiefer, C. Kull, M. Kuttel, E. Mosley-Thompson, J. T. Overpeck, N. Riedwyl, M. Schulz, A. W. Tudhope, R. Villalba, H. Wanner, E. Wolff, and E. Xoplaki. 2009. "High-resolution palaeoclimatology of the last millennium: a review of current status and future prospects." *Holocene* no. 19 (1):3-49. doi: 10.1177/0959683608098952.

Kalnay, E., M. Kanamitsu, R. Kistler, W. Collins, D. Deaven, L. Gandin, M. Iredell, S. Saha, G. White, J. Woollen, Y. Zhu, M. Chelliah, W. Ebisuzaki, W. Higgins, J. Janowiak, K. C. Mo, C. Ropelewski, J. Wang, A. Leetmaa, R. Reynolds, R. Jenne, and D. Joseph. 1996. "The NCEP/NCAR 40-year reanalysis project." *Bulletin of the American Meteorological Society* no. 77 (3):437-471. doi: 10.1175/1520-0477(1996)077<0437:tnyrp>2.0.co;2.

Kane, V. R., A. R. Gillespie, R. McGaughey, J. A. Lutz, K. Ceder, and J. F. Franklin. 2008. "Interpretation and topographic compensation of conifer canopy self-shadowing." *Remote Sensing of Environment* no. 112 (10):3820-3832. doi: 10.1016/j.rse.2008.06.001.

Kipfmueller, K. F., and M. W. Salzer. 2010. "Linear trend and climate response of five-needle pines in the western United States related to treeline proximity." *Canadian Journal of Forest Research-Revue Canadienne De Recherche Forestiere* no. 40 (1):134-142. doi: 10.1139/x09-187.

Klein, A. G., and A. C. Barnett. 2003. "Validation of daily MODIS snow cover maps of the Upper Rio Grande River Basin for the 2000-2001 snow year." *Remote Sensing of Environment* no. 86 (2):162-176. doi: 10.1016/s0034-4257(03)00097-x.

Klein, A. G., D. K. Hall, and G. A. Riggs. 1998. "Improving snow cover mapping in forests through the use of a canopy reflectance model." *Hydrological Processes* no. 12 (10-11):1723-1744.

Knowles, N., M. D. Dettinger, and D. R. Cayan. 2006. "Trends in snowfall versus rainfall in the Western United States." *Journal of Climate* no. 19 (18):4545-4559.

Kunkel, K. E., M. A. Palecki, K. G. Hubbard, D. A. Robinson, K. T. Redmond, and D. R. Easterling. 2007. "Trend identification in twentieth-century US snowfall: The challenges." *Journal of Atmospheric and Oceanic Technology* no. 24 (1):64-73. doi: 10.1175/jtech2017.1.

Lamarche, V. C. 1974a. "Frequency-Dependent Relationships between Tree-Ring Series along an Ecological Gradient and Some Dendroclimatic Implications." *Tree-Ring Bulletin* no. 34:1-20.

Lamarche, V. C., Jr. 1974b. "Paleoclimatic Inferences from Long Tree-Ring Records: Intersite comparison shows climatic anomalies that may be linked to features of the general circulation." *Science (New York, N.Y.)* no. 183 (4129):1043-8. doi: 10.1126/science.183.4129.1043.

Leathers, D. J., and D. A. Robinson. 1993. "The association between extremes in North-American snow cover extent and United-States temperature." *Journal of Climate* no. 6 (7):1345-1355.

Li, B. L., A. X. Zhu, C. H. Zhou, Y. H. Zhang, T. Pei, and C. Z. Qin. 2008. "Automatic mapping of snow cover depletion curves using optical remote sensing data under conditions of frequent cloud cover and temporary snow." *Hydrological Processes* no. 22 (16):2930-2942. doi: 10.1002/hyp.6891.

Li, W., K. Stamnes, H. Eide, and R. Spurr. 2007. "Bidirectional reflectance distribution function of snow: corrections for the Lambertian assumption in remote sensing applications." *Optical Engineering* no. 46 (6). doi: 06620110.1117/1.2746334.

Liston, G. E. 1999. "Interrelationships among snow distribution, snowmelt, and snow cover depletion: Implications for atmospheric, hydrologic, and ecologic modeling." *Journal of Applied Meteorology* no. 38 (10):1474-1487. doi: 10.1175/1520-0450(1999)038<1474:iasdsa>2.0.co;2.

Lu, D., H. Ge, S. He, A. Xu, G. Zhou, and H. Du. 2008. "Pixel-based Minnaert correction method for reducing topographic effects on a Landsat 7 ETM+ image." *Photogrammetric Engineering and Remote Sensing* no. 74 (11):1343-1350.

Lundquist, J. D., and M. D. Dettinger. 2005. "How snowpack heterogeneity affects diurnal streamflow timing." *Water Resources Research* no. 41 (5):14. doi: W0500710.1029/2004wr003649.

Marston, R. A., J. D. Mills, D. R. Wrazien, B. Bassett, and D. K. Splinter. 2005. "Effects of Jackson Lake Dam on the Snake River and its floodplain, Grand Teton National Park, Wyoming, USA." *Geomorphology* no. 71 (1-2):79-98. doi: 10.1016/j.geomorph.2005.03.005.

Masek, J. G., E. F. Vermote, N. E. Saleous, R. Wolfe, F. G. Hall, K. F. Huemmrich, F. Gao, J. Kutler, and T. K. Lim. 2006. "A Landsat surface reflectance dataset for North America, 1990-2000." *IEEE Geoscience and Remote Sensing Letters* no. 3 (1):68-72. doi: 10.1109/lgrs.2005.857030.

Matson, M., and D. R. Wiesnet. 1981. "New data-base for climate studies." *Nature* no. 289 (5797):451-456. doi: 10.1038/289451a0.

McCabe, G. J., and M. A. Palecki. 2006. "Multidecadal climate variability of global lands and oceans." *International Journal of Climatology* no. 26 (7):849-865. doi: 10.1002/joc.1289.

McCabe, G. J., and M. P. Clark. 2005. "Trends and variability in snowmelt runoff in the western United States." *Journal of Hydrometeorology* no. 6 (4):476-482.

McCabe, G. J., M. A. Palecki, and J. L. Betancourt. 2004. "Pacific and Atlantic Ocean influences on multidecadal drought frequency in the United States." *Proceedings of the National Academy of Sciences of the United States of America* no. 101 (12):4136-4141. doi: 10.1073/pnas.0306738101.

McCabe, G. J., and M. D. Dettinger. 2002. "Primary modes and predictability of year-to-year snowpack variations in the western United States from teleconnections with Pacific Ocean climate." *Journal of Hydrometeorology* no. 3 (1):13-25.

McCabe, G. J., and D. R. Legates. 1995. "Relationships between 700 hpa height anomalies and 1 April snowpack accumulations in the western USA " *International Journal of Climatology* no. 15 (5):517-530.

McGuire, M., A. W. Wood, A. F. Hamlet, and D. P. Lettenmaier. 2006. "Use of satellite data for streamflow and reservoir storage forecasts in the snake river basin." *Journal of Water Resources Planning and Management-Asce* no. 132 (2):97-110. doi: 10.1061/(asce)0733-9496(2006)132:2(97).

Meehl, G. A., J. M. Arblaster, G. Branstator, and H. van Loon. 2008. "A coupled air-sea response mechanism to solar forcing in the Pacific region." *Journal of Climate* no. 21 (12):2883-2897. doi: 10.1175/2007jcli1776.1.

Meehl, G. A., and H. Y. Teng. 2012. "Case studies for initialized decadal hindcasts and predictions for the Pacific region." *Geophysical Research Letters* no. 39. doi: L2270510.1029/2012gl053423.

Mehta, V., G. Meehl, L. Goddard, J. Knight, A. Kumar, M. Latif, T. Lee, A. Rosati, and D. Stammer. 2011. "Decadal climate predictability and prediction: Where are we?" *Bulletin of the American Meteorological Society* no. 92 (5):637-640. doi: 10.1175/2010bams3025.1.

Meko, D., E. R. Cook, D. W. Stahle, C. W. Stockton, and M. K. Hughes. 1993. "Spatial patterns of tree-growth anomalies in the United-States and Southeastern Canada." *Journal of Climate* no. 6 (9):1773-1786.

Meko, D. M., and C. H. Baisan. 2001. "Pilot study of latewood-width of conifers as an indicator of variability of summer rainfall in the North American Monsoon Region." *International Journal of Climatology* no. 21 (6):697-708. doi: 10.1002/joc.646.

Meko, D. M., R. Touchan, and K. J. Anchukaitis. 2011. "Seascorr: A MATLAB program for identifying the seasonal climate signal in an annual tree-ring time series." *Computers & Geosciences*. doi: 10.1016/j.cageo.2011.01.013.

Meko, D. M., and C. A. Woodhouse. 2005. "Tree-ring footprint of joint hydrologic drought in Sacramento and Upper Colorado river basins, western USA." *Journal of Hydrology* no. 308 (1-4):196-213. doi: 10.1016/j.jhydrol.2004.11.003.

Meko, D. M., C. A. Woodhouse, C. A. Baisan, T. Knight, J. J. Lukas, M. K. Hughes, and M. W. Salzer. 2007. "Medieval drought in the upper Colorado River Basin." *Geophysical Research Letters* no. 34 (10):5. doi: L1070510.1029/2007gl029988.

Menne, M. J., C. N. Williams, and R. S. Vose. 2009. "The US historical climatology network monthly temperature data, version 2." *Bulletin of the American Meteorological Society* no. 90 (7):993-1007. doi: 10.1175/2008bams2613.1.

Metsamaki, S., J. Vepsalainen, J. Pulliainen, and Y. Sucksdorff. 2002. "Improved linear interpolation method for the estimation of snow-covered area from optical data." *Remote Sensing of Environment* no. 82 (1):64-78. doi: 10.1016/s0034-4257(02)00025-1.

Meyer, P., K. I. Itten, T. Kellenberger, S. Sandmeier, and R. Sandmeier. 1993. "Radiometric corrections of topographically induced effects on Landsat TM data in an alpine environment." *ISPRS Journal of Photogrammetry and Remote Sensing* no. 48 (4):17-28.

Minder, J. R., P. W. Mote, and J. D. Lundquist. 2010. "Surface temperature lapse rates over complex terrain: Lessons from the Cascade Mountains." *Journal of Geophysical Research-Atmospheres* no. 115. doi: D1412210.1029/2009jd013493.

Michaelsen, J. 1987. "Cross-validation in statistical climate forecast models." *Journal of Applied Meteorology* no. 26:1589-1600.

Mitchell, T. D., and P. D. Jones. 2005. "An improved method of constructing a database of monthly climate observations and associated high-resolution grids." *International Journal of Climatology* no. 25 (6):693-712. doi: 10.1002/joc.1181.

Mitchell, V.L. 1976. "The regionalization of climate in the western United States." *Journal of Applied Meteorology* no. 15 (9):920-927.

Mock, C. J. 1996. "Climatic controls and spatial variations of precipitation in the western United States." *Journal of Climate* no. 9 (5):1111-1125.

Moore, J. N., J. T. Harper, and M. C. Greenwood. 2007. "Significance of trends toward earlier snowmelt runoff, Columbia and Missouri Basin headwaters, western United States." *Geophysical Research Letters* no. 34 (16):5. doi: L1640210.1029/2007gl031022.

Molotch, N. P., and R. C. Bales. 2005. "Scaling snow observations from the point to the grid element: Implications for observation network design." *Water Resources Research* no. 41 (11):16. doi: W1142110.1029/2005wr004229.

Mote, P. W., A. F. Hamlet, M. P. Clark, and D. P. Lettenmaier. 2005. "Declining mountain snowpack in western north America." *Bulletin of the American Meteorological Society* no. 86 (1):39-49. doi: 10.1175/bams-86-1-39.

Nolin, A. W. 2012. "Perspectives on Climate Change, Mountain Hydrology, and Water Resources in the Oregon Cascades, USA." *Mountain Research and Development* no. 32:S35-S46. doi: 10.1659/mrd-journal-d-11-00038.s1.

Nolin, A. W., and C. Daly. 2006. "Mapping "at risk" snow in the Pacific Northwest." *Journal of Hydrometeorology* no. 7 (5):1164-1171. doi: 10.1175/jhm543.1.

Ostrom, C. W. Jr. 1990. *Time Series Analysis, Regression Techiques*. second ed. Vol. 07-009. Newbury Park: Sage Publications.

Otterstrom, S. M., and J. M. Shumway. 2003. "Deserts and oases: the continuing concentration of population in the American Mountain West." *Journal of Rural Studies* no. 19 (4):445-462.

Owen, D.E. 2008. Geology of Craters of the Moon. Craters of the Moon National Monument and Preserve: Craters of the Moon Natural History Association.

Painter, T. H., K. Rittger, C. McKenzie, P. Slaughter, R. E. Davis, and J. Dozier. 2009. "Retrieval of subpixel snow covered area, grain size, and albedo from MODIS." *Remote Sensing of Environment* no. 113 (4):868-879. doi: 10.1016/j.rse.2009.01.001.

Pederson, G. T., S. T. Gray, C. A. Woodhouse, J. L. Betancourt, D. B. Fagre, J. S. Littell, E. Watson, B. H. Luckman, and L. J. Graumlich. 2011. "The Unusual Nature of Recent Snowpack Declines in the North American Cordillera." *Science* no. 333 (6040):332-335. doi: 10.1126/science.1201570.

Pederson, G. T., S. T. Gray, D. B. Fagre, and L. J. Graumlich. 2006. "Long-duration drought variability and impacts on ecosystem services: A case study from Glacier National Park, Montana." *Earth Interactions* no. 10:28. doi: 4.

Peterson, T. C., D. R. Easterling, T. R. Karl, P. Groisman, N. Nicholls, N. Plummer, S. Torok, I. Auer, R. Boehm, D. Gullett, L. Vincent, R. Heino, H. Tuomenvirta, O. Mestre, T. Szentimrey, J. Salinger, E. J. Forland, I. Hanssen-Bauer, H. Alexandersson, P. Jones, and D. Parker. 1998. "Homogeneity adjustments of in situ atmospheric climate data: A review." *International Journal of Climatology* no. 18 (13):1493-1517.

Pepe, M., P. A. Brivio, A. Rampini, F. R. Nodari, and M. Boschetti. 2005. "Snow cover monitoring in alpine regions using ENVISAT optical data." *International Journal of Remote Sensing* no. 26 (21):4661-4667.

Pierce, D. W., T. P. Barnett, H. G. Hidalgo, T. Das, C. Bonfils, B. D. Santer, G. Bala, M. D. Dettinger, D. R. Cayan, A. Mirin, A. W. Wood, and T. Nozawa. 2008. "Attribution of Declining Western US Snowpack to Human Effects." *Journal of Climate* no. 21 (23):6425-6444. doi: 10.1175/2008jcli2405.1.

Redmond, K. T., and R. W. Koch. 1991. "Surface climate and streamflow variablity in the western United-States and their relationship to large-scale circulation indexes." *Water Resources Research* no. 27 (9):2381-2399. doi: 10.1029/91wr00690.

Riggs, G. A., D. K. Hall, and V. V. Salomonson. 2006. "MODIS snow products user guide to collection 5."

Rittger, K., T. H. Painter, and J. Dozier. 2012. "Assessment of methods for mapping snow cover from MODIS." *Advances in Water Resources* (0). doi: 10.1016/j.advwatres.2012.03.002.

Robinson, D. A. 1991. "Merging operational satellite and historical station snow cover data to monitor climate change." *Global and Planetary Change* no. 90 (1-3):235-240.

Rosenthal, W., and J. Dozier. 1996. "Automated mapping of montane snow cover at subpixel resolution from the Landsat Thematic Mapper." *Water Resources Research* no. 32 (1):115-130.

Salminen, M., J. Pulliainen, S. Metsamaki, A. Kontu, and H. Suokanerva. 2009. "The behaviour of snow and snow-free surface reflectance in boreal forests: Implications to the performance of snow covered area monitoring." *Remote Sensing of Environment* no. 113 (5):907-918. doi: 10.1016/j.rse.2008.12.008.

Salomonson, V. V., and I. Appel. 2004. "Estimating fractional snow cover from MODIS using the normalized difference snow index." *Remote Sensing of Environment* no. 89 (3):351-360. doi: 10.1016/j.rse.2003.10.016.

———. 2006. "Development of the Aqua MODIS NDSI fractional snow cover algorithm and validation results." *IEEE Transactions on Geoscience and Remote Sensing* no. 44 (7):1747-1756. doi: 10.1109/tgrs.2006.876029.

Salzer, M. W., M. K. Hughes, A. G. Bunn, and K. F. Kipfmueller. 2009. "Recent unprecedented tree-ring growth in bristlecone pine at the highest elevations and possible causes." *Proceedings of the National Academy of Sciences of the United States of America* no. 106 (48):20348-20353. doi: 10.1073/pnas.0903029106.

Salzer, M. W., and K. F. Kipfmueller. 2005. "Reconstructed temperature and precipitation on a millennial timescale from tree-rings in the Southern Colorado Plateau, USA." *Climatic Change* no. 70 (3):465-487. doi: 10.1007/s10584-005-5922-3.

Schaaf, C. B., Z. S. Wang, and A. H. Strahler. 2011. "Commentary on Wang and Zender-MODIS snow albedo bias at high solar zenith angles relative to theory and to in situ observations in Greenland." *Remote Sensing of Environment* no. 115 (5):1296-1300. doi: 10.1016/j.rse.2011.01.002.

Seidel, K., F. Ade, and J. Lichtenegger. 1983. "Augmenting landsat mss data with topographic information for enhanced registration and classification " *Ieee Transactions on Geoscience and Remote Sensing* no. 21 (3):252-258.

Seidel, K., and J. Martinec. 2004. *Remote Sensing in Snow Hydrology Runoff Modeling, Effect of Climate Change*. Chichester, UK: Praxis Publishing.

Serreze, M. C., M. P. Clark, R. L. Armstrong, D. A. McGinnis, and R. S. Pulwarty. 1999. "Characteristics of the western United States snowpack from snowpack telemetry (SNOTEL) data." *Water Resources Research* no. 35 (7):2145-2160. doi: 10.1029/1999wr900090.

Service, R. F. 2004. "Water resources: As the West goes dry." *Science* no. 303 (5661):1124-1127.

Shinker, J. J. 2010. "Visualizing spatial heterogeneity of western U.S. climate variability." *Earth Interactions* no. 14. doi: 1010.1175/2010ei323.1.

Slaughter, R. A., and J. D. Wiener. 2007. "Water, adaptation, and property rights on the snake and Klamath Rivers." *Journal of the American Water Resources Association* no. 43 (2):308-321. doi: 10.1111/j.1752-1688.2007.00024.x.

Smith, J. A., T. L. Lin, and K. J. Ranson. 1980. "The Lambertian assumption and Landsat data." *Photogrammetric Engineering and Remote Sensing* no. 46 (9):1183-1189.

Sobolowski, S., G. Gong, and M. Ting. 2007. "Northern hemisphere winter climate variability: Response to North American snow cover anomalies and orography." *Geophysical Research Letters* no. 34 (16). doi: L1682510.1029/2007gl030573.

Song, C., C. E. Woodcock, K. C. Seto, M. P. Lenney, and S. A. Macomber. 2001. "Classification and change detection using Landsat TM data: When and how to correct atmospheric effects?" *Remote Sensing of Environment* no. 75 (2):230-244.

Stahle, D. W., M. K. Cleaveland, H. D. Grissino-Mayer, R. D. Griffin, F. K. Fye, M. D. Therrell, D. J. Burnette, D. M. Meko, and J. V. Diaz. 2009. "Cool- and Warm-Season Precipitation Reconstructions over Western New Mexico." *Journal of Climate* no. 22 (13):3729-3750. doi: 10.1175/2008jcli2752.1.

Stahle, D. W., E. R. Cook, M. K. Cleaveland, M. D. Therrell, D. M. Meko, H. D. Grissino-Mayer, E. Watson, and B. H. Luckman. 2000. "Tree-ring data document 16th century megadrought over North America." *EOS, Transactions, American Geophysical Union* no. 81 (12):121-132.

Stewart, I. T., D. R. Cayan, and M. D. Dettinger. 2005. "Changes toward earlier streamflow timing across western North America." *Journal of Climate* no. 18 (8):1136-1155. doi: 10.1175/jcli3321.1.

Stokes, M. A., and T. J. Smiley. 1996. *An Introduction to Tree-Ring Dating*. Tucson, Arizona: The University of Arizona Press.

Stroeve, J., M. M. Holland, W. Meier, T. Scambos, and M. Serreze. 2007. "Arctic sea ice decline: Faster than forecast." *Geophysical Research Letters* no. 34 (9). doi: L0950110.1029/2007gl029703.

Sturm, M., J. Holmgren, and G. E. Liston. 1995. "A seasonal snow cover classification-system for local to global applications." *Journal of Climate* no. 8 (5):1261-1283. doi: 10.1175/1520-0442(1995)008<1261:asccs>2.0.co;2.

Teillet, P. M., B. Guindon, and D. G. Goodenough. 1982. "On the slope-aspect correction of multispectral scanner data." *Canadian Journal of Remote Sensing* no. 8 (2):84-106.

Teng, H. Y., L. E. Buja, and G. A. Meehl. 2006. "Twenty-first-century climate change commitment from a multi-model ensemble." *Geophysical Research Letters* no. 33 (7). doi: 10.1029/2005GL024766.

Vautard, R., and M. Ghil. 1989. "Singular spectrum analysis in nonlinear dynamics, with applications to paleoclimatic time-series." *Physica D* no. 35 (3):395-424. doi: 10.1016/0167-2789(89)90077-8.

Vermote, E. F., and S. Kotchenova. 2008. "Atmospheric correction for the monitoring of land surfaces." *Journal of Geophysical Research-Atmospheres* no. 113 (D23). doi: D23s9010.1029/2007jd009662.

Vermote, E. F., D. Tanre, J. L. Deuze, M. Herman, and J. J. Morcrette. 1997. "Second Simulation of the Satellite Signal in the Solar Spectrum, 6S: An overview." *IEEE Transactions on Geoscience and Remote Sensing* no. 35 (3):675-686. doi: 10.1109/36.581987.

Warren, S. G. 1982. "Optical-properties of snow." *Reviews of Geophysics* no. 20 (1):67-89. doi: 10.1029/RG020i001p00067.

Watson, E., and B. H. Luckman. 2001. "Dendroclimatic reconstruction of precipitation for sites in the southern Canadian Rockies." *Holocene* no. 11 (2):203-213.

Westerling, A. L., H. G. Hidalgo, D. R. Cayan, and T. W. Swetnam. 2006. "Warming and earlier spring increase western US forest wildfire activity." *Science* no. 313 (5789):940-943. doi: 10.1126/science.1128834.

Whitlock, C., and P. J. Bartlein. 1993. "Spatial variations of Holocene climatic-change in the Yellowstone Region." *Quaternary Research* no. 39 (2):231-238.

Wigley, T. M. L., K. R. Briffa, and P. D. Jones. 1984. "On the average value of correlated time series, with applications in dendroclimatology and hydrometeorology." *Journal of Climate and Applied Meteorology* no. 23:201-213.

Wilks, D. S. 1995. *Statistical methods in the atmospheric sciences*. Boston: Academic Press.

Winther, J. G., and D. K. Hall. 1999. "Satellite-derived snow coverage related to hydropower production in Norway: present and future." *International Journal of Remote Sensing* no. 20 (15-16):2991-3008. doi: 10.1080/014311699211570.

Wiscombe, W. J., and S. G. Warren. 1980. "A model for the spectral albedo of snow. 1. pure snow." *Journal of the Atmospheric Sciences* no. 37 (12):2712-2733. doi: 10.1175/1520-0469(1980)037<2712:amftsa>2.0.co;2.

Wise, E. K. 2010. "Tree ring record of streamflow and drought in the upper Snake River." *Water Resources Research* no. 46. doi: W1152910.1029/2010wr009282.

Woodhouse, C. A., K. E. Kunkel, D. R. Easterling, and E. R. Cook. 2005. "The twentieth-century pluvial in the western United States." *Geophysical Research Letters* no. 32 (7). doi: L0770110.1029/2005gl022413.

Woodhouse, C. A., and J. T. Overpeck. 1998. "2000 years of drought variability in the central United States." *Bulletin of the American Meteorological Society* no. 79 (12):2693-2714. doi: 10.1175/1520-0477(1998)079<2693:yodvit>2.0.co;2.

Xin, Q. C., C. E. Woodcock, J. C. Liu, B. Tan, R. A. Melloh, and R. E. Davis. 2012. "View angle effects on MODIS snow mapping in forests." *Remote Sensing of Environment* no. 118:50-59. doi: 10.1016/j.rse.2011.10.029.

Yue, S., and C. Y. Wang. 2004. "The Mann-Kendall test modified by effective sample size to detect trend in serially correlated hydrological series." *Water Resources Management* no. 18 (3):201-218. doi: 10.1023/b:warm.0000043140.61082.60.